

Synechocystis Mutants Lacking Genes Potentially Involved in Carotenoid Metabolism

by

Christoph Trautner

A Dissertation Presented in Partial Fulfillment
of the Requirements for the Degree
Doctor of Philosophy

Approved January 2011 by the
Graduate Supervisory Committee:

Wim Vermaas, Chair
Douglas Chandler
Rajeev Misra
Scott Bingham

ARIZONA STATE UNIVERSITY

May 2011

ABSTRACT

Like most other phototrophic organisms the cyanobacterium *Synechocystis* sp. PCC 6803 produces carotenoids. These pigments often bind to proteins and assume various functions in light harvesting, protection from reactive oxygen species (ROS) and protein stabilization. One hypothesis was that carotenoids bind to the surface (S-)layer protein. In this work the *Synechocystis* S-layer protein was identified as Sll1951 and the effect on the carotenoid composition of this prokaryote by disruption of *sll1951* was studied. Loss of the S-layer, which was demonstrated by electron microscopy, did not result in loss of carotenoids or changes in the carotenoid profile of the mutant, which was shown by HPLC and protein analysis. Although $\Delta sll1951$ was more susceptible to osmotic stress than the wild type, the general viability of the mutant remained unaffected.

In a different study a combination of mutants having single or multiple deletions of putative carotenoid cleavage dioxygenase (CCD) genes was created. CCDs are presumed to play a role in the breakdown of carotenoids or apo-carotenoids. The carotenoid profiles of the mutants that were grown under conditions of increased reactive oxygen species were analyzed by HPLC. Pigment lifetimes of all strains were estimated by ^{13}C -labeling. Carotenoid composition and metabolism were similar in all strains leading to the conclusion that the deleted CCDs do not affect carotenoid turnover in *Synechocystis*. The putative CCDs either do not fulfill this function in cyanobacteria or alternative pathways for carotenoid degradation exist.

Finally, *slr0941*, a gene of unknown function but a conserved genome position in many cyanobacteria downstream of the ζ -carotene desaturase, was disrupted. Initially, the mutant strain was impaired in growth but displayed a rather normal carotenoid content and composition,

but an apparent second-site mutation occurred infrequently that restored growth rates and caused an accumulation of carotenoid isomers not found in the wild type. Based on the obtained data a role of the *slr0941* gene in carotenoid binding/positioning for isomerization and further conversion to mature carotenoids is suggested.

DEDICATION

This dissertation is dedicated to my mother, Christine,
for her support throughout all the years during my Master's and Doctoral work.

ACKNOWLEDGMENTS

Gratitude goes to my advisor Wim Vermaas
and my Committee Members Douglas Chandler, Rajeev Misra and Scott Bingham.

For their help with light- and electron microscopy I thank

Mr. David Lowry and Dr. Robert Roberson.

I also thank my friends and colleagues for their helpful input

and (not only scientifically) enlightening discussions,

Dmitri, Sawsan, Bing, Hatem, Miguel, Danny, Hongliang, Shuqin,
Dan Brune, Dan Jenk, Cathy, Yifei, Vicki, Ipsita, Raul, Wei, and Srin.

TABLE OF CONTENTS

LIST OF TABLES.....	x
LIST OF FIGURES.....	xi
CHAPTER	
I. INTRODUCTION.....	1
About the cyanobacterium <i>Synechocystis</i> and its pigments.....	1
Biosynthesis and structure of carotenoids.....	3
The functions of carotenoids in protein- and membrane stabilization as well as in photoprotection.....	8
Questions addressed in this work.....	9
References.....	11
II. METHODS - MOLECULAR BIOLOGY.....	14
Construction of mutant strains to analyze the function of Slr0941.....	14
Construction of dioxygenase deletion strains.....	26
Construction of Sll1951 (S-layer)-deficient strains.....	31
III. SLL1951 ENCODES THE S-LAYER PROTEIN OF <i>SYNECHOCYSTIS</i>	35
Abstract.....	35
Introduction.....	36
Methods.....	37
Cultivation of strains.....	37
Construction of the $\Delta sll1951$ deletion strain.....	37
Transmission electron microscopy.....	39
Discontinuous sucrose gradient centrifugation of cell extracts.....	40

CHAPTER	Page
Analysis of proteins by SDS-PAGE and mass spectroscopy.....	41
Analysis of carotenoids.....	42
Light microscopy.....	43
Results.....	45
The Sll1951 protein.....	45
The Δ sll1951 deletion mutant.....	46
Light- and electron microscopy.....	50
Analysis of the Δ sll1951 cell wall components.....	55
Transcript levels of S-layer mRNA in the <i>Synechocystis</i> wild type.....	61
Discussion.....	62
Preliminary identification of an S-layer candidate gene.....	62
Phenotype of Δ sll1951.....	64
Increased sensitivity of Δ sll1951 to osmotic stress.....	65
References.....	66
 IV. DELETION OF <i>SLR0941</i> PROMOTES THE DEVELOPMENT OF A CAROTENOID ACCUMULATING PHENOTYPE IN <i>SYNECHOCYSTIS</i>	 70
Abstract.....	70
Introduction.....	71
Methods.....	73
Analysis of carotenoid isomers.....	73
Results.....	74
Analysis of the <i>slr0941</i> coding region.....	74
Segregation of Δ slr0941 deletion strains.....	76

CHAPTER	Page
Pigment profiles of $\Delta slr0941$ deletion strains.....	78
Differences between <i>Synechocystis</i> wild type, $\Delta slr0941$ C and $\Delta slr0941$ G.....	92
Comparison of $\Delta slr0941$ with a carotenoid isomerase-less ($\Delta sll0033$) strain.....	93
Localization of accumulating carotenoids.....	94
Expression levels of <i>slr0941</i>	97
Discussion.....	98
Strains of $\Delta slr0941$ have markedly extended doubling times.....	99
$\Delta slr0941$ is prone to a secondary mutation leading to the accumulation of carotenoid isomers.....	100
Presence of functional isomerase genes in $\Delta slr0941$ suggest a structural role of Slr0941 at the stage of carotenoid isomerization.....	102
The restored doubling time of the $\Delta slr0941$ C mutant hints a secondary mutation.....	103
References.....	104
V. SLR1648 AND SLL1541 ARE PUTATIVE CAROTENOID CLEAVAGE DI- OXYGENASES OF <i>SYNECHOCYSTIS</i>	108
Abstract.....	108
Introduction.....	109
Methods.....	111
Labeling of carotenoids with ^{13}C -glucose.....	111
Fluorescence emission spectroscopy.....	113

CHAPTER	Page
Electron microscopy.....	113
Preparation of membrane profiles on sucrose density gradients.....	114
Calculation of chlorophyll contents of cells.....	115
Preparative analysis of pigments by HPLC.....	115
Results.....	116
Segregation of the mutants.....	116
Description of the fully segregated mutants.....	117
Analysis of the carotenoids of the <i>Synechocystis</i> wild-type strain and the dioxygenase mutants.....	118
Absence of detectable retinoids in the <i>Synechocystis</i> wild-type strain.....	122
Electron microscopy of the <i>Synechocystis</i> wild type and dioxygenase mutants.....	125
Membrane profiles of the <i>Synechocystis</i> wild type and dioxygenase mutants.....	128
Turnover of carotenoids in the <i>Synechocystis</i> wild type and carotenoid dioxygenase mutants monitored by ¹³ C-labeling.....	129
Discussion.....	135
Pigment profiles of dioxygenase strains.....	135
Effects of environmental stress on dioxygenase mutants.....	136
Electron microscopy and membrane profiles of dioxygenase mutants.....	137

CHAPTER	Page
¹³ C-labeling of carotenoids in the <i>Synechocystis</i> wild type and the dioxygenase mutants.....	138
Contribution of Sll1541 and Slr1648 to carotenoid turnover is negligible under high light conditions.....	138
References.....	140

LIST OF TABLES

Table	Page
I-1 Intermediates of the DOXP-pathway and corresponding <i>Synechocystis</i> genes/enzymes.....	4
I-2 Intermediates of the carotenoid biosynthesis pathway in <i>Synechocystis</i>	5
I-3 The four major carotenoids in <i>Synechocystis</i>	7
III-1 ORFs in the <i>Synechocystis</i> genome encoding hemolysin Ca ²⁺ binding motifs or S-layer homology (SLH) domain motifs.....	61
IV-1 Peak intensities of pigments in the carotenoid accumulating mutant $\Delta slr0941$ v2 compared to the <i>Synechocystis</i> wild-type strain.....	81
IV-2 Identification of carotenoids with respect to elution times, mass and online spectra.....	86
V-1 Chlorophyll contents of strains grown photomixotrophically at 200 $\mu\text{mol photons m}^{-2} \text{s}^{-1}$ supplemented with 20 μM atrazine.....	124

LIST OF FIGURES

Figure	Page
II-1 Map of pslr0941 v2 α	15
II-2 Map of pslr0941 v2.....	17
II-3 Map of pslr0940/0941 α	18
II-4 Map of pslr094X.....	19
II-5 Map of pslr0941 His.....	22
II-6 Map of pslr0941 His Sp.....	22
II-7 Map of psll0033 α	24
II-8 Map of psll0033.....	25
II-9 Map of psll1541 α	27
II-10 Map of psll1541.....	28
II-11 Map of pslr1648 α	29
II-12 Map of pslr1648.....	30
II-13 Map of psll1951 Cm.....	32
II-14 Map of psll1951 Km.....	34
III-1 PCR products of two fully segregated Δ <i>sll1951</i> mutant strains and the <i>Synechocystis</i> wild type	46
III-2 Growth of the wild type and the Δ <i>sll1951</i> mutant strain adapted to photoautotrophic growth at 45 $\mu\text{mol photons m}^{-2} \text{s}^{-1}$	47
III-3 Photomixotrophic growth performance of wild-type and mutant cultures.....	48
III-4 Absorption of supernatants of wild type and the Δ <i>sll1951</i> mutant.....	49
III-5 Antibiotic sensitivity test.....	50

Figure	Page
III-6 Whole cell images of HPF-fixed <i>Δsll1951</i> , <i>Δsll1213</i> and wild-type cells.....	52
III-7 High magnification images of the cell periphery of wild-type, <i>Δsll1951</i> and <i>Δsll1213</i> strains.....	53
III-8 Phosphotungstic acid negative stain images of wild-type cells and the <i>Δsll1951</i> mutant.....	53
III-9 DIC light microscopy on cells of <i>Synechocystis</i> wild type and <i>Δsll1951</i>	54
III-10 SDS-PAGE on protein isolates from the <i>Δsll1951</i> mutant and the <i>Synechocystis</i> wild type.....	56
III-11 SDS-PAGE of supernatants of <i>Synechocystis</i> wild-type and the <i>Δsll1951</i> mutant.....	57
III-12 SDS-PAGE of supernatant protein profiles of <i>Synechocystis</i> wild-type and the <i>Δsll1951</i> mutant after treatment with different concentrations of lauryl sarcosine.....	58
III-13 SDS-PAGE of supernatant protein profiles of <i>Synechocystis</i> wild-type and the <i>Δsll1951</i> mutant after treatment with different concentrations of Triton X-100.....	58
III-14 Sucrose gradients and isolated membrane/protein fractions of <i>Synechocystis</i> wild-type and the mutant <i>Δsll1951</i>	59
III-15 Carotenoid HPLC profiles of the <i>Synechocystis</i> wild-type and <i>Δsll1951</i> membrane fractions.....	60
IV-1 Biosynthesis of phytoene from dimethylallylpyrophosphate (DMAPP) via geranylgeranylpyrophosphate (GGPP).....	72
IV-2 Desaturation scheme of phytoene to lycopene in plants and cyanobacteria.....	73

Figure	Page
IV-3 Multiple sequence alignment of the ten most closely related cyanobacterial orthologs of <i>slr0941</i>	75
IV-4 Alignment of <i>slr0941</i> with the three <i>A. thaliana</i> orthologs.....	76
IV-5 Agarose gel image of PCR fragments of the <i>slr0941</i> loci in the <i>Synechocystis</i> wild-type strain and the fully segregated mutant Δ <i>slr0941</i> v2.....	76
IV-6 Growth performance at 5 μ mol photons $m^{-2} s^{-1}$ of photomixotrophically grown strains of wild type, carotenoid-phenotype mutant Δ <i>slr0941</i> C and slow-growth phenotype Δ <i>slr0941</i> G.....	77
IV-7 Growth performance of photomixotrophically grown strains of wild type, and slow-growth phenotype Δ <i>slr0941</i> G at 50 μ mol photons $m^{-2} s^{-1}$	78
IV-8 Overlay of elution profiles monitored at 480 nm of methanol extracts from segregated Δ <i>slr0941</i> v2 mutants grown at 5 μ mol photons $m^{-2} s^{-1}$	79
IV-9 Overlay of HPLC pigment elution profiles of wild type and Δ <i>slr0941</i> C grown at 5 μ mol photons $m^{-2} s^{-1}$	80
IV-10 A plate culture of slow-growing mutant Δ <i>slr0941</i> after several rounds of replating.....	81
IV-11 Three clones of Δ <i>slr0941</i> that had been transformed with <i>pslr0941</i> HIS Sp.....	82
IV-12 HPLC absorption traces of wild type, rescued Δ <i>slr0941</i> mutant (<i>slr0941R</i>) and Δ <i>slr0941</i> strains.....	82
IV-13 HPLC spectra of pigment extracts from Δ <i>slr094X</i> and Δ <i>slr0941</i> C grown photomixotrophically at 0.4 μ mol photons $m^{-2} s^{-1}$	83

Figure	Page
IV-14 HPLC spectrum of pigments accumulating in the mutant $\Delta slr0941$ C, separated by a 26-minute water/methanol/ethyl acetate gradient.....	84
IV-15 Combined mass trace/absorption profile of carotenoid precursors accumulating in LAHG-grown $\Delta slr0941$ C.....	85
IV-16 HPLC spectra of carotenoid precursors from $\Delta slr0941$ after increasing times of exposure of cells to $140 \mu\text{mol photons m}^{-2} \text{s}^{-1}$	88
IV-17 350 nm absorption trace of carotenoids purified between 16.5 and 18.5 min of an LAHG-adapted culture of $\Delta slr0941$ C after 0, 10, 60 and 360 min of illumination at $140 \mu\text{mol photons m}^{-2} \text{s}^{-1}$	89
IV-18 Absorption trace from the same experiment as in Fig. IV-17 but monitored at 480 nm to detect pigments that absorbed at higher wavelength.....	91
IV-19 Comparison of pigment profiles of <i>Synechocystis</i> wild type, $\Delta slr0941$ G and $\Delta slr0941$ C strains.....	92
IV-20 Agarose gel of PCR products of the <i>Synechocystis</i> wild type, and the mutant strains $\Delta sll0033$ and $\Delta sll0033/\Delta slr0941$	93
IV-21 Growth performance of wild type, carotenoid isomerase mutant $\Delta sll0033$ and the double mutant $\Delta sll0033/\Delta slr0941$	94
IV-22 Pigments isolated from CM fractions of the <i>Synechocystis</i> wild type and the $\Delta sll0033/\Delta slr0941$ double deletion mutant grown photomixotrophically at $5 \mu\text{mol photons m}^{-2} \text{s}^{-1}$	95

Figure	Page
IV-23 Pigments isolated TM of wild type and $\Delta sll0033/\Delta slr0941$ double deletion strains from the same experiment as in Fig. IV-22.....	96
IV-24 Tiling array data showing RNA probe abundances for the <i>slr0940/sl0941</i> locus including truncated up- and downstream ORFs in exponential growth phase and linear growth phase.....	97
V-1 Cleavage of carotenoids by 9- <i>cis</i> -epoxy carotenoid dioxygenase and by 15-15'-carotenoid dioxygenase	111
V-2 Agarose gel image of PCR products created from genomic DNA of wild type, $\Delta sll1541$, $\Delta slr1648$, and $\Delta sll1541/\Delta slr1648$	116
V-3 Agarose gel image of PCR products from wild type as well as mutants deficient in <i>sll1541</i> , <i>slr1648</i> and both genes.....	117
V-4 Combined HPLC spectra of strains grown at 5 $\mu\text{mol photons m}^{-2} \text{s}^{-1}$ – normalized to zeaxanthin – of <i>Synechocystis</i> wild type and the mutant strains $\Delta sll1648$ and $\Delta sll1541/\Delta slr1648$	118
V-5 Combined pigment profiles of low-light adapted wild type and $\Delta sll1541/\Delta slr1648$ strains after 10-minute exposure to 150 $\mu\text{mol photons m}^{-2} \text{s}^{-1}$	120
V-6 Combined pigment profiles of wild type and the double mutant $\Delta sll1541/\Delta slr1648$ after 2 h, 21 h and 29 h of exposure to 180 $\mu\text{mol photons m}^{-2} \text{s}^{-1}$	121
V-7 HPLC trace of pigments from the <i>Synechocystis</i> wild type combined with 1 μg of retinal standard.....	122

Figure	Page
V-8 Fluorescence emission of the <i>Synechocystis</i> wild type, $\Delta sll1541$, $\Delta slr1648$, and the double mutant.....	123
V-9 Photosystem ratios of all strains grown under high-light (200 $\mu\text{mol photons m}^{-2} \text{s}^{-1}$) and supplemented with 1 mM glucose.....	124
V-10 Low- and high magnification images of photoautotrophically grown, chemically fixed <i>Synechocystis</i> wild-type cells.....	126
V-11 Low- and high magnification TEM images of cells of $\Delta sll1541$	126
V-12 Cells of $\Delta slr1648$	127
V-13 The $\Delta sll1541/\Delta slr1648$ double mutant.....	127
V-14 Sucrose gradients of the <i>Synechocystis</i> wild type and all mutant strains ($\Delta sll1541$, $\Delta slr1648$ and the double mutant).....	128
V-15 Illumination of the gradients from Fig. V-14 with UV-light.....	129
V-16 Mass spectra of β -carotene in wild type.....	131
V-17 Mass spectra of echinenone of the wild type.....	132
V-18 Labeling of β -carotene in the double mutant $\Delta sll1541/\Delta slr1648$	133
V-19 Masses of echinenone in the double mutant $\Delta sll1541/\Delta slr1648$	134
V-20 Examples of carotenoid breakdown products.....	136

CHAPTER I. INTRODUCTION

*About the cyanobacterium *Synechocystis* and its pigments*

The model organism *Synechocystis* sp. PCC 6803 is a unicellular cyanobacterium and member of the group of coccus-shaped Chroococcales. Cyanobacteria are ubiquitous Gram-negative and, primarily, photoautotrophic prokaryotes, they harvest and use light during daytime as their energy source to maintain a membrane potential difference, generate ATP and fix inorganic carbon in the form of carbon dioxide (Bryant, 1994). Most phototrophic organisms have evolved highly specialized (sub-)cellular systems for efficient harvesting of light energy, while also minimizing the potentially destructive effects of excess light energy. Frequently, these systems involve pigments, chromophores that absorb at specific wavelengths and either dissipate or relay the energy. In cyanobacteria, pigments are commonly found embedded in membranes or protein complexes. Like other cyanobacteria, *Synechocystis* has three different types of membranes, the outer membrane (OM), the cytoplasmic membrane (CM) and the thylakoid membrane (TM).

The photosynthetic conversion of light energy into electro-chemical energy is catalyzed by a variety of multiprotein-enzyme complexes located in and on the TM. It commences with the extraction of electrons from water by photosystem II (PS II), a large heterodimeric protein complex that acts as a water-plastoquinone oxidoreductase, and is followed by a non-cyclic transfer of these highly energetic electrons along an electron transport chain to drive the pumping of protons. In plants and cyanobacteria electrons generated by PS II also contribute to the electron transport around photosystem I (PS I), a plastocyanin-ferredoxin oxidoreductase, for the reduction of NADP⁺. The structures of both PS I and PS II have been studied in great detail by several groups (Jordan *et al.*,

2001; Amunts *et al.*, 2007; Guskov *et al.*, 2009; Loll *et al.*, 2005). According to crystal structures a single PS I core complex of *Pisum sativum* on its own contains at least 167 chlorophyll molecules and an, as of yet, undefined number of carotenoids (Ben-Shem *et al.*, 2003), while in a PS II monomer 35 molecules of chlorophyll are accompanied by 12 carotenoid molecules (Guskov *et al.*, 2009). Light-harvesting complexes (LHC) of purple bacteria (Cogdell *et al.*, 1999), plants and algae also show a strong presence of (bacterio-)chlorophylls. The high abundance of chlorophylls in photosystems and LHCs underscores the importance of these pigments in photosynthetic processes. Chlorophylls are phytylated porphyrin pigments synthesized via 17 enzymatic steps from eight molecules of L-glutamic acid (Tanaka and Tanaka, 2007). Their characteristic absorption properties with maxima at 430 (Soret), 578 (Q_x) and 662 nm (Q_y) (for chlorophyll *a* in diethyl ether) are derived from a system of conjugated double-bonds that are distributed over the tetrapyrrole structure, and result in a high extinction coefficient of 90 mM⁻¹ cm⁻¹ (at 662 nm in diethyl ether). Although cyanobacteria produce a variety of different chlorophylls, the only type found in *Synechocystis* is chlorophyll *a*.

A different class of pigments is present in phycobilisomes (PBS), the light-harvesting antenna complexes of cyanobacteria and red algae (Grossman *et al.*, 1993; MacColl, 1998). Based on the photo-chemical properties of the phycobilins, the pigments bound to PBS, the spectral range of light that can be harvested by PBS is extended by approximately 100 nm down to about 560 nm if the PBS antenna contains phycoerythrin. PBS are TM-associated and relay energy in a highly directed manner to PS II or PS I by non-radiative Förster resonance- or exciton coupling transfer (Glazer *et al.*, 1985a; Glazer *et al.*, 1985b). The pigments involved in this process are (phyco-)bilins, linearized tetrapyrrole chromophores derived from the haem biosynthesis pathway. Like chlorophylls, bilins also possess several conjugated double-bonds and their extinction

coefficient is up to ca. $30 \text{ mM}^{-1} \text{ cm}^{-1}$ at their λ_{max} . Carotenoids represent the third class of pigments. Because of their functional versatility, carotenoids are found not only in cyanobacteria but in fact in all oxygenic phototrophic organisms. Since in this dissertation several aspects of carotenoid biosynthesis, localization, and turnover are addressed, a more detailed coverage of carotenoids is provided in the following sections of this introduction.

Biosynthesis and structure of carotenoids

In contrast to branched-chain chlorophylls and phycobilins, both of which are made of eight molecules of glutamic acid, carotenoids are chromophores that are based on single polyene chains consisting of usually eight C_5 -isoprenoid building blocks. In cyanobacteria these terpenoids are constructed from intermediates of glycolysis (glyceraldehyde 3-phosphate (G3P) and pyruvate (PYR)) and the sugar phosphates of the pentose phosphate cycle by the deoxy-xylulose 5-phosphate (DOXP-) pathway (Hunter, 2007). The DOXP pathway (a.k.a. non-mevalonate- or methyl-erythritol phosphate pathway) is also present in the plant chloroplast and starts with the decarboxylation-condensation of G3P and PYR to create 1-deoxy-D-xylulose 5-phosphate. Six additional enzymatic steps are required to form isopentenyl diphosphate (IPP) or dimethylallyl diphosphate (DMAPP), the building blocks for a vast variety of isoprenoid-based metabolites such as mono-, di- and triterpenes, ubiquinone, sterols, dolichols, zeatin, isoprene, phytol and carotenoids (Table I-1).

For carotenoid biosynthesis molecules of DMAPP are successively combined in a series of condensations catalyzed by geranylgeranyl diphosphate synthase (CrtE) via geranyl diphosphate and farnesyl diphosphate to geranylgeranyl diphosphate (GGPP). The carotenoid backbone phytoene is created by a head-to-head condensation of two

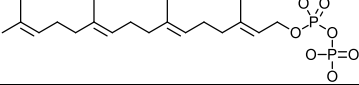
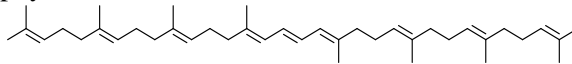
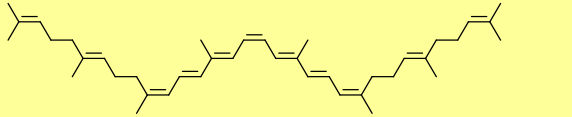
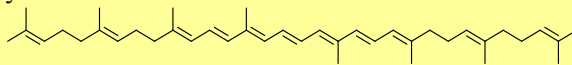
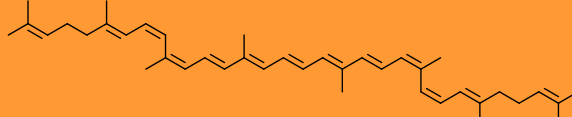
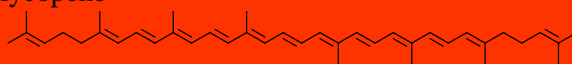
molecules of GGPP by phytoene synthase. Phytoene is then symmetrically desaturated either by a single bacterial-type desaturase, CrtI, or two distinct plant-type desaturases, CrtP and CrtQ, which are also present in most cyanobacterial species (Table I-2). Insertion of double bonds along the hydrocarbon backbone of the carotenoid has a crucial effect on its absorption characteristics. Incomplete desaturation and subsequent absence of native carotenoids dramatically increases the light sensitivity of affected strains of *Synechocystis* (Bautista *et al.*, 2005; Sozer *et al.*, 2010; this work).

Interestingly, while carotenoid biosynthesis down to the level of neurosporene (a linear, partially desaturated carotenoid intermediate with nine conjugated double bonds) or lycopene (table I-2) appears to be highly conserved throughout the kingdoms of eukaryotes and prokaryotes, the variety among carotenoids is created by additional modifications of the desaturated intermediates, resulting in hundreds of different compounds. Cyclization at the polyene-terminus by ring formation between C-1 and C-6 which is initiated by a H⁺-attack on the C-2-position (Hornero-Méndez and Britton, 2002) is a very common modification, and increases the overall stability of the polyene (Edge *et al.*, 1997).

Table I-1: Intermediates of the DOXP-pathway (grey background) and corresponding *Synechocystis* genes/enzymes. Steps leading to carotenoid biosynthesis have a white background.

Step	Substrate(s)	ORF	Gene
1	pyruvate and D-glyceraldehyde 3-phosphate	<i>sll1945</i>	Dxs
2	1-deoxy-D-xylulose 5-phosphate	<i>sll0019</i>	Dxr
3	2-C-methyl-D-erythrol 4-phosphate	<i>slr0951</i>	IspD
4	4-(cytidine 5-diphospho)-2-C-methyl-D-erythritol	<i>sll0711</i>	IspE
5	2-phospho-4-(cytidine 5'-diphospho)-2-C-methyl-D-erythritol	<i>slr1542</i>	IspF
6	2-C-ethyl-D-erythritol 2,4-cyclodiphosphate	<i>slr2136</i>	GcpE
7	1-hydroxy-2-methyl-2-butenyl 4-diphosphate	<i>slr0348</i>	IspH
8	isopentenyl diphosphate and dimethylallyl diphosphate	<i>sll1556</i>	Ipi
9	dimethylallyl diphosphate	<i>slr0739</i>	CrtE
	geranylgeranyl diphosphate		

Table I-2: Intermediates of the carotenoid biosynthesis pathway in *Synechocystis*. Colors of carotenoids are indicated as an approximation of their natural coloration.

Step	Substrate(s)	λ_{\max} (nm)	ORF	Gene
1	geranylgeranyl diphosphate 	n/a	<i>slr1255</i>	CrtB
2	phytoene 	276, 286, 297 ^{1,2}	<i>slr1254</i>	CrtP
3	9,15,9'-tri- <i>cis</i> - ζ -carotene 	(296,) 377, 399, 424 ⁴	<i>slr1599</i>	n/a
4	ζ -carotene 	378, 400, 425 ^{1,2}	<i>slr0940</i>	CrtQ
5	prolycopene 	414, 436, 463 ^{1,2}	<i>sll0033</i>	CrtH
6	lycopene 	444, 470, 502 ^{1,3}		

⁽¹⁾ data from Britton *et al.*, 2004

⁽²⁾ in hexane

⁽³⁾ in petroleum

⁽⁴⁾ data from Breitenbach and Sandmann, 2005

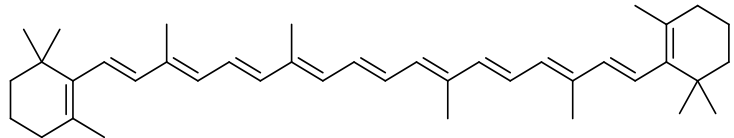
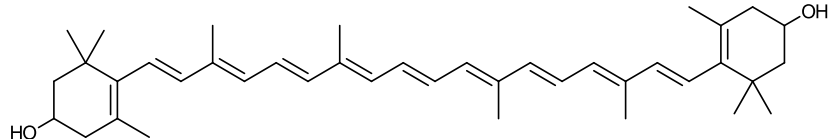
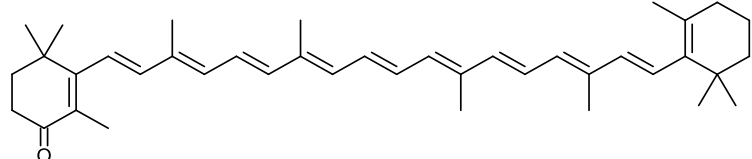
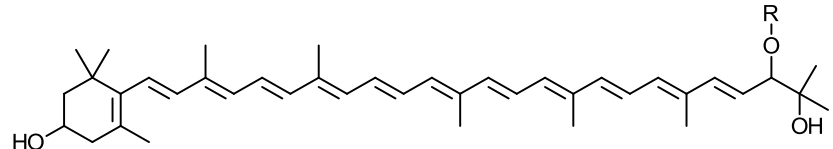
Depending on the position of the ring double-bond and the specificity of the cyclase, β - (C-5,6), ϵ - (C-4,5) or γ - (C-5,18) rings are formed. *Synechocystis* exclusively produces carotenoids with rings of the β -type and the corresponding β -cyclase is presumed to be Sll0147 (Maresca *et al.*, 2007). β -carotene (Table I-3) is formed by the symmetric di-cyclization of all-*trans*-lycopene.

Additional modifications involving the incorporation of oxygen atoms into the carotenoid structure produce xanthophylls, for instance, by hydroxylation, ketolation or epoxidation. In fact, the vast majority of naturally occurring carotenoids are xanthophylls and, except for β -carotene, all carotenoids of *Synechocystis* are xanthophylls: Echinenone

(Table I-3), a carotenoid predominantly found in the CM and as a structural component of the cytochrome *b₆f* complex (Boronowsky *et al.*, 2001; this work) is identical to β -carotene except for a single ring-keto group at position C-4, which is introduced by the asymmetrically acting ring-ketolase Slr0088 (Fernandez-Gonzalez *et al.*, 1997).

Zeaxanthin (Table I-3) is produced by hydroxylation of both β -ionone rings of β -carotene via β -cryptoxanthin (the mono-hydroxylated carotenoid intermediate), a reaction that is catalyzed by the β -carotene hydroxylase Sll1468 (Masamoto *et al.*, 1998). In plants and algae zeaxanthin plays an important role in quenching of reactive oxygen species (ROS) in the TM where it is part of the xanthophyll cycle (Jahns *et al.*, 2009). Although cyanobacteria do not have a xanthophyll cycle, zeaxanthin is abundant in the TM of *Synechocystis* as well (this work).

Table I-3: The four major carotenoids in *Synechocystis*.

Carotenoid	λ_{\max} (nm) ¹
<p>β-carotene</p> 	425, 450, 477 (in hexane)
<p>Zeaxanthin</p> 	428, 450, 478 (in petroleum)
<p>Echinenone</p> 	458 (in petroleum)
<p>Myxoxanthophyll</p> 	446, 472, 502 (in acetone)

⁽¹⁾ data from Britton *et al.*, 2004

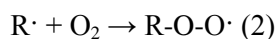
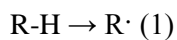
Glycosylated carotenoids are very common in cyanobacteria. The biosynthesis route for myxoxanthophyll (Table I-3) in cyanobacteria has not been identified in full detail, but it differs significantly from all other carotenoids as myxoxanthophyll is a monocyclic xanthophyll glycoside. In *Synechocystis* Sll0254 has been proposed as the monocyclassase responsible for the formation of a β - ψ -type carotene, the un-glycosylated backbone for myxoxanthophyll (Mohamed and Vermaas, 2006). Furthermore, a specific C-3',4' desaturase is required to extend the system of conjugated double bonds to twelve (Mohamed and Vermaas, 2004) in addition to hydroxylations at the C-1' and C-2' positions. The sugar moiety of myxoxanthophyll, which is O-linked to the hydroxyl-group at C-2', is strain dependent, and represents a di-methyl fucoside in *Synechocystis*. Of the four major carotenoids in *Synechocystis* myxoxanthophyll is probably the most

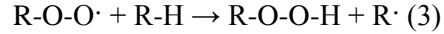
potent photoprotectant (Steiger *et al.*, 1999). Mohamed *et al.* (2006) have also shown the importance of this pigment in maintaining thylakoid organization and cell wall structure.

The functions of carotenoids in protein- and membrane stabilization, as well as in photoprotection

Because of the lipophilic nature of most carotenoids, they are located in similarly lipophilic environments, i.e. the lipid moieties of lipid bilayers and in proteins. In membranes carotenoids assume a specific orientation based on the presence (if any) of functional groups. For example, zeaxanthin (Table I-3) is inserted into the monolayer of a bilayer perpendicularly to the membrane plane, with its hydroxyl-groups facing both the hydrophilic surface and the membrane core. On the other hand, while β -carotene (Table I-3) is distributed exclusively in the lipid moieties of membranes its orientation is less restricted (Jürgens and Mäntele, 1991). Both carotenoids have important effects on membrane fluidity: The rigid polyene chain of zeaxanthin lowers membrane fluidity, while β -carotene disturbs the lipid tails and thus antagonizes zeaxanthin.

Carotenoids are potent quenchers of ROS. The formation of peroxy radicals occurs at unsaturated bonds in membranes and is particularly dangerous as it could result in a radical chain reaction leading to an accumulation of lipid peroxides. Di-oxygen plays a key-role in the propagation of peroxy radicals (Guo *et al.*, 2009). Initially, a radical starter forms a lipid radical by abstraction of hydrogen (eq. 1, where R is the lipid carbon chain). Under the presence of di-oxygen a peroxy radical is created (eq. 2) which, in turn, abstracts hydrogen from a neighboring lipid moiety. In this reaction sequence the lipid is oxidized to an (unstable) lipid peroxide and another lipid radical is created (eq. 3).





The antioxidative properties of carotenoids allow a variety of chemical reactions with radical species to stop the propagation thereof, and form a generally less reactive compound. Such reactions are oxidation, reduction, addition and hydrogen abstraction (Britton, 1995), which involve unpaired-electron transfers from or to the carotenoid. Usually, the resulting carotenoid radical is significantly less reactive due to its system of de-localized π -electrons. In the previous example hydrogen abstraction from a carotenoid molecule would work as indicated in eq. 4:



Carotenoids can also have protective functions in proteins where ROS such as chlorophyll triplets ($^3\text{Chl}^*$) or oxygen singlets ($^1\text{O}_2$) are frequently formed, e.g., in PS II or LHCs. Although singlet oxygen cannot be produced by optical excitation, triplet-to-triplet energy transfer can occur from $^3\text{Chl}^*$ to $^3\text{O}_2$, resulting in the highly reactive singlet oxygen. This compound can diffuse hundreds of nanometers prior to a decay back to the ground state (Triantaphylidès and Havaux, 2009). Carotenoids can quench both of these ROS because of their lower energy triplet state, however, this happens by means of Dexter electron transfer and thus requires a wavefunction overlap between donor and acceptor molecules. The carotenoid then undergoes internal conversion and dissipates the energy non-radiatively by heat emission.

Questions addressed in this work

The chapters three to five of this work deal with various aspects of carotenoid metabolism in *Synechocystis*. The functions of several genes presumed to be important in the biosynthesis and turnover of these pigments, as well as their contribution to the cell wall stability was studied by the construction and analysis of mutants lacking single and

multiple of these genes. Based in on the previous characterization of a myxoxanthophyll-deficient strain ($\Delta sll1213$) (Mohamed *et al.*, 2005) that was shedding large amounts of protein into the growth medium, the surface (S-)layer protein of *Synechocystis* was identified. Absence of myxoxanthophyll resulted in a disrupted thylakoid organization and a markedly altered cell wall structure, accompanied by the loss of the S-layer in the deletion strain. In this work it was assessed whether the S-layer is required to maintain the wild-type carotenoid profile. Additional tests were performed on the S-layer deletion mutant to elucidate the function of the *Synechocystis* S-layer protein.

In chapter four of this work the role of a cyanobacterial ORF (*slr0941*), whose position on the genome immediately downstream of the ζ -carotene desaturase gene is highly conserved in many cyanobacteria, was probed for a possible contribution to carotenoid metabolism. Profiles and localization of carotenoid in the membranes of the resulting deletion mutant were studied by preparative and analytical HPLC.

Very little is known about the turnover or the breakdown of damaged carotenoids in prokaryotes. Animals and plants possess a variety of carotenoid cleavage enzymes (von Lintig *et al.*, 2001; Schwartz *et al.*, 1997). In eukaryotes, the products created by these enzymes are present in photoreceptors such as rhodopsin, or are precursors of plant hormones such as abscisic acid. Similar carotenoid processing enzymes have been discovered recently in cyanobacteria. Ruch *et al.* (2005) have identified and biochemically characterized enzymes in *Synechocystis* that are capable of cleaving carotenoids with a shortened polyene chain. The fifth chapter of this work deals with the *in vivo* characterization of deletion mutants lacking these putative cyanobacterial carotenoid cleavage dioxygenases.

References

- Amunts, A., Drory O., and Nelson N. (2007) The structure of a plant photosystem I supercomplex at 3.4 Å resolution. *Nature* **447**: 58-63.
- Bautista, J.A., Rappaport F., Guergova-Kuras M., Cohen R.O., Golbeck J.H., Wang J.Y., *et al.* (2005) Biochemical and biophysical characterization of photosystem I from phytoene desaturase and zeta-carotene desaturase deletion mutants of *Synechocystis* sp. PCC 6803: evidence for PsaA- and PsaB-side electron transport in cyanobacteria. *J Biol Chem* **280**: 20030-20041.
- Ben-Shem, A., Frolow F., and Nelson, N. (2003) The crystal structure of plant photosystem I. *Nature* **426**: 630-635.
- Boronowsky, U., Wenk S.O., Schneider D., Jäger C., and Rögner M. (2001) Isolation of membrane protein subunits in their native state: evidence for selective binding of chlorophyll and carotenoid to the b_6 subunit of the cytochrome b_6/f complex. *Biochim Biophys Acta* **1506**: 55-66.
- Breitenbach, J., and Sandmann G. (2005) ζ -carotene cis isomers as products and substrates in the plant poly-cis carotenoid biosynthetic pathway to lycopene. *Planta* **220**: 785-793.
- Britton, G., Liaaen-Jensen S., and Pfander H. (2004) Carotenoids Handbook. Birkhäuser Verlag, Basel/Boston/Berlin.
- Britton, G. (1995) Structure and properties of carotenoids in relation to function. *FASEB J* **9**: 1551-1558
- Bryant, D.A. (1994) The Molecular Biology of Cyanobacteria. Kluwer Academic Press, Dordrecht.
- Cogdell, R.J., Isaacs N.W., Howard T.D., McLuskey K., Fraser N., and Prince S.M. (1999) How photosynthetic bacteria harvest solar energy. *J Bacteriol* **181**: 3869-3879.
- Edge, R., McGarvey D.J., and Truscott T.G. (1997) The carotenoids as anti-oxidants - a review. *J Photochem Photobiol B* **41**:189-200.
- Fernandez-Gonzalez, B., Sandmann G., and Vioque A. (1997) A new type of asymmetrically acting beta-carotene ketolase is required for the synthesis of echinenone in the cyanobacterium *Synechocystis* sp. PCC 6803. *J Biol Chem* **272**: 9728-9733.
- Glazer, A.N., Chan C., Williams R.C., Yeh S.W., and Clark J.H. (1985a) Kinetics of energy flow in the phycobilisome core. *Science* **230**: 1051-1053.
- Glazer, A.N., Yeh S.W., Webb S.P., and Clark J.H. (1985b) Disk-to-disk transfer as the rate-limiting step for energy flow in phycobilisomes. *Science* **227**: 419-423.

- Grossman, A.R., Schaefer M.R., Chiang G.G., and Collier J.L. (1993) The phycobilisome, a light-harvesting complex responsive to environmental conditions. *Microbiol Rev* **57**:725-749.
- Guo, J., Hsieh H., and Hu C. (2009) Chain-breaking activity of carotenes in lipid peroxidation: A theoretical study. *J Phys Chem B* **113**: 15699-15708
- Guskov, A., Kern J., Gabdulkhakov A., Broser M., Zouni A., and Saenger W. (2009) Cyanobacterial photosystem II at 2.9 Å resolution and the role of quinones, lipids, channels and chloride. *Nat Struct Biol* **16**: 334-342.
- Hornero-Méndez, D., and Britton G. (2002) Involvement of NADPH in the cyclization reaction of carotenoid biosynthesis. *FEBS Lett* **515**: 133-136.
- Hunter, W.N. (2007) The non-mevalonate pathway of isoprenoid precursor biosynthesis. *J Biol Chem* **282**: 21573-21577.
- Jahns, P., Latowski D., and Strzalka K. (2009) Mechanism and regulation of the violaxanthin cycle: The role of antenna proteins and membrane lipids. *Biochim Biophys Acta* **1787**: 3-14.
- Jordan, P., Fromme P., Witt H.P., Klukas O., Saenger W., and Krauss N. (2001) Three-dimensional structure of cyanobacterial photosystem I at 2.5 Å resolution. *Nature* **411**: 909-917.
- Jürgens, U.W., and Mäntele W. (1991) Orientation of carotenoids in outer membrane of *Synechocystis* PCC 6714 (Cyanobacteria). *Biochim Biophys Acta* **1067**: 208-212.
- von Lintig, J., Dreher, A., Kiefer, C., Wernet, M.F., and Vogt, K. (2001) Analysis of the blind *Drosophila* mutant *ninaB* identifies the gene encoding the key enzyme for vitamin A formation in vivo. *Proc Natl Acad Sci USA* **98**: 1130-1135.
- Loll, B., Kern J., Saenger W., Zouni, A., and Biesiadka, J. (2005) Towards complete cofactor arrangement in the 3.0 Å resolution structure of photosystem II. *Nature* **438**: 1040-1044.
- MacColl, R. (1998) Cyanobacterial phycobilisomes. *J Struct Biol* **124**: 311-334.
- Maresca, J.A., Graham J.E., Wu M., Eisen J.A., and Bryant D.A. (2007) Identification of a fourth family of lycopene cyclases in photosynthetic bacteria. *Proc Natl Acad Sci USA* **104**: 11784-11789.
- Masamoto, K., Misawa N., Kaneko T., Kikuno R., and Toh H. (1998) Beta-carotene hydroxylase gene from the cyanobacterium *Synechocystis* sp. PCC6803. *Plant Cell Physiol* **39**: 560-564.
- Mohamed, H.E., and Vermaas W. (2004) Slr1293 in *Synechocystis* sp. strain PCC 6803 is the C-3',4' desaturase involved in myxoxanthophyll biosynthesis. *J Bacteriol* **186**: 5621-5628.

- Mohamed, H.E., van de Meene A.M.L., Roberson R.W., and Vermaas W.F.J. (2005) Myxoxanthophyll is required for normal cell wall structure and thylakoid organization in the cyanobacterium, *Synechocystis* sp strain PCC 6803. *J Bacteriol* **187**: 6883-6892.
- Mohamed, H.E., and Vermaas W.F.J. (2006) Sll0254 (CrtL(diox)) is a bifunctional lycopene cyclase/dioxygenase in cyanobacteria producing myxoxanthophyll. *J Bacteriol* **188**: 3337-3344.
- Ruch, S., Beyer P., Ernst H., and Al-Babili S. (2005) Retinal biosynthesis in Eubacteria: in vitro characterization of a novel carotenoid oxygenase from *Synechocystis* sp. PCC 6803. *Mol Microbiol* **55**:1015-1024.
- Schwartz, S.H., Tan, B.C., Gage, D.A., Zeevart, J.A., and McCarty, D.R. (1997) Specific oxidative cleavage of carotenoids by VP14 of maize. *Science* **276**: 1872-1874.
- Sozer, O., Komenda J., Ughy B., Domonkos I., Laczkó-Dobos H., Malec P. *et al.* (2010) Involvement of carotenoids in the synthesis and assembly of protein subunits of photosynthetic reaction centers of *Synechocystis* sp PCC 6803. *Plant Cell Physiol* **51**: 823-835.
- Steiger, S., Schäfer L., and Sandmann G. (1999) High-light-dependent upregulation of carotenoids and their antioxidative properties in the cyanobacterium *Synechocystis* PCC 6803. *J Photochem Photobiol* **52**: 14-18.
- Tanaka, R., and Tanaka A. (2007) Tetrapyrrole biosynthesis in higher plants. *Ann Rev Plant Biol* **58**: 321-346.
- Triantaphylidès, C., and Havaux M. (2009) Singlet oxygen in plants: production, detoxification and signaling. *Trends Plant Sci* **14**: 219-228.

CHAPTER II. METHODS - MOLECULAR BIOLOGY

Construction of mutant strains to analyze the function of Slr0941

In addition to an *slr0941* deletion strain (Δ *slr0941*) a series of other mutant strains were created to facilitate studying the function of the ORF that is located immediately downstream of the zeta-carotene desaturase gene (*slr0940*). A deletion strain expressing a kanamycin (Km) cassette in the opposite direction of *slr0941* (Δ *slr0941*) led to an *slr0940* knockdown phenotype and, unlike the mutant strain expressing this cassette in the *slr0941* direction (Δ *slr0941* v2), could not be fully segregated. The combined disruption of *slr0940* and *slr0941* in the strain Δ *slr094X*, however, could be segregated to homozygosity at high antibiotic concentration under low light intensity ($<0.5 \mu\text{mol photons m}^{-2} \text{s}^{-1}$). To examine a possible interaction between Slr0941 and other proteins, a strain encoding His-tagged *slr0941* was created (slr0941-His). After the discovery of the carotenoid phenotype of Δ *slr0941*, mutant strains were constructed with deletions of either the carotenoid isomerase (*sll0033*) only, or of both, *sll0033* and *slr0941* (Δ *sll0033*, and Δ *sll0033/\Delta*slr0941*), respectively, to allow for a comparison of the phenotypes of both deletion strains. Finally, to rescue (and thus confirm) the Δ *slr0941* carotenoid phenotype, a construct based on the slr0941-His plasmid with a spectinomycin (Sp) cassette swapped for the Km cassette was prepared.*

Δ *slr0941* v2:

First, a 838 bp PCR product encoding the whole *slr0941* ORF including flanking regions was created using the primers with engineered restriction sites (modified bases are *italicized*, restriction sites underlined, 5'-genomic position in parenthesis):

slr0941 FWD (*SacI*)

(2005908) 5'-CACCGGGCATGGAGCTCTTC-3'

and

slr0941 REV (*HindIII*)

(2006745) 5'-GAATCTCTGCAAGCTTTCTCCATCC-3'

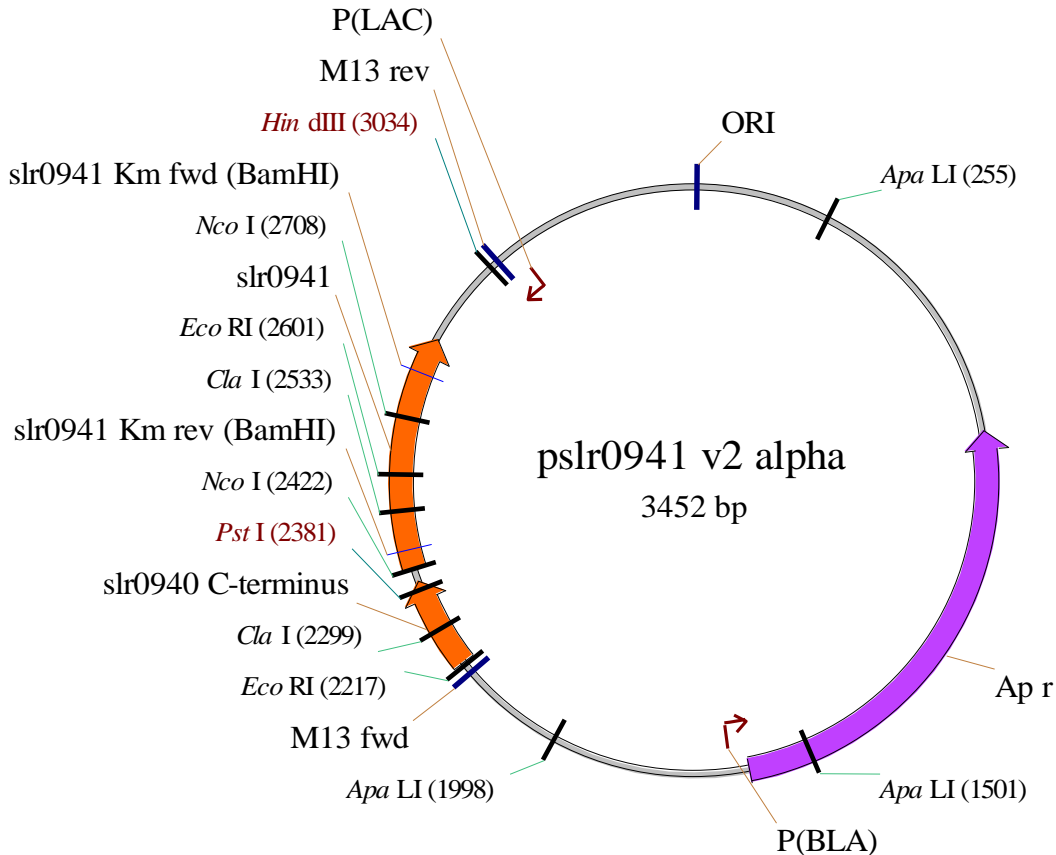


Fig. II-1: Schematic representation of plasmid pslr0941 v2 α , indicating positions and orientations of the cloned *slr0941* ORF and the ampicillin resistance gene (*Ap r*). Primer binding sites for the amplification of the plasmid including *slr0941* flanking regions are indicated (“slr0941 Km fwd/rev”). ORI – origin of plasmid replication. P(LAC) – lac operon promoter. P(BLA) – promoter of the β -lactamase (*Ap r*) gene. M13 fwd/rev – primer binding sites for M13 sequencing primers.

and then cloned into the corresponding pUC19 polylinker sites. This resulted in a disruption of pUC19's *lacZ* α gene, and transformants carrying the desired plasmid pslr0941 v2 α (Fig. II-1) were selected by screening for white colonies.

Next, a part of *pslr0941 v2 α* was amplified by PCR using primers with engineered *Bam*HI restriction sites:

*slr0941Km FWD (Bam*HI)

5'-GGTGGGATCCACTATTCAAGCTG-3'

and

*slr0941Km REV (Bam*HI)

5'-CAATTCGATGGGGGGATCC-3'

76.5% (340 bp) of the *slr0941* coding sequence was not amplified in this procedure. The PCR product included 245 bp upstream (plus 39 bp of the *slr0941* 5'-end) and 232 bp downstream (plus 65 bp of the *slr0941* 3'-end), respectively. The 3135-bp PCR product was cut with *Bam*HI. A Km resistance cassette was cut with *Bam*HI from the donor plasmid pUC4K and then ligated to the PCR product from *pslr0941 v2 α*. Correct *pslr0941 v2* (Fig. II-2) target clones were selected by screening for colonies that were resistant to both kanamycin and ampicillin, as well as restriction analysis. *pslr0941 v2* was checked for the presence of any point mutations by sequencing the subcloned *Synechocystis* locus on both ends in both directions, and no mutations could be detected.

Δ *slr094X*:

A 2905 bp PCR product comprising *slr0940* and *slr0941* ORFs was created with the following engineered primers:

*slr094X FWD (Ehe*I)

(2004221) 5'-GACACCACTGGCGCCTCA-3'

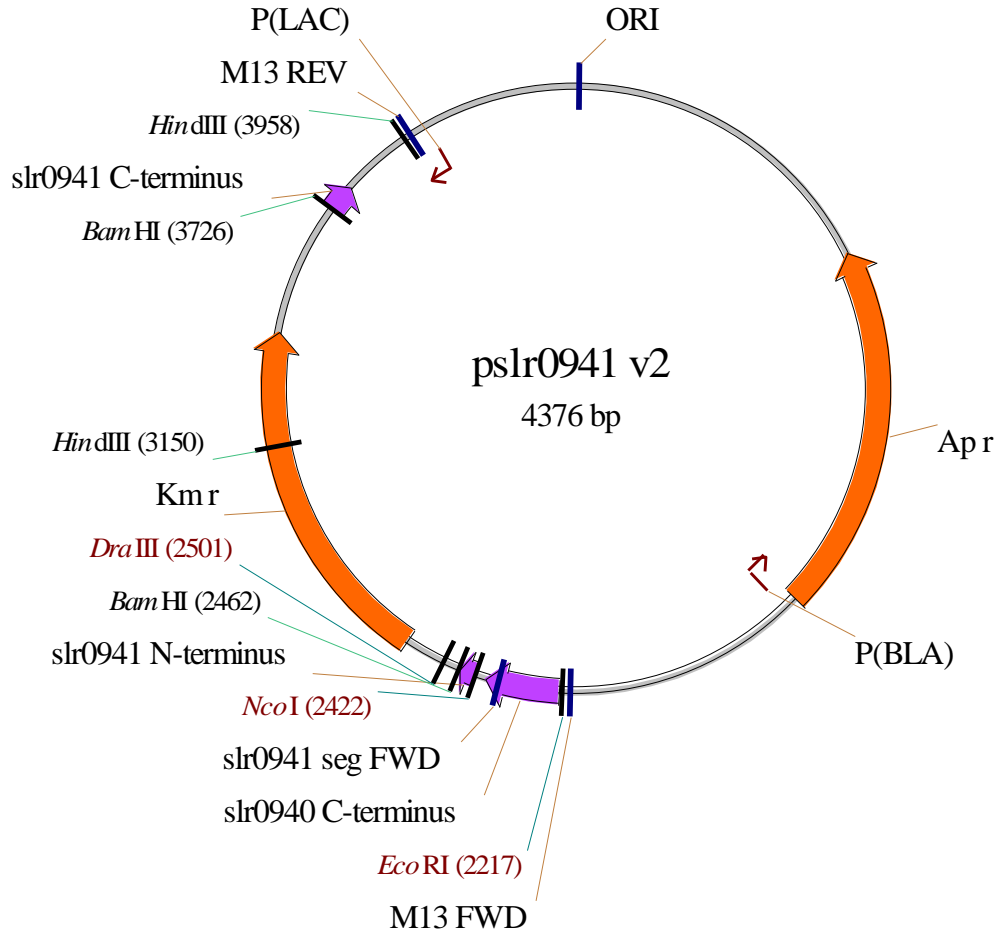


Fig. II-2: Schematic representation of plasmid pslr0941 v2, indicating positions and orientations of the interrupted *slr0941* ORF, as well as kanamycin (Km r)- and ampicillin (Ap r) resistance genes.

and

slr094X REV

5'-ACGCGGTTTTACCTGCTCTC-3' (2007126)

This PCR product was cut with *EheI* and *HindIII* (genomic position 2006948) and cloned into pUC19, resulting in complete removal of the polylinker and most of the *lacZ* gene.

The length of the constructed plasmid pslr0940/0941 α (Fig. II-3) was 5192 bp.

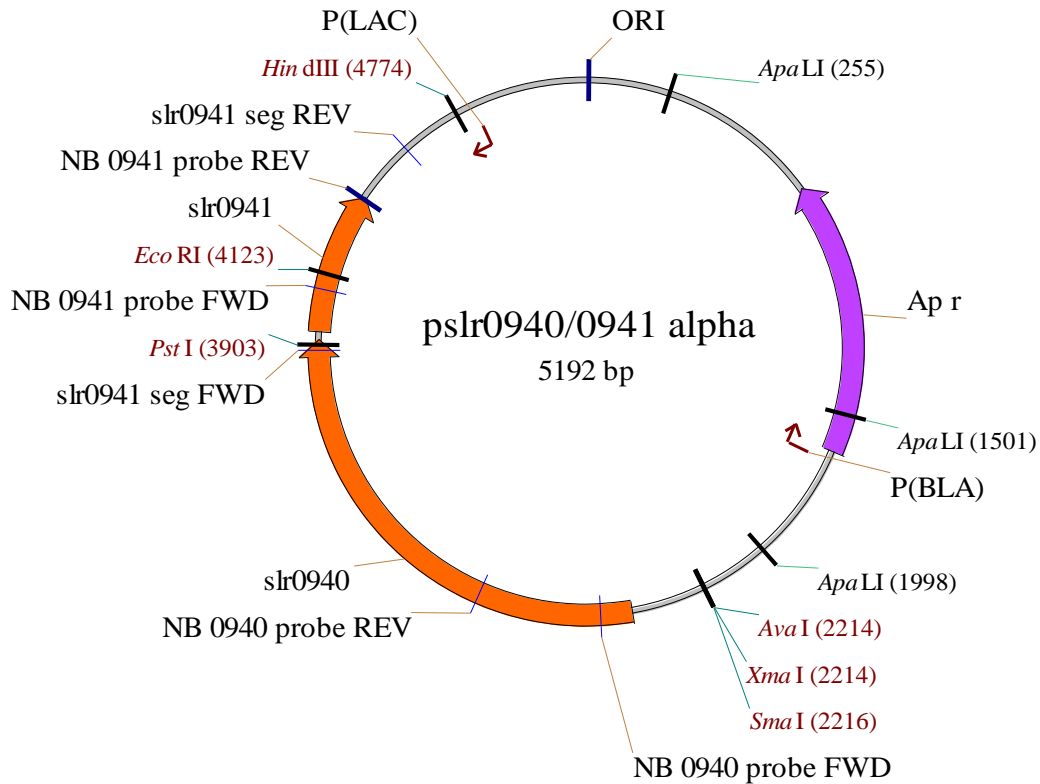


Fig. II-3: Map of the plasmid pslr0940/0941 showing positions and orientations of the subcloned ORF *slr0940* and *slr0941* as well as the ampicillin resistance gene (*Ap r*). Primer binding sites for Northern blot probes are indicated as “NB 0941 probe FWD” and “NB 0941 probe REV”, as they also are for *slr0940*. Primer binding sites to check for complete segregation are indicated as “slr0941 seg FWD” and “slr0941 seg REV”.

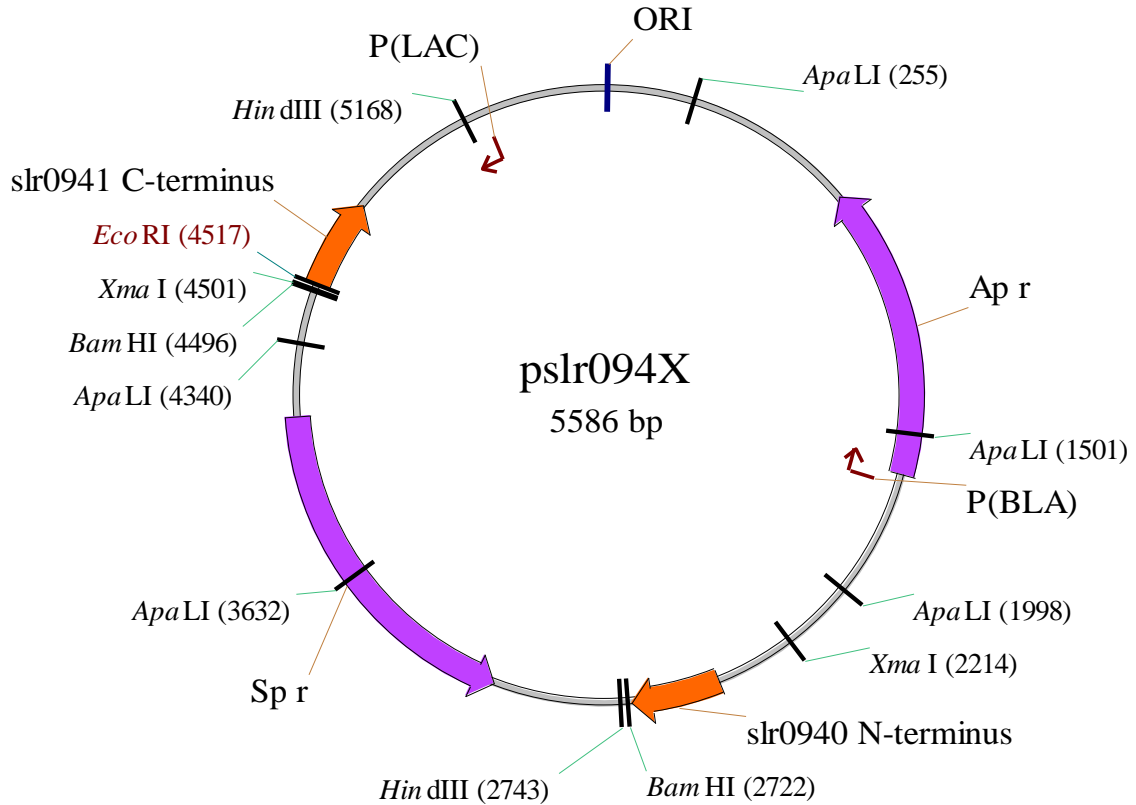


Fig. II-4: Schematic representation of the plasmid pslr094X, a derivative of pslr0940/0941 α for the deletion of the *slr0940/sl0941* locus. The ORFs of both genes were interrupted with a spectinomycin resistance cassette (Sp r) in antisense orientation.

This plasmid was cut with *HincII* and *EcoRI*, resulting in the removal of 1411 bp (>82%) of *slr0940* and 180 bp (>40%) of *slr0941* intragenic regions. A spectinomycin resistance cassette from pSpec was cut with the same enzymes and the obtained 1809 bp fragment was cloned into pslr0940/0941 α , creating the 5586 bp deletion construct pslr094X (Fig. II-4).

Primers for segregation check:

094X seg FWD

(2004854) 5'-CTACGGCTCAAGGAACATACC-3'

094X seg REV

(2006326) 5'-CTTAGTAATCCGGGACAACC-3'

slr0941 His:

Based on pslr0941 v2 α , primers were designed to amplify the subcloned *slr0941* locus for HIS-tagging.

slr0941 His FWD

5'-GTTGTT GGATCC TGCGCTGAATAGTAGAACTAAGGCTAATGG-3'

*Bam*HI *slr0941* downstream region, part of pslr0941v2 α

and

slr0941 His REV

5'-GTTGTT GGATCC TCATCA ATGATGATGATGATGATG ...

*Bam*HI STOP His-tag

... GGAAGCCTGCAAATTATTGATATATTCCC-3'

slr0941 native 3'-end, part of pslr0941v2 α

PCR using these primers on pslr0941 α as template produced a 3489 bp fragment carrying *Bam*HI sites on both ends for subcloning a Km- (or a Sp-) resistance cassette. The region downstream of the final construct pslr0941 His (Fig. II-5) has 164 bp complementary to the *Synechocystis* wild-type locus, whereas the upstream region retains a 647 bp complementary to the wild type locus comprising *slr0941* and the 3'-end of *slr0940*. A Km cassette from pUC4K was ligated to the *Bam*HI sites of the PCR product.

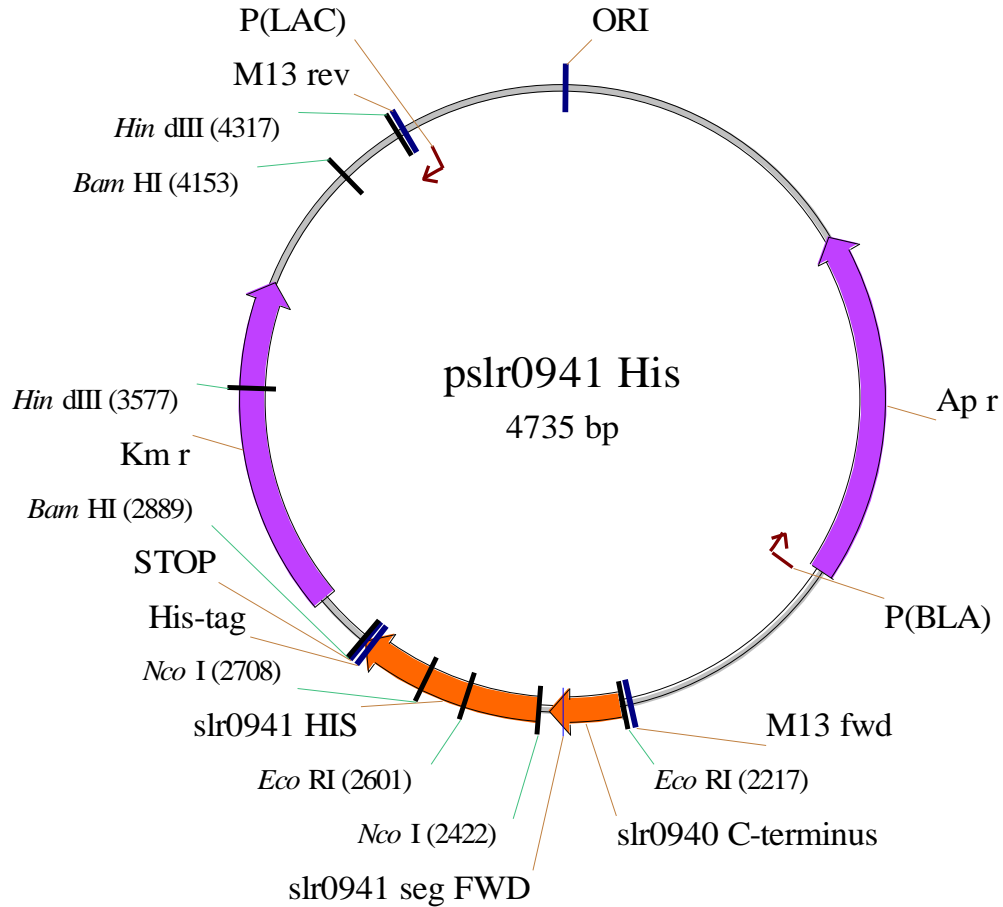


Fig. II-5: Map of pslr0941 His, a plasmid derived from pslr0941 α for purification of the Slr0941 protein and assessment of possible protein/protein interaction. Position of the His-tag followed by the engineered stop codon is indicated.

Although pslr0941 His plasmids with the Km cassette of both orientations were isolated, only the one facing downstream of the *slr0941* ORF was transformed into the *Synechocystis* wild-type strain to avoid a potential transcriptional repression of *slr0941*.

To rescue the carotenoid phenotype of the Δ *slr0941* deletion strain, a plasmid based on pslr0941 His was constructed: pslr0941 His Sp (Fig. II-6). In this vector the Km resistance cassette was replaced by a spectinomycin resistance cassette.

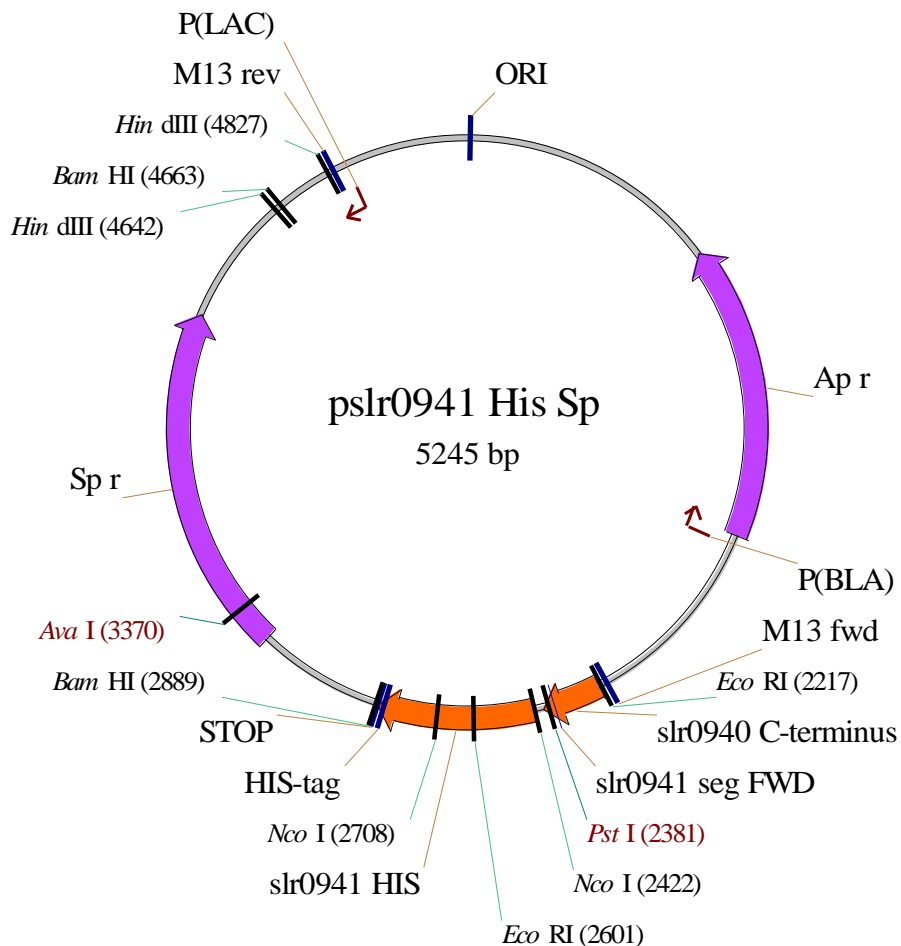


Fig. II-6: Map of pslr0941 His Sp, a plasmid identical to pslr0941 His encoding spectinomycin resistance (Sp r) instead of kanamycin resistance. This plasmid was used to rescue the $\Delta slr0941$ mutant strain.

$\Delta sll0033$:

First, a 2263 bp PCR product consisting of the *sll0033* ORF and its flanking regions was created using the following engineered primers:

sll0033 FWD (*EcoRI*)

(3164562) 5'-GCTAGACAGCAGAATTCCTTGCC-3'

and

sll0033 REV (*SphI*)

(3162300) 5'-CCTTGGCATGCCGTTGCA-3'

This PCR product was cut with *EcoRI* and *SphI*, and cloned into the polylinker of pUC19 at these sites, disrupting the *lacZ* α gene of the receiving vector. A blue/white screen was performed and white colonies were selected. The constructed plasmid psl10033 α (Fig. II-7) contained three *BstEII* restriction sites, all of which were located in the *sl10033* coding region.

To create the *sl10033* deletion plasmid, psl10033 α was cut with *BstEII* and a chloramphenicol resistance cassette from pCh1 that had been created by PCR was inserted into the vector fragment. The PCR product carrying the Chloramphenicol Acetyl-Transferase (CAT) gene was amplified using the following pair of engineered primers:

pCh1 FWD (*BstEII*)

5'-GACAGGTCACCCGACTGG-3'

and

pCh1 REV (*BstEII*)

5'-GTTGGGTAACCCAGGGTTTT-3'

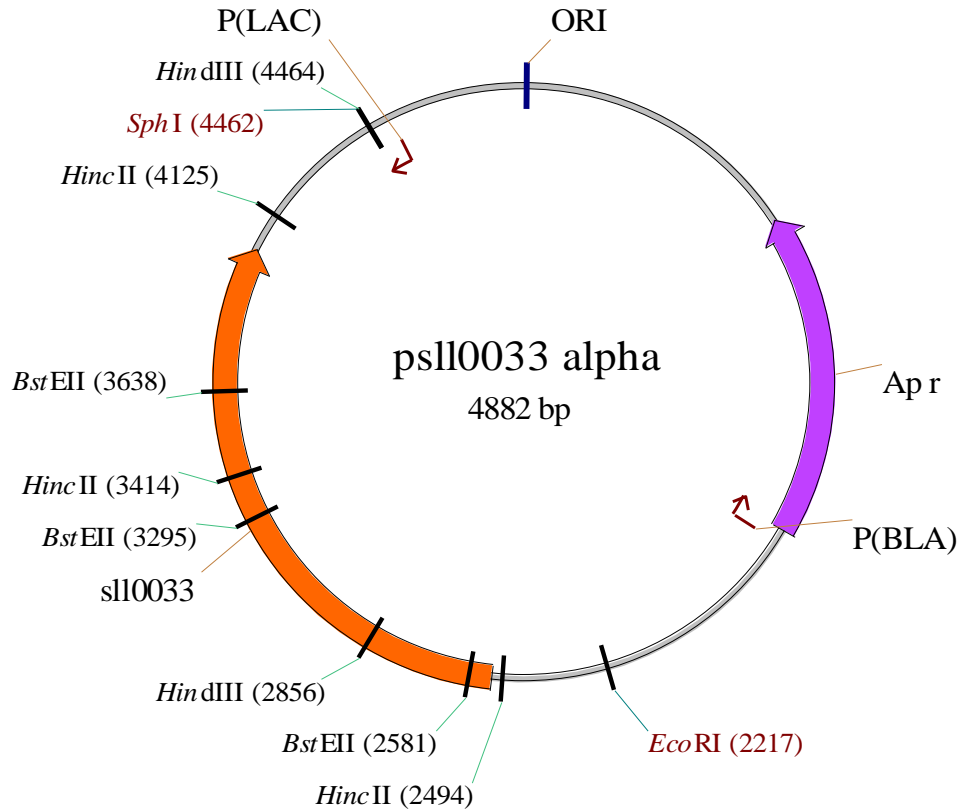


Fig. II-7: Map of *psII0033 alpha* encoding the *Synechocystis* prolycopene isomerase SII0033. After cutting the PCR product with *BstEII* it was inserted into the corresponding restriction sites at the *psII0033 alpha* positions 3002 and 4059, as confirmed by sequencing, resulting in the replacement of 1057 bp (~70.5 %) of the *sII0033* coding region (Fig. II-8).

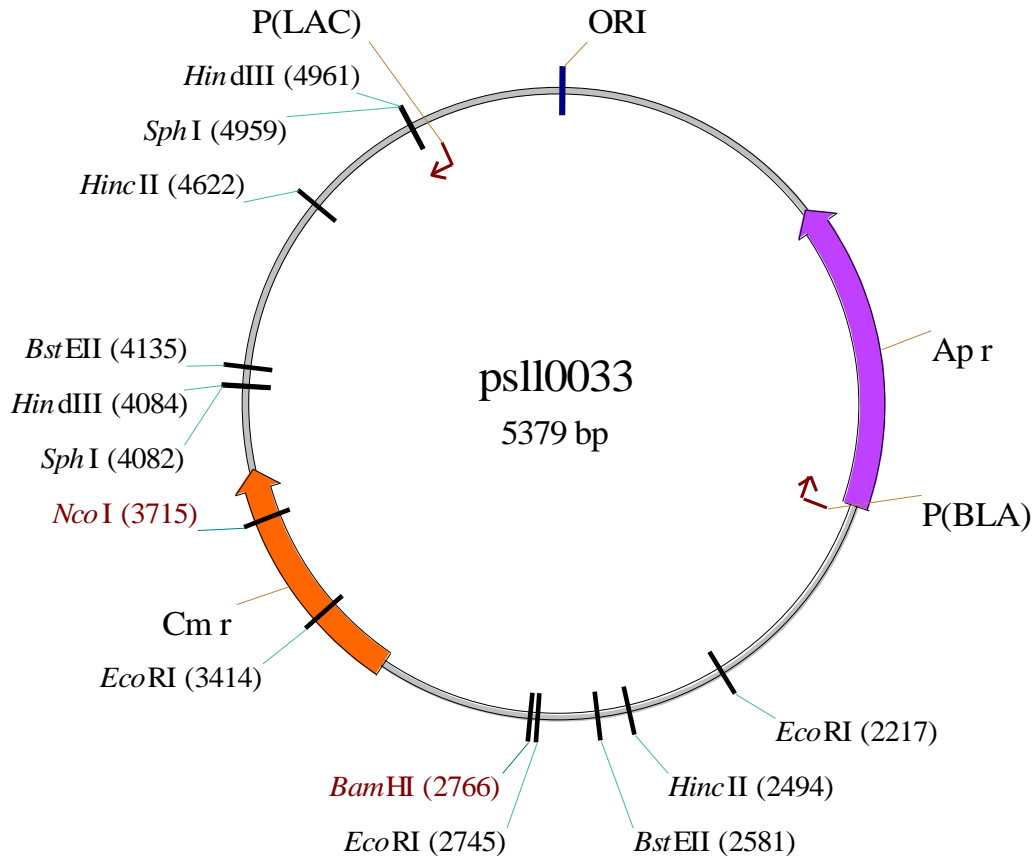


Fig. II-8: Schematic representation of psl10033, the plasmid that was used to disrupt the polycopene isomerase of *Synechocystis*. Positions of resistance genes are indicated for chloramphenicol (Cm r) and ampicillin (Ap r).

Construction of dioxygenase deletion strains

Δsll1541:

A 2416 bp PCR fragment of the native *sll1541* locus of *Synechocystis* was created with the following primers:

sll1541 FWD (*Hind*III)

(2032930) 5'-CCACCGGATCAAAGCTTTGTGCATC-3'

and

sll1541 REV (*Sac*I)

(2030514) 5'-CAGTGGACTGGTGAGCTCTTATGGA-3'

This fragment was digested with *Hind*III and *Sac*I, then cloned into the corresponding polylinker sites of pUC19, thus disrupting the *lacZ* gene of this vector. A blue/white colony screen was performed to identify target clones carrying the *sll1541* locus (psll1541 α , Fig. II-9). A 3648 bp part from psll1541 α containing the *sll1541* flanking regions as well as the beta-lactamase gene was amplified by PCR using primers with engineered restriction sites:

sll1541 FL FWD (*Bam*HI)

5'-CCTGCACGGATCCTGGGC-3'

and

sll1541 FL REV (*Pst*I)

5'-CAGCCAATCCTGCAGACTGTAGG-3'

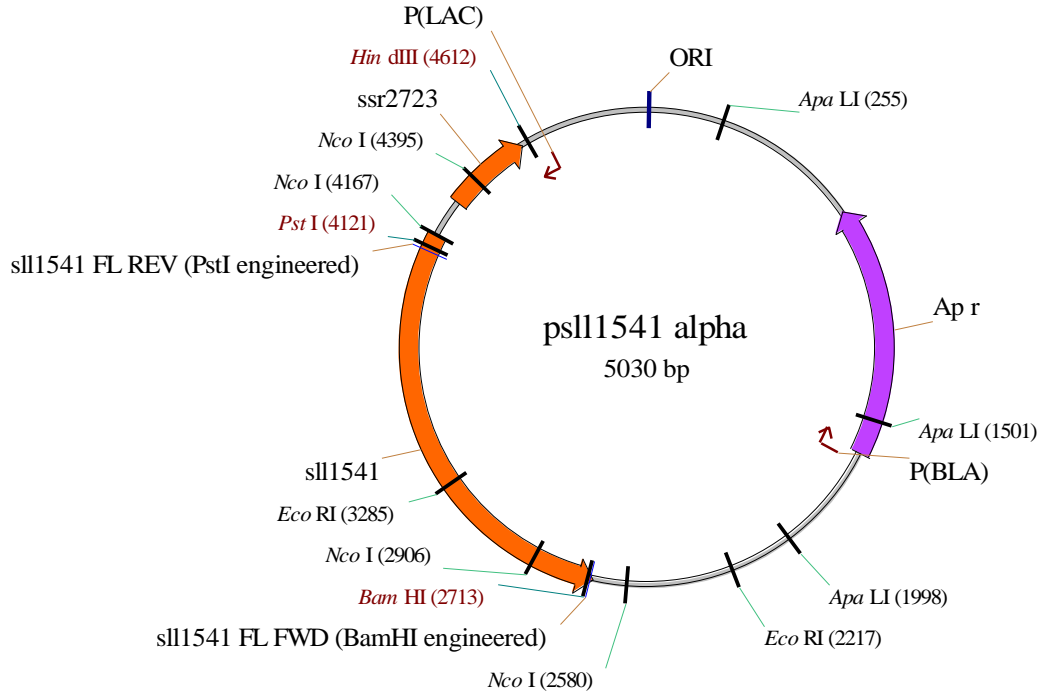


Fig. II-9: Map of the psl1541 α carrying the putative apo-carotenoid dioxygenase gene *sll1541*. Primer binding sites with engineered restriction sites to amplify the *sll1541* flanking regions are indicated (“sll1541 FL FWD/REV”).

Additionally, the Km cassette from pUC4K was amplified by PCR using primers with engineered restriction sites. A *PstI* restriction site located downstream of pUC4K's Km resistance cassette site would have interfered with the cloning process and was therefore removed in the FWD primer.

Km FWD -*PstI* (*BamHI*)

5'-CCCGGATCCTTCGACTTGCAGGG-3'

BamHI Δ *PstI*

and

Km REV (*EcoRI*)

5'-CAGCTATGACCATGATTACGAATTCCCCG-3'

After restriction digest with *BamHI* and *PstI* both PCR products were ligated and the resulting deletion plasmid psl1541 (Fig. II-10) was used to transform the *Synechocystis*

wild-type strain. 95% of the coding region (1404 of 1473 bp) of the *sll1541* ORF are deleted in the $\Delta sll1541$ deletion construct, whereas 491 bp upstream as well as 486 bp downstream of the *sll1541* locus remain on *psll1541* for homologous recombination. Complete segregation of the $\Delta sll1541$ mutant was confirmed by PCR.

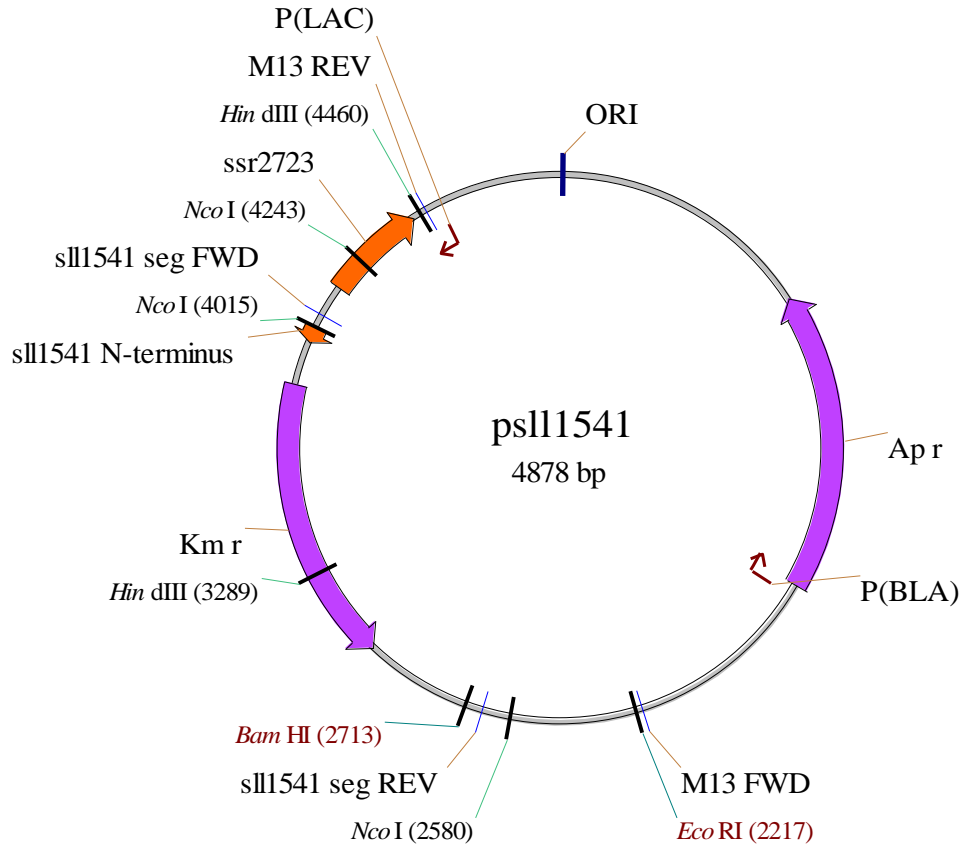


Fig. II-10: Map of the deletion vector *psll1541*. The native ORF was interrupted with a kanamycin resistance cassette (*Km r*) in sense of the gene. Positions of primer binding sites to check for complete segregation are indicated (“*sll1541 seg FWD/REV*”). The ORF upstream of *sll1541* is *ssr2723*.

$\Delta slr1648$:

To create the plasmid *pslr1648* α (Fig. II-11) a 2174 bp PCR fragment of the *Synechocystis* *slr1648* locus from position 2072812 to 2074986 was subcloned into the polylinker of *pUC19* at its sites *KpnI* and *HindIII*.

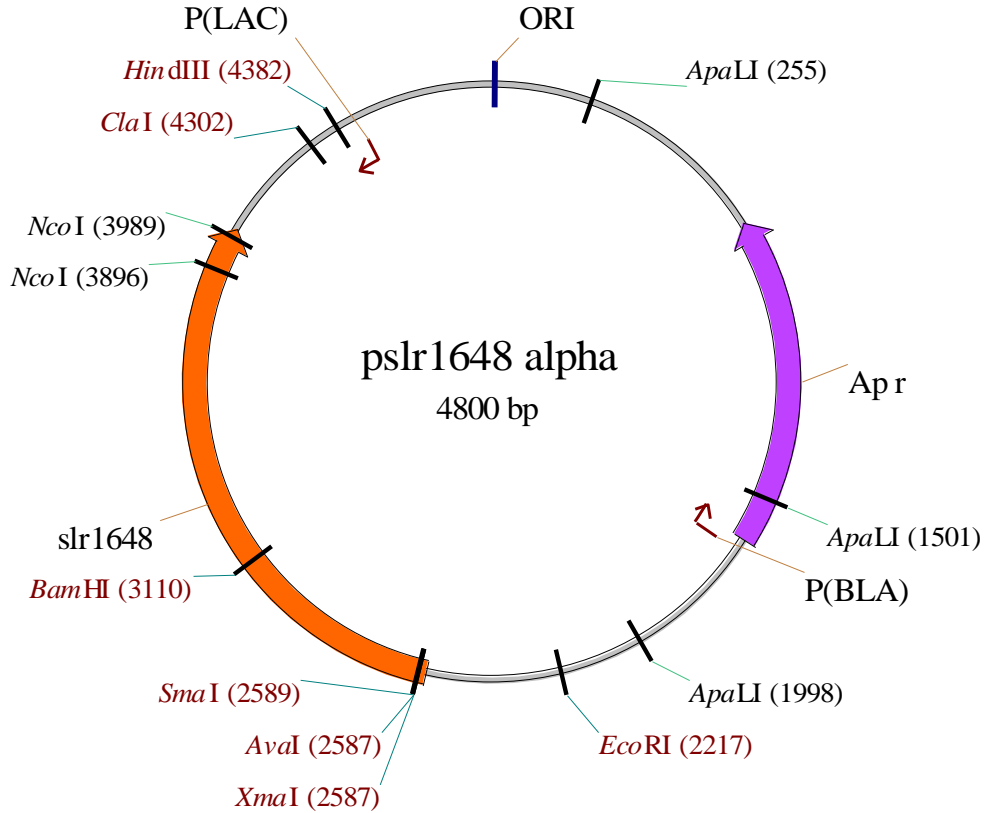


Fig. II-11: Map of the plasmid pslr1648 α , carrying the putative *Synechocystis* dioxygenase gene *slr1648*.

The native *Synechocystis* locus was amplified with the following primers:

slr1648 FWD (*KpnI*)

(2072812) 5'-CACCTTGGTACCATTGCAG-3'

and

slr1648 REV (*HindIII*)

(2074986) 5'-CATGCCAAGAAAGCTTGGTAAAG-3'

This procedure disrupted pUC19's *lacZ* α gene, and a blue/white screen was performed to identify target clones carrying the insert.

pslr1648 α was cut with *BamHI* and *PshAI*, and a spectinomycin resistance cassette from pSpec, cut with *BamHI* as well as *XmnI*, was inserted in the orientation opposite to the

disrupted ORF, resulting in the final $\Delta slr1648$ deletion vector pslr1648 (Fig. II-12). The flanking regions consisted of 878 bp (5'-*slr1648*) and 529 bp (*slr1648*-3'). In this construct, 750 bp of 1443 bp (~52 %) of the *slr1648* coding sequence were deleted. The segregation of the mutant was monitored by PCR using the following pair of primers:

slr1648 Sp seg FWD

(2072758) 5'-CCTCAATGCCTCGGTCTATC-3'

and

slr1648Sp REV

(2075074) 5'-CATCAAAAAGGATCCCTGGC-3'

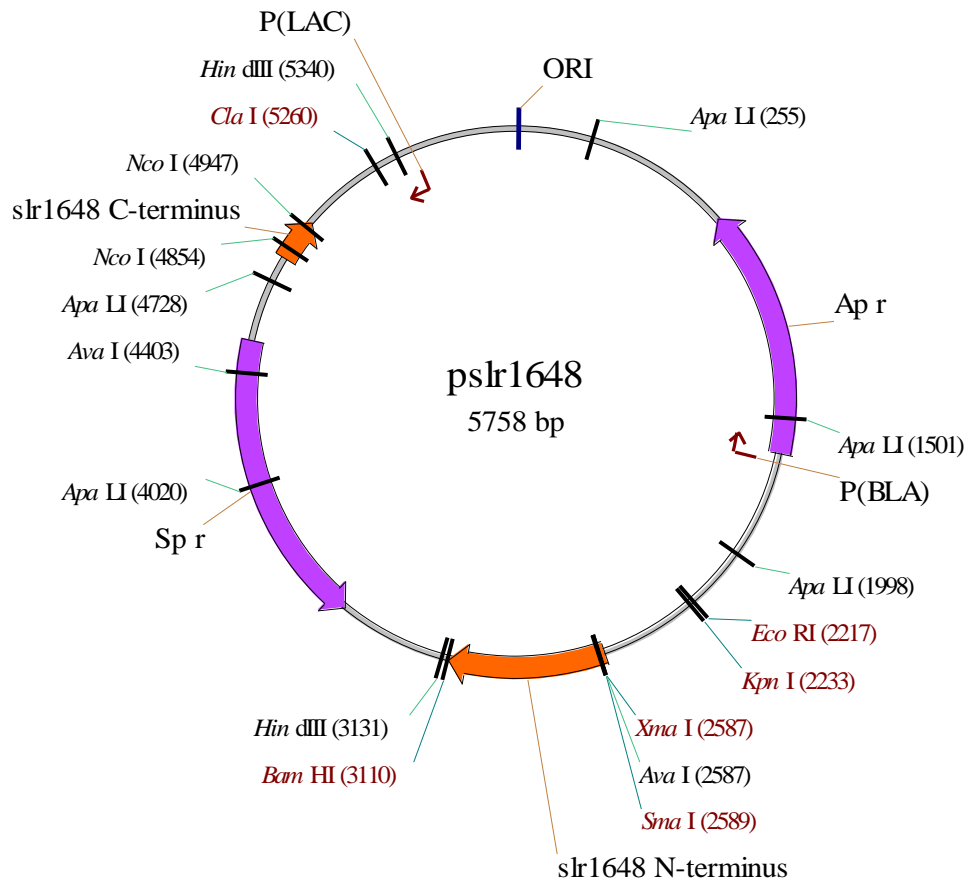


Fig. II-12: Map of the deletion vector pslr1648. The native *slr1648* was interrupted with a spectinomycin cassette in anti-sense orientation of the gene.

Construction of Sll1951 (S-layer)-deficient strains

A 398 bp upstream region including 50 bp of the *sll1951* ORF, as well as a 569 bp downstream region (1422150 – 1422716) including 293 bp of the *sll1951* ORF were amplified by PCR using the forward primer

5sll1951 FWD (*EagI*)

(1422142) 5'-GGAATCGGCCGGCTTTAGC-3' with an engineered *EagI* site, and the reverse primer

5sll1951 REV (*BamHI*)

(1422726) 5'-CGATCGGATCCTTAATGCCTCTGC-3'

with an engineered *BamHI* site for the downstream region, as well as a forward primer

3sll1951 FWD (*PstI*)

(1427588) 5'-CGGATACACCACTGCAGGTGTAC-3' with engineered *PstI*- and removed *EagI* sites, and the reverse primer

3sll1951 REV (*SalI*)

(1428019) 5'-GAAAGTAAGGGAGGTCGACAAAGGTG-3'

including an engineered *SalI* site for the upstream region.

The chloramphenicol resistance cassette of pChl (a derivative of pACYC184, Acc.# X06403) was amplified by PCR using primers to create termini complementary to both the 5'-region upstream and the 3'-region downstream of the previously created PCR products, as indicated in bold letters:

5'-**GATGTTATTAGCAGAGGCATTAAGGATCCTCTAGAGTCACTTCAC**-3' and

5'-**CTACAGATCATGTACACCTGCAGGTCGGCATTGAGAAGC**-3'.

In another PCR all three products were combined together resulting in a linear 2.3 kb deletion-fragment that was used to transform the *Synechocystis* wild-type strain.

For future reference, the deletion-fragment was also cloned into pBluescript II KS- (Acc.# X52329) at its polylinker sites *Sal*I and *Eag*I (Fig. II-13).

Δ *sll1951*:

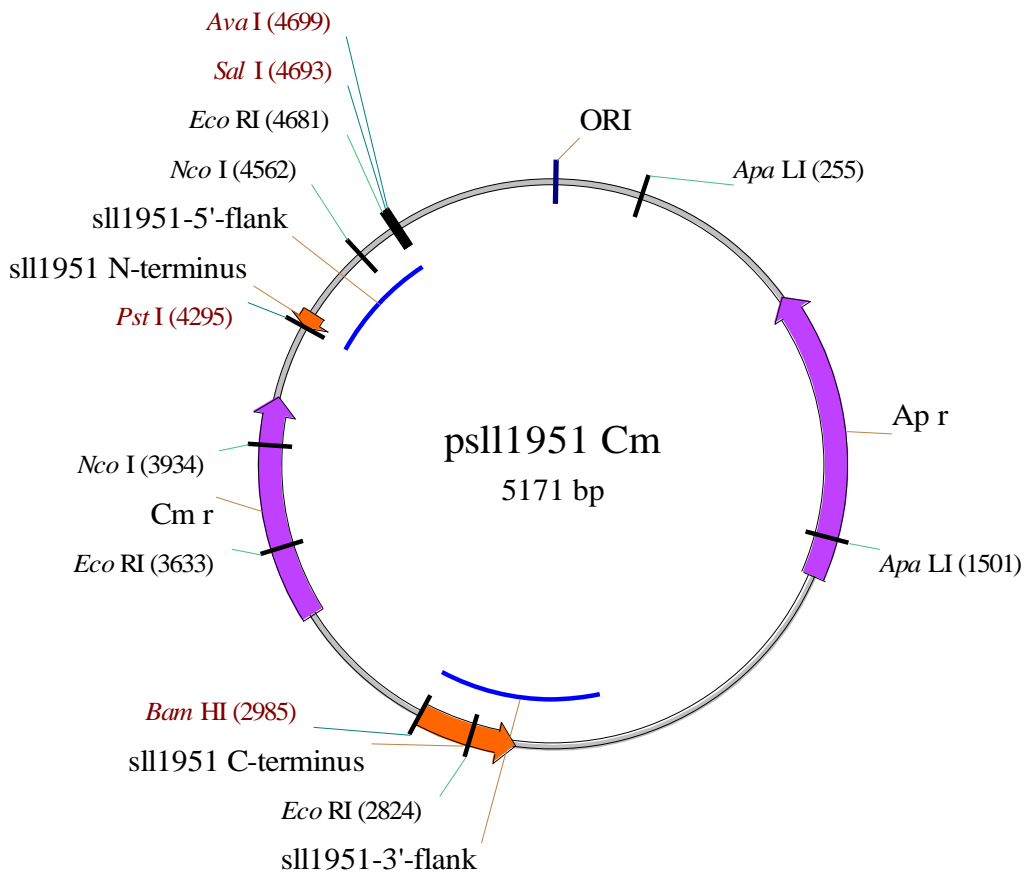


Fig. II-13: Map of psl11951 Cm, a derivative of pBluescript II KS- carrying a chloramphenicol resistance cassette (*Cm r*) flanked by sequences complementary to the 5'- and 3'-termini of *sll1951*, the S-layer gene of *Synechocystis*.

Since the created S-layer deficient strain was possibly amenable to facilitated secretion of lipids and/or fatty acids, an additional plasmid was constructed with a kanamycin

resistance cassette in place of the Cm resistance cassette for greater flexibility with antibiotic selection markers, psII1951 Km (Fig. II-14). The Km resistance cassette in this plasmid was amplified from pUC4K by PCR with primers previously used for the construction of psII1541:

Km FWD -*Pst*I (*Bam*HI)

5'-CCCGGATCCTTCGACTTGCAGGG-3'

*Bam*HI

Δ *Pst*I

and

Km REV (*Eco*RI)

5'-CAGCTATGACCATGATTACGAATTCCCCG-3'

Δ *sII1951* Km:

This deletion vector was used to transform the fatty acid producing strains TE/*ΔsIrl609* and TesA/*ΔsIrl609* (Fig. II-14).

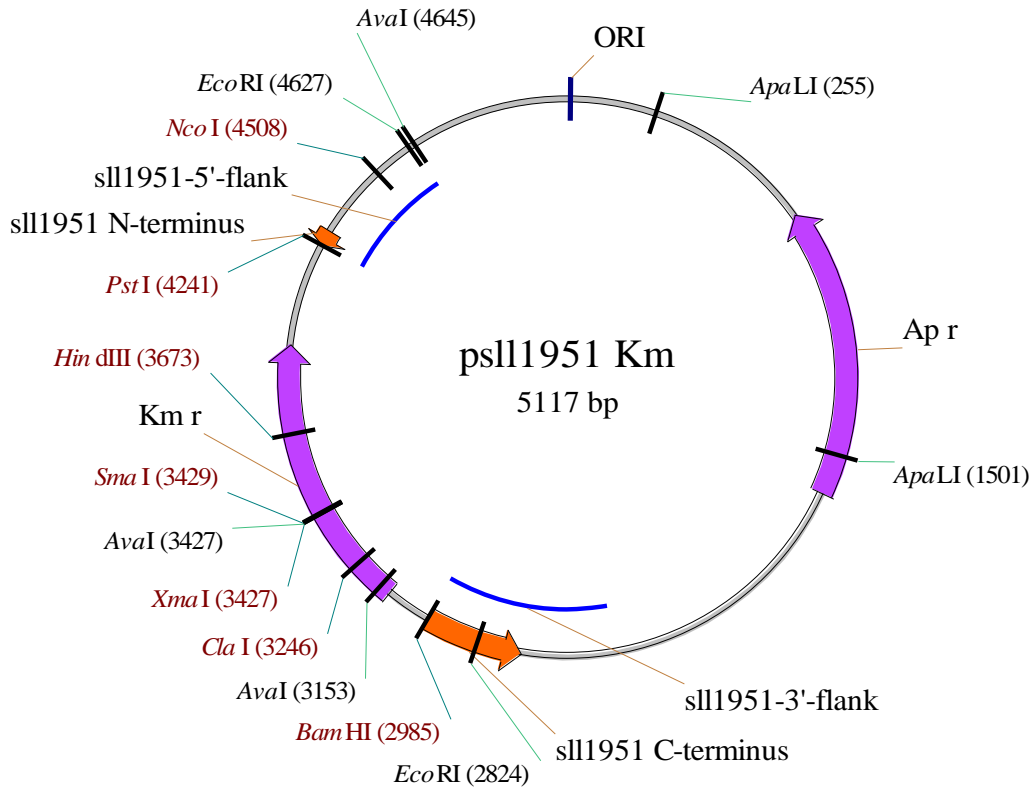


Fig. II-14: Map of psII1951 Km, the S-layer deletion vector to create the fatty acid producing strains TE/ Δ *slr1609*/ Δ *sII1951* and TesA/ Δ *slr1609*/ Δ *sII1951*. This plasmid is identical to psII1951 except for the kanamycin resistance cassette (Km r) replacing the chloramphenicol resistance cassette.

CHAPTER III. SLL1951 ENCODES THE S-LAYER PROTEIN OF *SYNECHOCYSTIS*

Abstract

Potential surface layer (S-layer) candidate open reading frames (ORFs) in the *Synechocystis* genome were examined in silico and experimentally by studying a protein-shedding mutant strain. An insertion-deletion in the ORF of the most promising candidate, the hemolysin-like protein Sll1951, was easily segregated to homozygosity under laboratory conditions. Concomitantly, the 178 kDa protein, present on PAGE gels of wild type derived from S-layer preparations, was completely absent in the protein profiles of the mutant strain. Apart from the 178-kDa protein cell wall and cell membrane protein profiles, as well as carotenoid profiles of both strains remained identical with myxol being dominant in the cell wall, and β -carotene as well as echinenone being the major carotenoids of the cell membrane. Pigments were not detected in the supernatant of the mutant. Thin section- and negative stain transmission electron microscopy showed the presence of a ca. 50 nanometer wide S-layer lattice covering the cell surface of wild type cells, the mutant, however, was devoid of this layer. Although the overall growth performance of the mutant was comparable to the wild type strain, the viability of Δ sll1951 was reduced upon exposure to lysozyme treatment and hypo-osmotic stress, suggesting a contribution of the S-layer to the integrity of the *Synechocystis* cell wall.

Introduction

More than half a century has passed since the first description of a bacterial protein surface layer (Houwink, 1953). Over time it has become obvious that surface layer (S-layer) proteins are a very common feature among a wide variety of prokaryotes, including the archaeal and bacterial domains. S-layers are highly ordered structural, paracrystalline layers of protein on the surface of bacteria, often glycosylated and usually in non-covalent contact with an underlying membrane or peptidoglycan. The structural organization of S-layers is relatively simple as most of them consist of only a single protein type. After export to the cell surface an entropy-driven self-assembly of the subunits occurs to form a lattice structure (Sleytr and Messner, 1983). Being exceptionally rigid and durable (Peters *et al.*, 1995; Mescher and Strominger, 1976; Engelhardt, 2007), archaeal S-layers assume primarily the functions of peptidoglycan in bacteria, thus stabilizing the cell shape, while in bacteria the roles of S-layers are more diverse. For example, the dense lattice formed by the protein subunits that are associated to oblique, tetragonal or hexagonal symmetry may hinder the diffusion of molecules greater than 10 kDa such as exoenzymes or antibodies, and enable strains to fend off predators, or pathogens to evade the immune systems of their hosts (Calabi *et al.*, 2002; Kern and Schneewind, 2010; Buck *et al.*, 2005). In cyanobacteria, S-layers have also been reported to be involved in biomineralization processes such as carbon sequestration (Schultze-Lam and Beveridge, 1994; Jansson and Northen, 2010). Their role as an immunogen as well as their delicate physico-chemical properties with potential for a variety of biotechnological applications (Sleytr *et al.*, 2007) have led to extensive study of S-layer proteins in a variety of strains. Even though cyanobacterial S-layers have been described in many instances since the early days of their discovery in 1973 (Jensen and Sicko, 1973; Simon, 1981; Karlsson *et al.*, 1983; Hoiczky and Baumeister, 1995;

reviewed by Smarda 2002), actual identifications of S-layer encoding genes in cyanobacteria are not available to date, with *Synechococcus* sp. strain WH 8102 being the only exception (McCarren *et al.*, 2005). In this work the gene coding for the S-layer protein of *Synechocystis* sp. PCC 6803 is identified, and a phenotypical and biochemical analysis of a mutant lacking this gene is provided.

Methods

Cultivation of strains

Strains of *Synechocystis* wild type and $\Delta slr1951$ were grown axenically in BG-11, supplemented with 10 mM TES (N-tris hydroxymethyl methyl-2-aminoethane sulfonic acid-)NaOH (pH 8.2) at 30 °C and continuous white fluorescent-light irradiation between 25 to 60 $\mu\text{mol photons m}^{-2} \text{s}^{-1}$ on a rotary shaker. Plate cultures were maintained on BG-11 with 1.5 % (w/v) of Difco agar as well as 0.3 % (w/v) of sodium thiosulfate added to it. For photomixotrophic growth glucose was added to a final concentration of 5 mM. All liquid cultures of the $\Delta slr1951$ mutant were started supplemented with 25 $\mu\text{g/ml}$ of chloramphenicol. Culture densities were measured with a Shimadzu UV-160 spectrophotometer at 730 nm. The *E. coli* strain DH10B, carrying the $\Delta psll1951$ deletion construct, was maintained at 37 °C on Luria-Bertani plates with 25 $\mu\text{g/ml}$ of chloramphenicol added.

Construction of the $\Delta sll1951$ deletion strain

A 398 bp upstream region (*Synechocystis* genome position 1427604 – 1428001, CyanoBase (<http://genome.kazusa.or.jp/cyanobase>) including 50 bp of the *sll1951* ORF, as well as a 569 bp downstream region (1422150 – 1422716) including 293 bp of the *sll1951* ORF were amplified by PCR using the forward primer 5'-

GGAATCGGCCGGCTTTAGC-3' with an engineered *EagI* site, and the reverse primer 5'-CGATCGGATCCTTAATGCCTCTGC-3' with an engineered *BamHI* site for the downstream region, as well as a forward primer 5'-CGGATACACCACTGCAGGTGTAC-3' with engineered *PstI*- and removed *EagI* sites, and the reverse primer 5'-GAAAGTAAGGGAGGTCGACAAAGGTG-3' including an engineered *SalI* site for the upstream region.

The chloramphenicol resistance cassette of pChl was amplified by PCR using primers to create termini complementary to both the 5'-region upstream and the 3'-region downstream of the previously created PCR products, as indicated in bold letters:

5'-**GATGTTATTAGCAGAGGCATTAAGGATCCTCTAGAGTCACTTCAC**-3' and 5'-**CTACAGATCATGTACACCTGCAGGTCGGCATTGAGAAGC**-3'. In another PCR all three products were combined resulting in a linear 2.3 kb deletion-fragment that was used to transform the *Synechocystis* wild type strain. The transformation procedure was described previously (Vermaas *et al.*, 1987). For future reference, the deletion-fragment was also cloned into pBluescript II KS- (Acc.# X52329) at its polylinker sites *SalI* and *EagI*. Transformed cells were initially grown on 0.4 µm pore-size Nuclepore Track-Etch polycarbonate membranes (Whatman Inc., Piscataway, NJ) on BG-11 supplied with 5 mM glucose and 5 µg/ml chloramphenicol. Five colonies were picked, and the transformants re-plated, gradually increasing the chloramphenicol concentration up to 62.5 µg/ml, at which complete segregation was achieved as confirmed by PCR.

Transmission electron microscopy

Liquid cultures of *Synechocystis* wild type and $\Delta sll1951$ mutant were grown in BG-11 at 50 $\mu\text{mol photons m}^{-2} \text{ s}^{-1}$ under continuous active aeration to an OD_{730} between 0.5 and 0.6, then filtered onto a 0.4 μm -pore size Nuclepore Track-Etch membranes with very mild suction applied to them. The membranes were placed onto fresh BG-11 plates to prevent drying of the cells. Prior to fixation by means of High Pressure Freezing (HPF), the cells were scraped off the membranes with a toothpick and smeared into a slot-grid that was “sandwiched” between two halves of inverted copper planchets. HPF was performed at 210,000 kPa and $-196\text{ }^{\circ}\text{C}$ on a Bal-Tec HPM 010 High Pressure Freezer (Bal-Tec Corporation, Middlebury, CT). Kept at $-80\text{ }^{\circ}\text{C}$, the planchets were transferred into 10 ml of anhydrous acetone, dehydrated three times and post-fixed for 2 h in fresh 1% (w/v) OsO_4 in acetone. The planchets were warmed to $-20\text{ }^{\circ}\text{C}$ for 2 h, then to $4\text{ }^{\circ}\text{C}$ for 1 h, and washed again three times with 10 ml of acetone. Chunks of fixed cells were isolated from the planchets and infiltrated with increasing concentrations (25%, 50%, 75%, and three times 100%) of Spurr's resin (Spurr, 1969) in acetone for 12 hours each. The specimen were transferred into plastic molds and polymerized in a convection oven at $60\text{ }^{\circ}\text{C}$ overnight. Thin sections of 70 nm were cut on a Leica Ultracut R microtome (Leica, Vienna, Austria), then attached to Formvar-coated copper slot grids, and subsequently post-stained either with 1% uranyl acetate in 50% ethanol for 6 min only, or with uranyl acetate for 6 min and Sato's lead citrate (Sato, 1967) for 3 min. Electron micrographs were taken on a Philips CM12S transmission electron microscope (Philips Electronic Instruments, Co., Mahwah, NJ) equipped with a Gatan 791 CCD 1,024- by 1,024-pixel-area digital camera (Gatan, Inc., Pleasanton, CA) using Gatan Digital Micrograph 3.9.1 software, at 80 kV.

Discontinuous sucrose gradient centrifugation of cell extracts

For a preliminary analysis of the density distribution of membrane/protein fractions, cells were grown photoautotrophically in 100 ml cultures at $50 \mu\text{mol photons m}^{-2} \text{ s}^{-1}$ in BG-11 with continuous active aeration to an OD_{730} of approximately 1. The cells were harvested by centrifugation at $10,500 \times g$ at room temperature (RT) and the pellets were gently resuspended in 2 ml of 50 mM MES-NaOH (pH 6.5) that contained a protease inhibitor cocktail (1 mM phenylmethanesulfonyl fluoride, 1 mM benzamidine, and 1 mM ϵ -amino caproic acid). 1.2 ml of cell suspension was transferred into 2 ml screw-cap tubes filled with ~0.8 ml of glass beads (100 μm \emptyset), and then chilled on ice. Cells were broken in 10 cycles of grinding in a MiniBeadbeater (BioSpec Products, Bartlesville, OK) for 30 s with the tubes being cooled on ice for two minutes between the cycles. The extract was centrifuged for 5 min at $3000 \times g$ to remove most of the unbroken cells. The remaining suspension was loaded on top of a discontinuous gradient consisting of the following sucrose concentrations (w/v)/volumes (ml): 90/0.8, 55/2, 48/4, 45/1, 30/2 and 10/1 (bottom to top). Ultracentrifugation was carried out in an SW-41 rotor (Beckman Coulter Inc., Brea, CA) at $130,000 \times g$ at RT for 16 h.

To analyze carotenoids and proteins in different density fractions, 100 ml pre-cultures of wild type and mutant strains were grown photomixotrophically at $50 \mu\text{mol photons m}^{-2} \text{ s}^{-1}$ in BG-11, supplemented with 5 mM glucose (and 25 $\mu\text{g/ml}$ chloramphenicol for the mutant) to an OD_{730} of at least 1, and then used to inoculate 3.5 l of BG-11 in Erlenmeyer flasks. These subcultures were grown photoautotrophically at $120 \mu\text{mol photons m}^{-2} \text{ s}^{-1}$ with continuous active aeration until an OD_{730} of approximately 0.7 was reached. Cells were harvested by a 10-min centrifugation at $10,800 \times g$ at RT. The pellets were washed in 50 mM MES-NaOH (pH 6.5), decanted and then frozen at $-80 \text{ }^\circ\text{C}$.

Pellets were thawed, then resuspended with a brush in 5 ml of 20% (w/v) sucrose in 40 mM MES-NaOH (pH 6.5), 4 mM EDTA, and protease inhibitor cocktail. After diluting the volume to 25 ml, the cells were cooled on ice and then broken by three cycles in the French-Press at 13.8 MPa. Unbroken cells were removed by a 10-min centrifugation at $4,400 \times g$ at 4 °C. Ten ml aliquots of protein extract were used as the 20% sucrose step in a 38-ml discontinuous gradient consisting of the following sucrose concentrations (w/v)/volumes (ml): 80/3, 60/10, 48/10, 20/10 and 10/5 (bottom to top).

Proteins were separated by ultracentrifugation for 18 h at $112,000 \times g$ at 4 °C in an SW-28 rotor (Beckman Coulter Inc., Brea, CA). The colored fractions were removed and stored at -80 °C.

Analysis of proteins by SDS-PAGE and mass spectroscopy

Proteins were separated by SDS-PAGE on gels prepared according to Ikeuchi and Inoue (1988) either with 6 % stacking- and 12 to 20 % (w/v) continuous gradient acrylamide-, or 6% stacking and 15 % acrylamide running gels, respectively.

For mass spectroscopy protein bands were cut from gels with a scalpel and the pieces trimmed to small cubes of about 1 mm^3 . The cubes were incubated in $\sim 150 \mu\text{l}$ of double deionized (dd) water for 1 h at RT. To dehydrate the sample, $200 \mu\text{l}$ of 35% (v/v) acetonitrile in 20 mM freshly prepared ammonium bicarbonate was added and the incubation at RT was resumed for another 75 min. This dehydration step was repeated. The liquid was removed and the gel pieces containing proteins were dried in a Speed-vac for 20 min. Proteins samples were put on ice and re-hydrated for 90 min with a solution of 20 mM ammonium bicarbonate, containing $5 \mu\text{g/ml}$ Sequencing grade modified trypsin (Promega Corporation, Madison, WI), followed by in-gel digestion overnight at 37 °C. Of the suspension, $3 \mu\text{l}$ was loaded onto a μ -Precolumn cartridge (Dionex Acclaim

PepMap 100 C₁₈, 5 µm) that was connected in line with the main column (Dionex Acclaim PepMap 100 C₁₈, 75 µm ID, 15 cm), with flow rates of 5 µl/min for the precolumn but 300 nl/min for the main column, respectively. Elution of protein fragments was carried out on a Dionex UltiMate 3000 LC system (Dionex, Sunnyvale, CA). Proteins were eluted continuously with a the solvent mixture of 5% acetonitrile and 0.1% formic acid in water on the precolumn whereas the main column was developed with an increasing concentration of acetonitrile, initially up until the 5th minute also with 5% acetonitrile (in 0.1% formic acid). The content of acetonitrile was then increased as follows (concentration %/min): 20/11.5, 50/51.5, 65/59 and 95/69. Eluted fragments were ESI-ionized and their masses were determined on a Bruker microTOF-Q (Bruker Daltonics Inc., Billerica, MA) mass spectrometer. Mass data were deconvoluted in Bruker's DataAnalysis v4.0 software, and then imported into BioTools v3.1 (Bruker Daltonics Inc., Billerica, MA). The data were then submitted to one of the following MASCOT databases: MSDB, SwissProt or NCBIInr, as semi-Trypsin digested MS-MS fragments with the variable modifications Oxidation and Propionamide.

Analysis of carotenoids

For analysis by High Performance Liquid Chromatography (HPLC) pigments were extracted from cell pellets with 100% methanol, and aliquots were loaded onto a semipreparative Waters Spherisorb C₁₈ ODS2 4.0 × 250 mm column.

Pigments in distinct membrane fractions were extracted differently depending on their sucrose content: Of the high density cell wall fraction, 100 µl aliquots were washed twice with 1 ml of 50 mM MES-NaOH (pH 6.5) to minimize the sucrose content, and the pellets were extracted twice with 300 µl of 100% methanol. Of the extract, 200 µl was loaded onto the semi-preparative column.

For the lower density cell membrane fraction, 100 μl aliquots were diluted with 900 μl of 50 mM MES-NaOH (pH 6.5), and, since the cell membrane fraction could not be pelleted, the resulting suspension was extracted with 500 μl of chloroform. The solvent was evaporated under a stream of nitrogen and the pigments redissolved in 500 μl of 100% methanol. Of the extract, 200 μl aliquots were loaded onto the semipreparative column.

The pigments were separated on an HP-1100 Chemstation using a 24-min gradient of ethyl acetate (EtAc) in water/methanol, with an initial water content of 10%, continuously decreasing to 0% to the third minute. The content of ethyl acetate was continuously added to the methanol mobile phase to create a concentration gradient of 0 to 70% from minutes 3 to 11, then from 70% to 100% until the 21st minute. The elution of carotenoids was recorded at 452 and 475 nm.

Light microscopy

Cells were grown photomixotrophically at 40 $\mu\text{mol photons m}^{-2} \text{ s}^{-1}$ and then harvested by centrifugation for 30 min in the clinical centrifuge at 1,200 rpm. The cell density was adjusted to $\text{OD}_{730} = 1$ and cells were resuspended in 50 mM HEPES-NaOH (pH 7.2) with either 0.5 % (w/v) lauryl sarcosine or 0.5 % (v/v) Triton X-100. Light microscopy was carried out after a one-hour exposure to the detergents. To assess osmotic effects on wild type and mutant cells, approximately 3×10^8 cells of equally cultivated strains were exposed for two hours to 10 mg/ml lysozyme containing 2.5 mM EDTA in 50 mM HEPES-NaOH (pH 7.2), harvested by centrifugation and then resuspended in 50 mM HEPES-NaOH (pH 7.2) containing 5 mM CaCl_2 . The cells were left to sit at RT for 30 min. After that the volumes were split and transferred to new tubes, and then pelleted by

centrifugation. Immediately before light microscopy the cell pellets were resuspended in either 1 M aqueous sucrose solution or dd water.

For Differential Interference Contrast microscopy, 20 μ l of cell suspension was pipetted onto a glass slide and covered with a 22- by 22 mm coverslip. The cells were inspected with an Axioscop microscope (Carl Zeiss, Thornwood, NY) using a Plan-Neofluar 100 x oil-immersion objective with a 1.3-numerical aperture and a 1.4-numerical aperture oil immersion condenser lens. Images were taken with a Hamamatsu C3200-07 CCD.

Results.

The Sll1951 protein

In silico analysis, previously published findings (Sakiyama *et al.*, 2006) as well as unpublished observations in our laboratory on a mutant strain shedding significant amounts of Sll1951 into the growth medium made this protein a potential candidate for the *Synechocystis* S-layer protein. Due to the presence of a GGXGXDXUX nonapeptide motif, several predicted hemolysin-like calcium-binding regions, and serralyisin-like metalloprotease motifs, Sll1951 has been classified as one of eleven hemolysin-like proteins (HLP) encoded on the *Synechocystis* genome. These types of proteins are typically exported through the type I secretion machinery (Awram and Smit, 2001; Kawai *et al.*, 1998; Thompson *et al.*, 1998). Although Sll1951 shares local similarity with other proteins because of the motifs present, neither orthologs nor paralogs covering the entire coding region were found. The 1741-amino acid Sll1951 protein appears to lack any transmembrane regions, and sulfur-containing amino acids are largely under-represented in its primary structure with only seven methionines (0.4%) and a complete absence of cysteine. Microarray data show high levels of transcription of *sll1951* under standard growth conditions (Hihara *et al.*, 2001), and its codon sequence is optimized for rapid translation (Mrazek *et al.*, 2001). A possible ribosome binding site is located -19 bp from the start codon, whereas the most probable -10 and -35 transcriptional signals appear to be distant at positions -187 and -206, respectively, not uncommon for S-layer proteins (Adachi *et al.*, 1989). Other potential, alternative transcription initiation sites are present in the non-coding region upstream of the *sll1951* ORF.

The $\Delta sll1951$ deletion mutant

Strains of *Synechocystis* wild type that had been transformed with *psll1951* segregated to homozygosity after only six passages on BG-11 plates supplemented with 5 mM glucose, eventually containing 62.5 $\mu\text{g/ml}$ chloramphenicol (Fig. III-1).

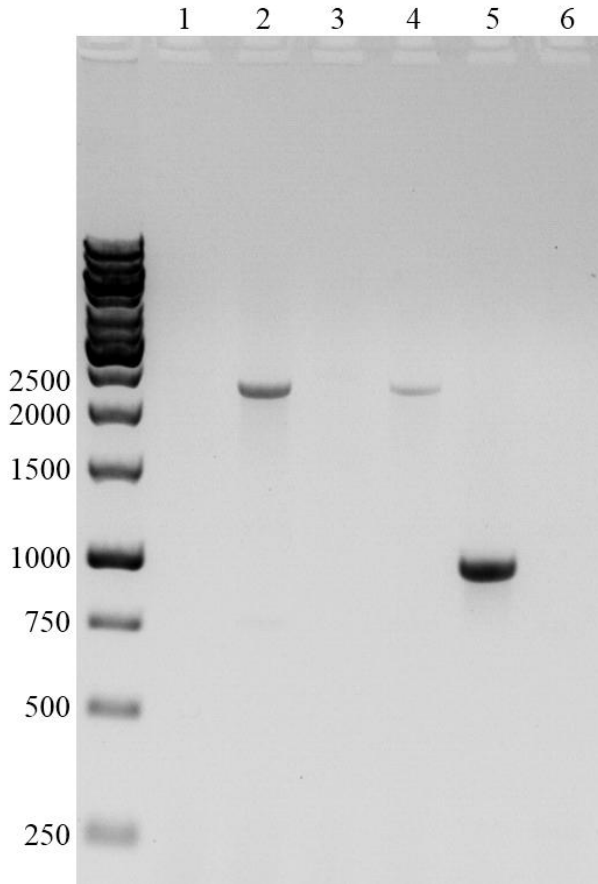


Fig. III-1: PCR products of two fully segregated $\Delta sll1951$ mutant strains (lanes 1 - 4) and the *Synechocystis* wild type (5, 6) to demonstrate complete segregation of the mutants. The reactions were carried out with pair of external primers (lanes 2, 4, 6) located at positions up- and downstream of *slr1951*, and a pair of external/*sll1951* internal primers (1, 3, 5). The 7081-bp wild type native locus could not be amplified in this reaction (lane 6). The internal/external primer pair amplified a 1010-bp 3'-region of *sll1951*, which was deleted in the mutant strains (lane 5). In the mutant strains a large part of the *sll1951* coding region was replaced by a much shorter chloramphenicol cassette which resulted in product length of 2298 bp (Fig. II-13).

Compared to the *Synechocystis* wild type, the colonies of the mutant strain appeared to have similar pigmentation but less convex curvature, and a shiny surface. The doubling time of a freshly inoculated mutant when grown photoautotrophically at 45 $\mu\text{mol photons m}^{-2} \text{ s}^{-1}$ was twice that of the wild type 24 hours after inoculation (omitted in the growth curve). During exponential phase, however, growth performance was about the same as the wild type strain (Fig. III-2).

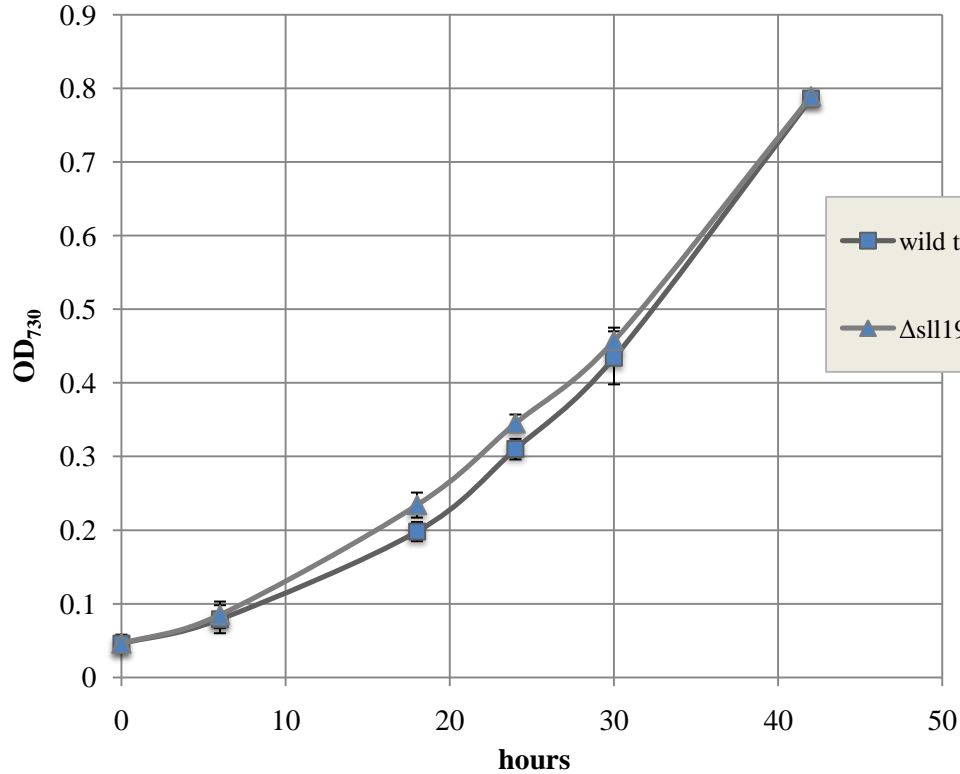


Fig. III-2: Growth of the wild type and the $\Delta sl11951$ mutant strain (three culture average) adapted to photoautotrophic growth at $45 \mu\text{mol photons m}^{-2} \text{s}^{-1}$. Freshly inoculated strains of the mutant grew significantly slower than the wild-type (WT) strain. Data presented are the average of three independent determinations.

Mutant cultures at optical densities above 0.5 exhibited an increased tendency to foam. Incubation at light intensities less than $2 \mu\text{mol photons m}^{-2} \text{s}^{-1}$ resulted in long initial lag-phases of 12+ hours, but doubling times similar to the wild type during exponential growth phase, while photomixotrophic growth of the mutant at $0.15 \mu\text{mol photons m}^{-2} \text{s}^{-1}$ or under Light Activated Heterotrophic Growth (LAHG, 15 min of $50 \mu\text{mol photons m}^{-2} \text{s}^{-1}$ per 24 h) conditions was not possible at all: An increase in optical density was not observed for the mutant cultures even after 30 hours of incubation (Fig. III-3).

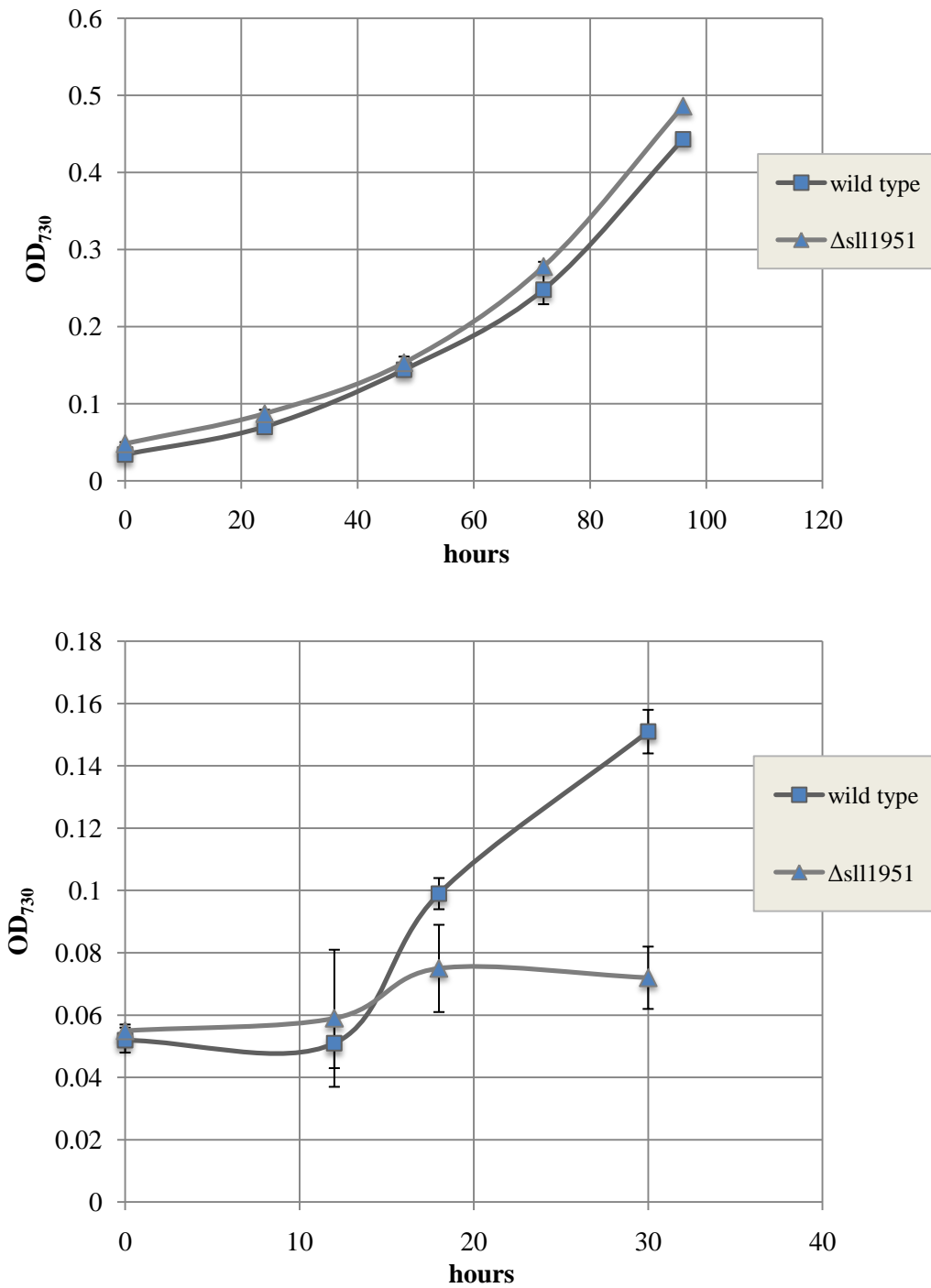
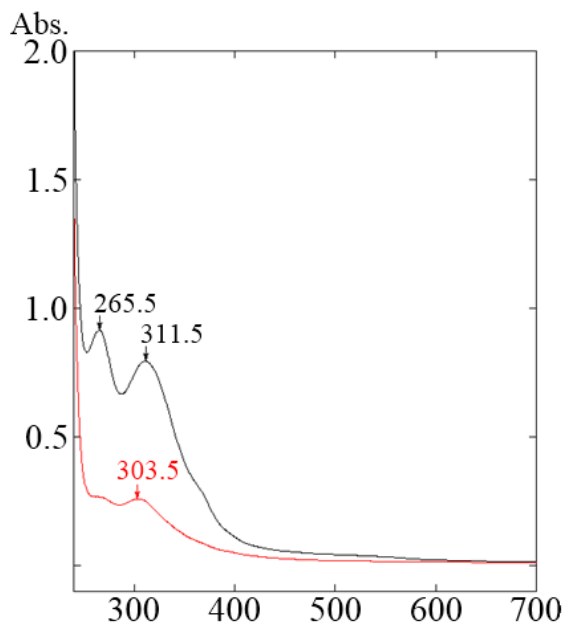


Fig. III-3: Photomixotrophic growth performance of wild-type and mutant cultures (triplicates). Cultures were grown at $1.5 \mu\text{mol photons m}^{-2} \text{s}^{-1}$ (top graph) and $0.15 \mu\text{mol photons m}^{-2} \text{s}^{-1}$ (bottom graph). After an initial lag phase the $\Delta sll1951$ mutant strains assumed doubling times similar to the wild type. Values are the average of three independent experiments.

The plate-grown mutant strain developed a sensitivity to low concentrations of chloramphenicol (5 – 25 $\mu\text{g/ml}$) upon exposure to regular light intensities (50 $\mu\text{mol photons m}^{-2} \text{s}^{-1}$). This effect could be remedied by initially incubating the plates at $\sim 5 \mu\text{mol photons m}^{-2} \text{s}^{-1}$. One possible explanation is the orientation of the chloramphenicol acetyl transferase (CAT) cassette in the mutated locus whose transcription may be competing with the *sll1951* promoter being transcribed in the antisense direction, thus leading to a knockdown of the CAT mRNA and a virtual absence of CAT. This may limit the survival rate of individual CFUs. Regardless of the growth conditions, liquid cultures of the mutant strain always assumed a lightly yellow tint presumably due to increased export of compounds into the medium. This phenomenon intensified at less than 2 $\mu\text{mol photons m}^{-2} \text{s}^{-1}$, when mutant supernatants developed a brownish coloration. A comparison of the supernatants taken from three strains, the wild type, $\Delta\text{sll1951}$ and the fucose synthetase mutant $\Delta\text{sll1213}$ showed almost no absorption in the VIS region and therefore absence of chlorophyll or fully desaturated carotenoids. Conversely, absorption in the UV with peaks at 312 and 265 nm often was barely detectable in the wild type



strain, increased in $\Delta\text{sll1951}$ and dramatically increased in $\Delta\text{sll1213}$ (Fig. III-4, data not shown for $\Delta\text{sll1213}$).

Fig. III-4: Absorption of supernatants of wild type (red line) and the $\Delta\text{sll1951}$ mutant (black line) after photomixotrophic growth to high optical densities of 4.95 (WT) and 4.60 ($\Delta\text{sll1951}$). Abscissa: wavelength in nm.

The absorption maximum above 300 nm could originate from mycosporin-like amino acids which are very common UV-protectants in a wide variety of organisms (Cockell and Knowland, 1999). Recently such compounds have also been found in *Synechocystis* (Zhang *et al.*, 2007). Attempts to identify the cause for the color change by extracting or precipitating the supernatant were made, but were unsuccessful.

Assessment of sensitivity of wild type and mutants strains to the antibiotics polymyxin B, carbenicillin and colistin by a non-standardized Antibiotic Sensitivity Test (AST) showed almost equal zones of inhibition (ZOI) (Fig. III-5).

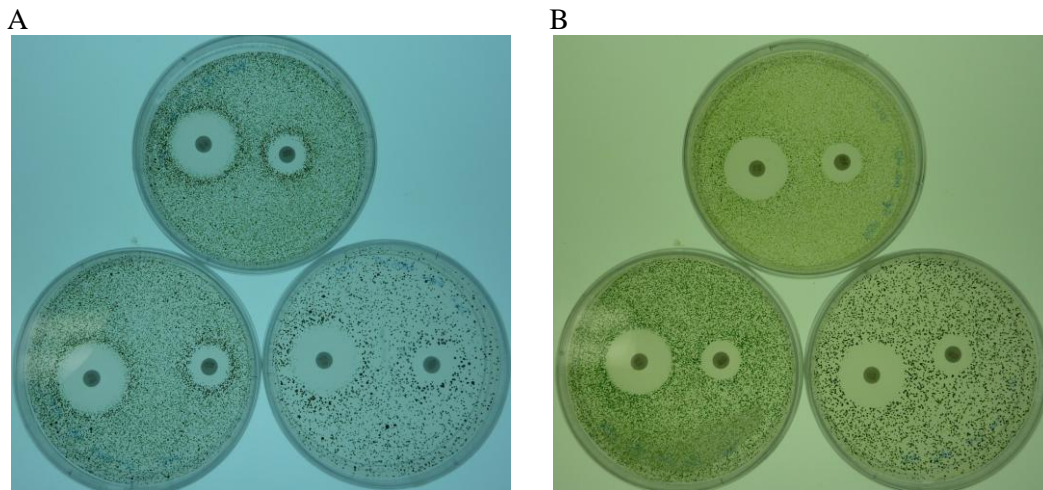


Fig. III-5: Antibiotic sensitivity test performed with polymyxin B (large ZOI) and colistin (small ZOI) on wild type (A) and $\Delta sll1951$ mutant cells (B). The amounts of cells plated were 1000, 500 and 100 cm^{-2} (top, bottom left, bottom right).

Light- and electron microscopy

HPF TEM was performed on photoautotrophically grown strains of *Synechocystis* wild type, the $\Delta sll1951$ mutant as well as $\Delta sll1213$, a strain lacking myxoxanthophyll due to a deletion of the fucose synthetase gene (Mohamed *et al.*, 2005). Both mutant strains showed a severely altered cell wall: Wild type cells were surrounded by a glycocalyx at a distance of approximately 20 nm from the outer membrane, whereas this surface protein

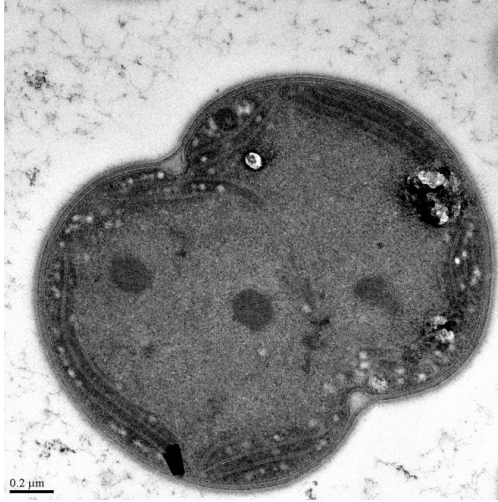
layer was completely absent in both mutant strains (Fig. III-6, 7, 8). Cells of the $\Delta sll1951$ strain were in direct contact with the environment via the outer membrane, which appeared to be covered with a diffuse, weakly electron dense layer of about 5 – 10 nm thickness, protruding from the outer membrane's (OM) phospholipid head group, and could therefore represent the LPS layer that is normally in contact with glycosylated moieties of the S-layer protein (Fig. III-7). Even though the glycocalyx was absent in the myxoxanthophyll-deficient mutant as well, its OM seemed to be covered by a fairly electron dense layer with an appearance and thickness similar to a membrane bilayer.

The peptidoglycan layer of the wild type-strain was located centrally in the periplasmic space between CM and OM, and its electron density was slightly higher than the peptidoglycan of $\Delta sll1951$ but markedly higher than the corresponding layer in $\Delta sll1213$. Consequently, both the *Synechocystis* wild type and the $\Delta sll1951$ mutant cells were less prone to cell wall deformation during the fixation of specimen for electron microscopy than $\Delta sll1213$. The CM bilayer was much less pronounced in both mutants than it was in the wild type, even on micrographs that clearly displayed the details of both outer membrane monolayers (Fig. III-7). This phenomenon has been observed before (Graham and Beveridge, 1990) and is probably due to compression of the CM by the cytoplasm.

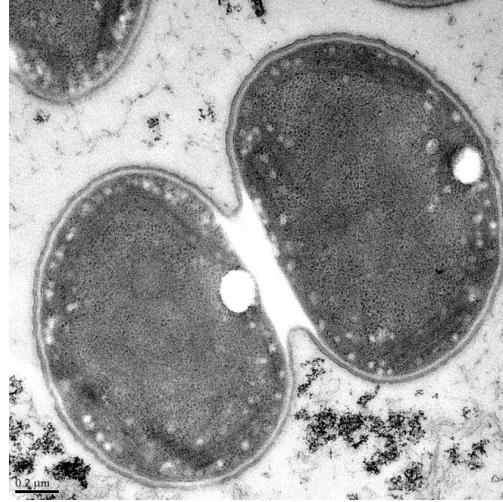
The thylakoid membranes remained unaltered in the $\Delta sll1951$ mutant compared to wild type with four layers on average. By contrast, the thylakoid membranes of the myxoxanthophyll mutant were not only fewer but also less organized (data not shown).

In support of the TEM data, negative stain EM performed on the *Synechocystis* wild type and the $\Delta sll1951$ mutant revealed the honeycomb-like surface layer on the wild-type strain, which was absent in the mutant (Fig. III-8).

A



B



C



Fig. III-6: Whole cell image of HPF-fixed $\Delta sll1951$ (A), $\Delta sll1213$ (B) and wild-type cells (C). Scale bar is 0.2 μm .

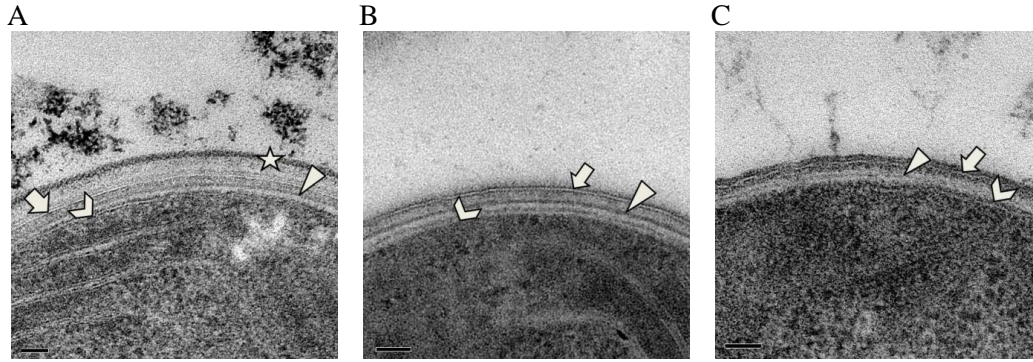


Fig. III-7: High magnification images of the cell periphery of wild type (A), $\Delta sll1951$ (B) and $\Delta sll1213$ (C) strains. Scale bar is 50 nm. Arrow – outer membrane, arrowhead – peptidoglycan, chevron – cytoplasmic membrane, star – surface layer.

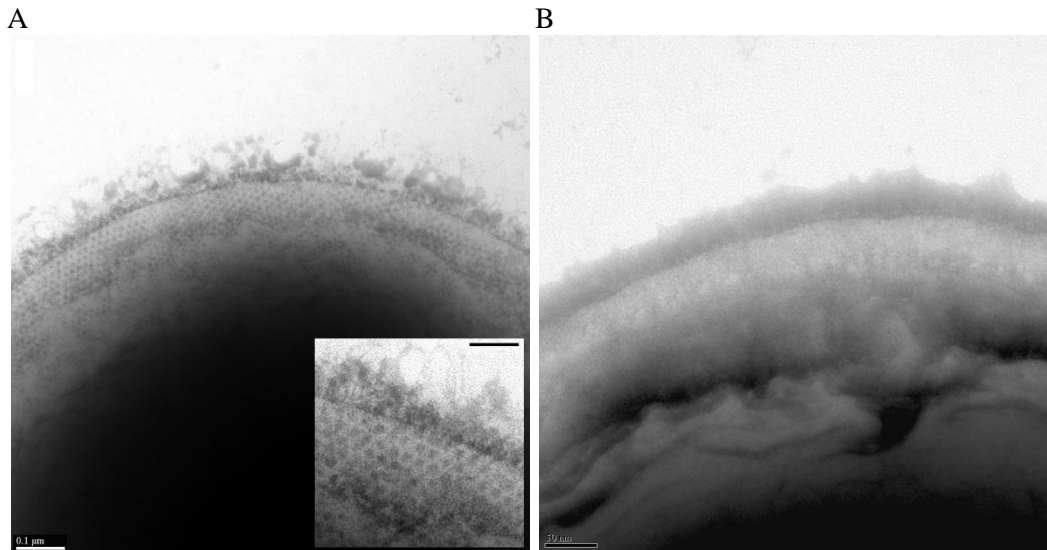


Fig. III-8: Phosphotungstic acid negative stain images of wild type cells (A) and the $\Delta sll1951$ mutant (B). The surface layer of honeycomb-like structure is visible at the periphery of the wild-type strain, shifting out of the focal plane towards the bottom of the image. The S-layer is absent in the mutant cell. Scale bars are 100 nm for image A (50 nm for the higher magnification inset) and 50 nm for image B, respectively.

Differential Interference Contrast (DIC) light microscopy was performed on cells of *Synechocystis* wild type and the $\Delta sll1951$ mutant (Fig. III-9). Without any pre-treatment both strains looked identical (data not shown). Similarly, a 20-minute exposure of both strains to lysozyme (10 mg/ml) did not seem to have any effect on the appearance of the cells.

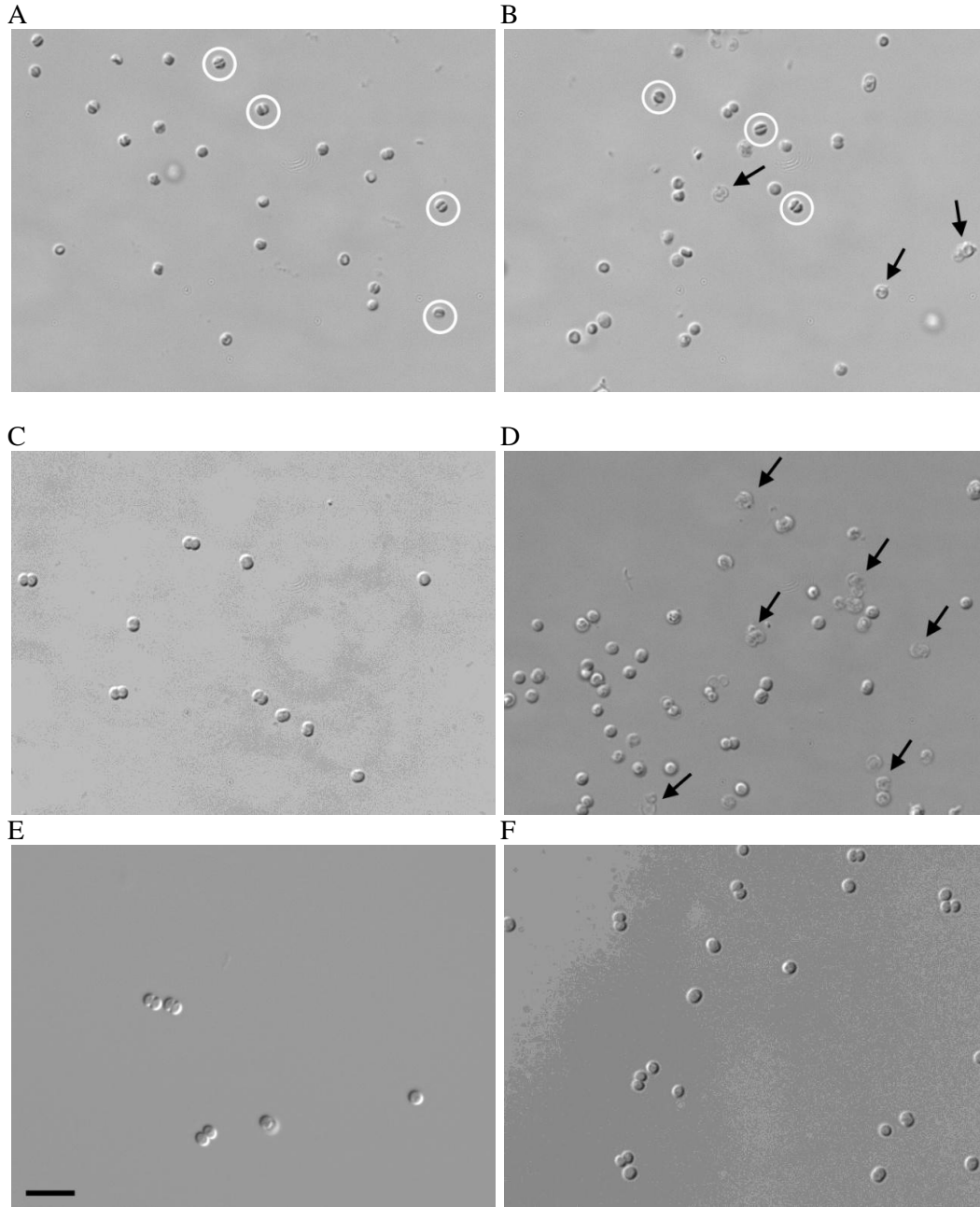


Fig. III-9: DIC light microscopy on cells of *Synechocystis* wild type (A, C, E) and $\Delta sl11951$ (B, D, F) after lysozyme-treatment and hyper-osmotic shock (A, B) and hypo-osmotic shock (C, D). Water efflux cause significant cell shrinkage (circles). The mutant was significantly more susceptible to hypo-osmotic effects leading to a high degree of lysis and ghost-like cells (arrows). E and F are untreated controls. Scale bar in (E) is 5 μm and applies to all images.

Cyanobacteria are generally less susceptible to lysozyme treatment due to a peptidoglycan sacculus that is thicker and has a greater degree of cross-linking than in most other Gram-negative prokaryotes (Hoiczky and Hansel, 2000). However, a combination of lysozyme treatment followed by exposure to osmotic stress had a much more severe effect on the mutant. Although hyperosmosis caused by 1 M sucrose led to very little cell lysis, which was most obvious on dividing cells, washing cells with de-ionized water after lysozyme treatment resulted in a significant degree of lysis, and the appearance of ghost-like cells in case of the $\Delta sll1951$ mutant whereas only very few wild type cells were destroyed under hypoosmotic conditions (Fig. III-9).

Analysis of the $\Delta sll1951$ cell wall components

To confirm the absence of Sll1951 in the mutant strain, PAGE was performed with protein extracts isolated from large (3.5 l) cultures of the wild type strain and $\Delta sll1951$. Protein profiles of both strains were mostly identical except for a complete absence of several high molecular weight bands (>100 kDa) in the mutant.

MASCOT analysis of the two strongest bands of >100 kDa after trypsin digest revealed the presence of two co-migrating proteins, Sll1951 with a coverage of 16%, and Slr0335, the phycobilisome core-membrane linker protein, ApcE, with a relatively high coverage of 53% in the higher molecular weight band (Fig. III-10, H).

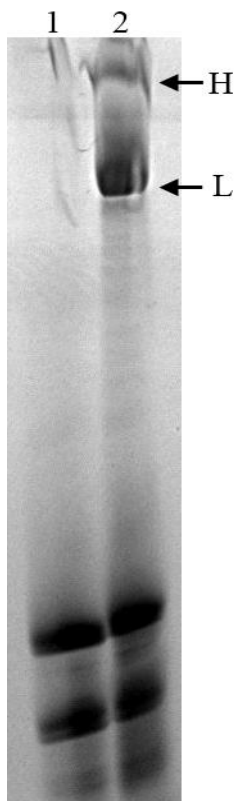


Fig. III-10: SDS-PAGE on protein isolates from the $\Delta sll1951$ mutant (lane 1) and the *Synechocystis* wild type (lane 2). Bands of >100 kDa that were analyzed by MS are indicated by arrows.

The other isolated, lower molecular weight band contained markedly more protein. Although Sll1951 and Slr0335 were present, their coverages were different with 19% and 18%, respectively (Fig. III-10, L). Taking into account that Sll1951 is probably glycosylated, both proteins are larger than 100 kDa and have strongly opposing predicted pIs of 3.5 (Sll1951) and 9.25 (Slr0335), an interaction between the denatured strands of both proteins is likely, resulting in co-migrating bands. Furthermore, the migration speed of high molecular weight proteins frequently does not correlate well with their masses. Due to the lower sequence coverage of Slr0335 in the lighter, more intensely stained band, this band was designated the main Sll1951 band, whereas other, heavier bands were presumed to contain lower amounts of Sll1951, but with a higher degree of glycosylation.

The supernatant protein profiles of $\Delta sll1951$ and wild type cultures that had been exposed to denaturing environments such as high temperature (60° C) with 5 mM EDTA, or 6 M urea with 5 mM EDTA were analyzed (Fig. III-11). While this treatment had minimal effect on the wild-type strain, resulting in only one dominating high-molecular-weight band on the gel, a wide spectrum of proteins were extracted from the mutant. The 6 M urea / 5 mM EDTA treatment had a more severe effect on the mutant than increased temperature with 5 mM EDTA. In both instances, however, a high-molecular-weight protein was isolated from the wild type strain but was absent from the mutant samples.

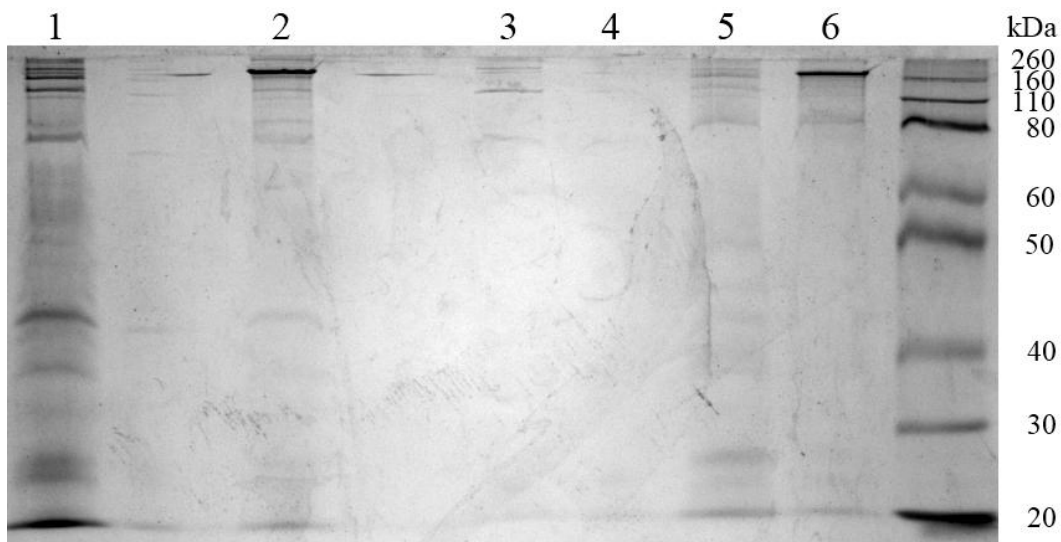


Fig. III-11: SDS-PAGE (10%) of supernatants of *Synechocystis* wild type and the $\Delta sll1951$ mutant strain after treatment with 6 M urea/5 mM EDTA (1 = mutant, 2 = wild type), 1.5 M guanidine hydrochloride (3 = mutant, 4 = wild type), and 5 mM EDTA at 60 °C for one hour (5 = mutant, 6 = wild type). The combination of urea and EDTA had a severe effect on the mutant, resulting in a spectrum of proteins, whereas guanidine hydrochloride was particularly ineffective.

Although light microscopy on cells that had been treated with various concentrations of Triton X-100 and lauryl sarcosine did not demonstrate any effect on either wild type or mutant cells (data not shown), the effect of different amounts (0.1, 0.5 and 5%) of these detergents on $\Delta sll1951$ was assessed biochemically. In contrast to the light microscopy data, both detergents appeared to solubilize and isolate the same four proteins from the wild type cell wall (Fig. III-12, 13).

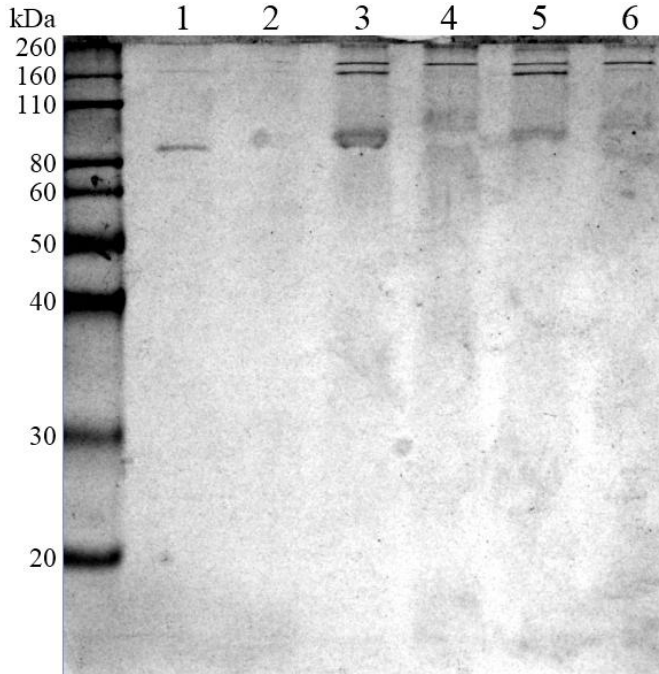


Fig. III-12: SDS-PAGE (10%) of supernatant protein profiles of *Synechocystis* wild type and the $\Delta sll1951$ mutant after treatment with different concentrations of lauryl sarcosine. Wild-type protein was loaded onto odd-numbered lanes and proteins extracted from $\Delta sll1951$ was loaded onto even-numbered lanes. Detergent concentrations were 0.1 % (lanes 1, 2), 0.5 % (lanes 3, 4) and 5 % (lanes 5, 6)

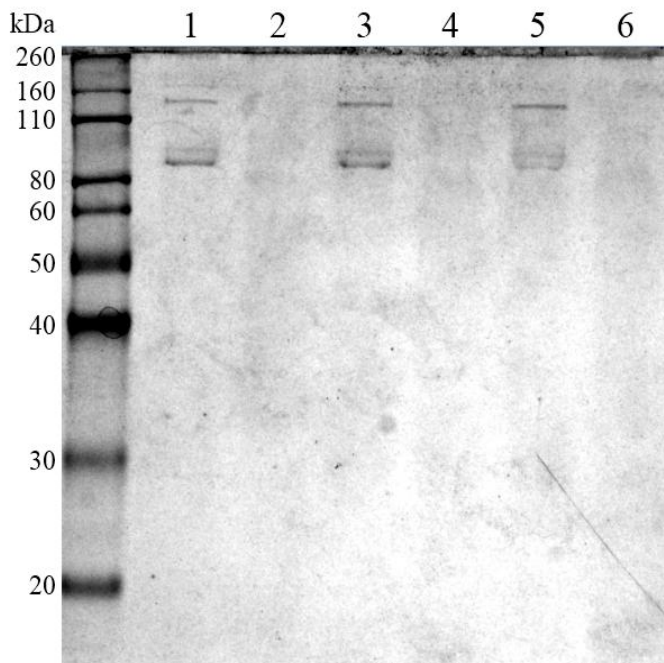


Fig. III-13: SDS-PAGE (10%) of supernatant protein profiles of *Synechocystis* wild type and the $\Delta sll1951$ mutant after treatment with different concentrations of Triton X-100. Wild-type protein was loaded onto odd-numbered lanes and proteins extracted from $\Delta sll1951$ was loaded onto even-numbered lanes. Detergent concentrations were 0.1 % (lanes 1, 2), 0.5 % (lanes 3, 4) and 5 % (lanes 5, 6).

Carotenoid contents of both strains were analyzed with focus on the cell periphery of both strains. Distribution and concentration of carotenoids in the mutant remained largely unchanged (Fig. III-14, 15; HPLC spectra of carotenoids were identical for both strains and the mutant trace was therefore omitted in Fig. III-15). The cell wall (CW) fractions including peptidoglycan and outer membrane were of highest density and accumulated at the bottom of the centrifugation tubes. This fraction was of orange-light brown color in both strains and accumulated an unidentified carotenoid which eluted early in the hydrophilic range of the methanol/EtAc gradient, indicating possible sites of hydroxylation and/or glycosylation (Fig. III-15). In contrast to the cell wall fraction the yellow cytoplasmic membrane (CM) fraction was of lowest density and barely penetrated the sucrose on top of the gradient. The CM contained mostly β -carotene and echinenone. As expected, all isolated fractions were virtually chlorophyll-free. Loss of the S-layer had apparently no effect on the carotenoid content of the cell periphery.

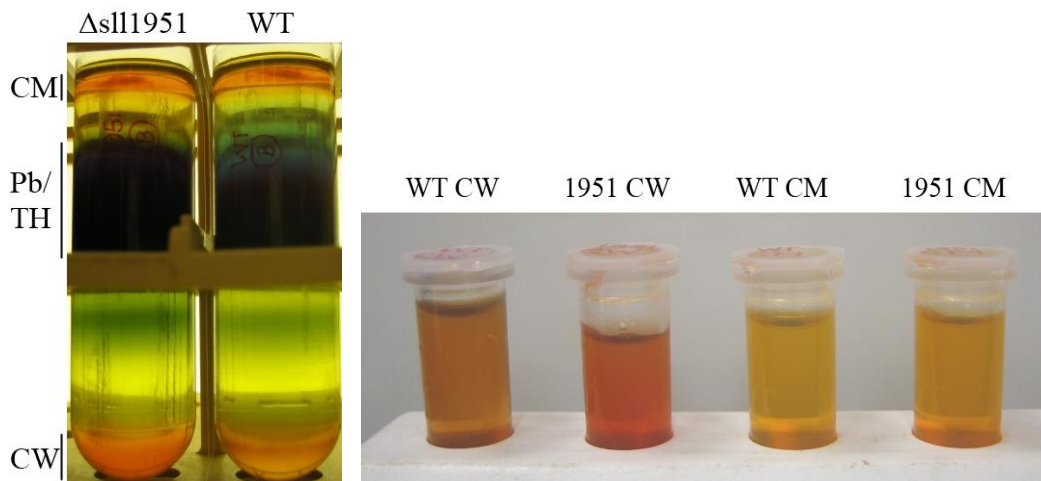


Fig. III-14: Sucrose gradients and isolated membrane/protein fractions of *Synechocystis* wild type (WT) and the mutant $\Delta sll1951$ (1951). Cytoplasmic membrane = CM, phycobilisome/thylakoid = Pb/TH, cell wall = CW.

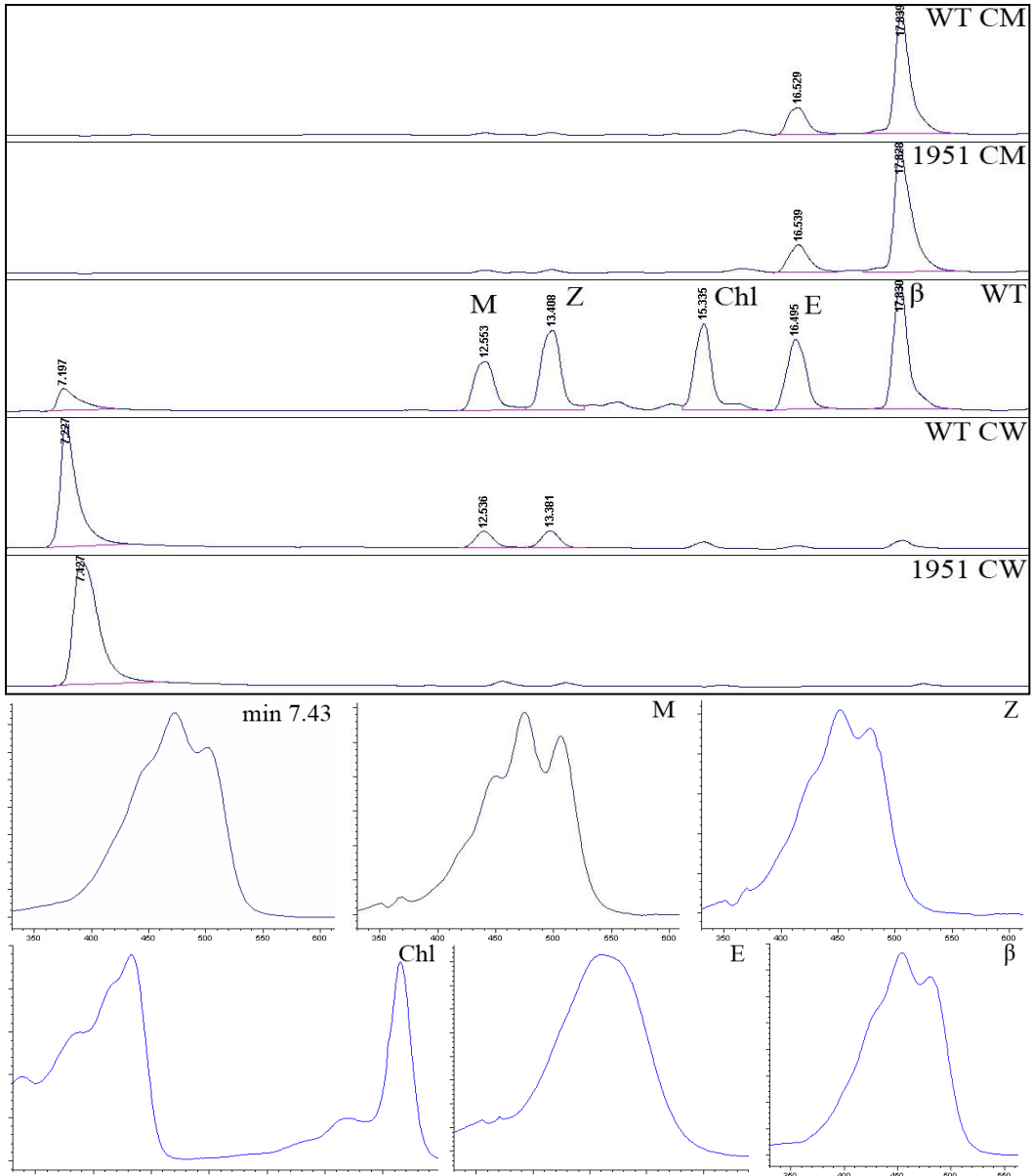


Fig. III-15: Carotenoid HPLC profiles of the *Synechocystis* wild-type and $\Delta sll1951$ membrane fractions. Predominant carotenoids of the cytoplasmic membrane fraction (WT CM, 1951 CM) were echinenone (E) and β -carotene (β) as indicated by a whole cell pigment extract from wild-type cells (WT). Extracts from $\Delta sll1951$ looked identical. The pellets that also contained the cell wall fractions were mostly devoid of carotenoids with the exception of an unidentified carotenoid that eluted between minute $\sim 7 - 7.5$. Elution times are indicated above peaks. Corresponding online spectra are indicated. Y-axis is absorbance on all images.

Transcript levels of S-layer mRNA in the Synechocystis wild type

In a tiling array approach the abundances of mRNAs of *slr1951*, ORFs related to *slr1951*, as well as a variety of *Synechocystis* proteins encoding for a putative S-layer homology domain (SLH) were analyzed for exponential growth phase- ($OD_{730} = 0.5$) and early stationary phase- ($OD_{730} = 1.5$) cultures of the wild type (Table II-1). Under these conditions, of all analyzed genes *slr1951* had by far the highest transcript levels. In fact, mRNA levels of other ORFs carrying putative hemolysin Ca^{2+} binding domains were very low (data not shown).

Although SLH motifs are a very uncommon feature in S-layers of Gram negatives, expression levels of ORFs coding for predicted SLHs were examined as well. Of the transcript levels of these proteins only Slr1841 showed expression comparable to Slr1951. The corresponding protein, however, could never be detected in S-layer preparations and the presence of an N-terminal transmembrane helix as well as the predicted porin-like structure makes Slr1841 likely a candidate for a membrane anchored- but not an S-layer protein.

Table III-1: ORFs in the *Synechocystis* genome encoding hemolysin Ca^{2+} binding motifs or S-layer homology (SLH) domain motifs. Predicted sizes are in amino acids.

ORF	Size	Notes	SLH
<i>sll1951</i>	1741	hemolysin Ca^{2+} binding, Sakiyama <i>et al.</i> , 2006	no
<i>sll1009</i>	591	hemolysin Ca^{2+} binding, peptidase domains, iron regulated	no
<i>sll0721</i>	1290	hemolysin Ca^{2+} binding, carbamate kinase, Y-rich domains	no
<i>slr1403</i>	3016	hemolysin Ca^{2+} binding, integrin α , Y-rich domains	no
<i>sll0723</i>	1771	hemolysin Ca^{2+} binding	no
<i>slr5005</i>	3797	hemolysin Ca^{2+} binding, integrin α	no
<i>slr2000</i>	312	SLH, Zhang <i>et al.</i> 2009; Claus <i>et al.</i> , 2005	2
<i>sll1550</i>	544	SLH, probable porin	1
<i>slr1272</i>	254	SLH, probable porin, Huang <i>et al.</i> 2004	1
<i>sll1271</i>	572	SLH, probable porin	1
<i>slr1841</i>	630	SLH, probable porin, Claus <i>et al.</i> , 2005; Huang <i>et al.</i> 2004	1
<i>slr1908</i>	591	SLH, Huang <i>et al.</i> 2004	1
<i>slr0042</i>	576	SLH	1

Discussion

The cyanobacterium *Synechocystis* sp. PCC 6803 has become a very important model organism over the last few decades, with a majority of research devoted to studying its plant-like photosynthesis, and, more recently, because of its obvious potential for producing biofuels (Schirmer *et al.*, 2010). Efficient secretion of endogenously produced hydrocarbons such as lipids or fatty acids that are amenable as precursors for biofuels may require a solid understanding of the cell wall properties of the engineered organism, yet our knowledge about the *Synechocystis* cell wall, and especially its surface layer protein, is still limited. In this chapter the identification of the gene encoding the *Synechocystis* S-layer protein is reported. Its identification was based on the analysis of a *Synechocystis* mutant, $\Delta sll1213$ (Mohamed *et al.*, 2005), shedding significant amounts of S-layer protein into the medium, on comparative analysis of transcript levels of possible surface layer target genes, and the characterization of a deletion mutant that lacks the ability to synthesize S-layer protein.

Preliminary identification of an S-layer candidate gene

As reported by Mohamed *et al.* (2005) Sll1213 is a putative fucose synthetase that is essential for the biosynthesis of myxoxanthophyll, a native *Synechocystis* sp. PCC 6803 carotenoid. Deletion of this enzyme in the $\Delta sll1213$ strain resulted not only in an irregular thylakoid organization, but also in an altered cell wall and a complete loss of the S-layer. Fucose had been identified as a building block in the S-layer glycan of *Geobacillus tepidamans* (Kahlig *et al.*, 2005) and may be important for proper anchoring of the S-layer protein to the underlying lipopolysaccharide (LPS). Changes in composition of LPS or (if present) the S-layer glycan frequently lead to a loss of the glycocalyx (Belland and Trust, 1985; Walker *et al.*, 1994). The predominant protein in supernatants of $\Delta sll1213$

cultures was identified as Sll1951, a hemolysin-like protein that had been characterized previously by Sakiyama *et al.* (2006). A predicted extracellular protein (Yu *et al.*, 2010), Sll1951 is particularly prone to shedding when changes to the structural organization of the cell wall occur (Bhaya *et al.*, 1999). It has several characteristics making it a likely candidate for a surface layer protein: Firstly, its primary structure with an absence of cysteines and by a low amount of methionines, resulting in a very low abundance of sulfur-containing amino acids. Secondly, the theoretical pI of 3.50 that is due mainly to the presence of 193 (11.1 %) aspartate and 80 (4.6 %) glutamate residues. With few exceptions for archaeal S-layer proteins, pIs in the acidic range are common for the majority of S-layer proteins that have been described to date. Thirdly, *sll1951* a codon sequence that is obviously highly optimized for rapid translation (Mrazek *et al.*, 2001), as well as a transcription initiation region with multiple possible start sites (Adachi *et al.*, 1989, Kahala *et al.* 1997). In certain fast growing strains, S-layer proteins range among the most highly expressed proteins with synthesis rates of up to 500 subunits per minute (Sleytr and Beveridge, 1999). Tiling array data support this observation showing very high mRNA levels (i.e., similar to levels for the D1 protein) for *sll1951* during logarithmic and early stationary phase growth. Curiously, despite the characterization of Sll1951 by Sakiyama *et al.*, (2006) and the attempted annotation of S-layer candidates by other authors (Zhang *et al.*, 2009; Claus *et al.*, 2005; Huang *et al.*, 2004) experimental evidence for the function of Sll1951 was missing.

Phenotype of $\Delta sll1951$

Based on these findings a mutant strain was created with a chloramphenicol resistance cassette inserted into the ORF of *sll1951*. Segregation of this mutant to homozygosity in the mutated locus did not require high concentrations of chloramphenicol. Although the *Synechocystis* wild type strain has kept its S-layer over many years of culturing, axenically grown laboratory strains may not have an immediate evolutionary disadvantage from losing their surface layer due to lack of competition and optimized growth conditions. In fact, growth rates of the $\Delta sll1951$ mutant were similar to those of the wild type strain. A possible slight growth advantage of the mutant can most likely be attributed to the reduced metabolic load from the absence of Sll1951.

In contrast to the wild type strain, densely grown cultures of $\Delta sll1951$ exhibited an increased tendency to foam possibly due to accumulation of exported proteins and metabolites in the growth medium that are usually retained in the wild type.

In addition to a variety of mostly high molecular weight proteins, $\Delta sll1213$ exported large amounts of Sll1951 into the medium. Mass spectrometry confirmed the presence of S-layer protein in the wild type strain as well, yet to a much lower degree (data not shown). Unlike in $\Delta sll1213$ however, other proteins were barely detectable in the *Synechocystis* wild type supernatant. Sll1951 was completely absent in the S-layer mutant (Fig. III-10). This strain may be capable of assembling a mature, fully functional LPS/exopolysaccharide (EPS) as its outer-most cell layer whereas a structurally crippled LPS with limited functionality is likely present in the fucose-lacking strain $\Delta sll1213$ (Fig. III-7).

The *Synechocystis* S-layer polycrystalline structure was examined by negative staining of the surface of whole cells. A rapid method, negative staining of the *Synechocystis* wild type displayed Sll1951 as a regularly ordered protein layer (Fig. III-

8). Thin sections of HPF cells demonstrated markedly altered cell surface features of both mutant strains, which appeared fuzzy in $\Delta sll1951$ but smooth in $\Delta sll1213$ (Fig. III-6, 7). The weakly electron dense surface of $\Delta sll1951$ represented an intact LPS/EPS and hence the point of contact with the S-layer glycan. This was in contrast to the $\Delta sll1213$ mutant that, in spite of expressing Sll1951, could not anchor the exported protein to its LPS (Walker *et al.*, 1994; Awram and Smit, 2001). EM images also show that the peptidoglycan sacculus of $\Delta sll1213$ was less electron dense than in the S-layer mutant or the *Synechocystis* wild type. Of the three strains examined in this study, the cell periphery of the fucose deficient strain was structurally most altered and it is presumed that this was the reason for the increased loss of cellular components into the growth medium.

Increased sensitivity of $\Delta sll1951$ to osmotic stress

Assessment of the viability of the S-layer deficient strain upon exposure to environmental stresses suggests a protective role of Sll1951. While treatment of cyanobacterial cells with lysozyme usually has little effect due to their robust peptidoglycan layers (Hoiczky and Hansel, 2000), the number of CFUs in one experiment was reduced by 38 percent in the S-layer deficient strain when compared to wild type. However, these findings could not be reproduced in another experiment. Hypoosmosis of lysozyme-treated $\Delta sll1951$ resulted in a high degree of cell lysis whereas the wild type cells appeared largely unaffected (Fig. III-9). Growth inhibition of wild type cells and the S-layer mutant by the antibiotics carbenicillin (an inhibitor of peptidoglycan synthesis), polymyxin B (a cationic ionophor that binds to lipid A) and colistin (binds to cell membrane lipids and disrupts the cell wall integrity) was identical for both strains (Fig. III-5). Hence, the S-layer may not pose a barrier to low molecular weight antibiotics such as the ones tested regardless of their charge. However, lysozyme is more than an order of magnitude larger

than the antibiotics and its diffusion through the S-layer may be limited in the wild type strain.

Despite the increased sensitivity to osmotic stress $\Delta sll1951$ appears to have no obvious growth disadvantage when compared to the *Synechocystis* wild-type strain. Based on these observations and the general assumption that S-layers are molecular sieves it would be feasible to evaluate the applicability of engineered, S-layer-less strains of phototrophic bacteria with respect to the secretion of metabolites that can be converted into biofuels, e.g., fatty acids or lipids. Experiments with the mutant strain created in this work are currently in progress.

References

- Adachi, T., Yamagata H., Tsukagoshi N., and Udaka S. (1989) Multiple and tandemly arranged promoters of the cell wall protein operon in *Bacillus brevis* 47. *J Bacteriol* **171**: 1010-1016.
- Awram, P., and Smit J. (1998) The *Caulobacter crescentus* paracrystalline S-layer protein is secreted by an ABC transporter (type I) secretion apparatus. *J Bacteriol* **180**: 3062-3069.
- Awram, P., and Smit J. (2001) Identification of lipopolysaccharide O antigen synthesis genes required for attachment of the S-layer of *Caulobacter crescentus*. *Microbiol* **147**: 1451-1460.
- Belland, R.J., and Trust T.J. (1985) Synthesis, export and assembly of *Aeromonas salmonicida* A-layer analyzed by transposon mutagenesis. *J Bacteriol* **163**: 877-881.
- Bhaya, D., Watanabe N., Ogawa T., and Grossman A.R. (1999) The role of an alternative sigma factor in motility and pilus formation in the cyanobacterium *Synechocystis* sp. strain PCC 6803. *Proc Natl Acad Sci USA* **96**: 3188-3193.
- Buck, B.L., Alterman E., Svinegerod T., and Klaenhammer T.R. (2005) Functional analysis of putative adhesion factors in *Lactobacillus acidophilus* NCFM. *Appl Environ Microbiol* **71**:8344-8351.
- Calabi, E., Calabi F., Phillips A.D., and Fairweather N.F. (2002) Binding of *Clostridium difficile* surface layer proteins to gastrointestinal tissues. *Infect Immun* **70**:5770-5778.

- Claus, H., E. Akca, Debaerdemaeker T., Evrard C., Declercq J., Harris J., Schlott B., and König H. (2005) Molecular organization of selected prokaryotic S-layer proteins. *Can J Microbiol* **51**: 731-743.
- Cockell, C.S., and Knowland J. (1999) Ultraviolet screening compounds. *Biol Rev* **74**: 311-345
- Engelhardt, H. (2007) Are S-layers exoskeletons? The basic function of protein surface layers revisited. *J Struct Biol* **160**: 115-124.
- Ester, L., Foster J., and Brinkman F.S. (2010) PSORTb 3.0: improved protein subcellular localization prediction with refined localization subcategories and predictive capabilities for all prokaryotes. *Bioinformatics* **26**: 1608-1615.
- Garduno, R.A., Phipps B.M., and Kay W.W. (1995) Physical and functional S-layer reconstitution in *Aeromonas salmonicida*. *J Bacteriol* **177**: 2684-2694.
- Graham, L.L., and Beveridge T.J. (1990) Effect of chemical fixatives on accurate preservation of *Escherichia coli* and *Bacillus subtilis* structure in cells prepared by Freeze-Substitution. *J Bacteriol* **172**: 2150-2159.
- Hanaichi, T., Sato T., Iwamoto T., Malavasi-Yamashiro J., Hoshino M., and Mizuno N. (1986) A stable lead by modification of Sato's method. *J Electron Microsc* **35**: 304-306.
- Hihara, Y., Kamei A., Kanehisa M., Kaplan A., and Ikeuchi M. (2001) DNA microarray analysis of cyanobacterial gene expression during acclimation to high light. *Plant Cell* **13**: 793-806.
- Hoiczyk, E., and Baumeister W. (1995) Envelope structure of four gliding filamentous cyanobacteria. *J Bacteriol* **177**: 2387-2395.
- Hoiczyk, E., and Hansel A. (2000) Cyanobacterial cell walls: News from an unusual prokaryotic envelope, Minireview. *J Bacteriol* **182**: 1191-1199.
- Houwink, A.L. (1953) A macromolecular monolayer in the cell wall of *Spirillum* spec. *Biochim Biophys Acta* **10**: 360-366.
- Huang, F., Hedman E., Funk C., Kieselbach T., Schröder W.P., and Norling B. (2004) Isolation of outer membrane of *Synechocystis* sp. PCC 6803 and its proteomic characterization. *Mol Cell Proteomics* **6**: 586-595.
- Ikeuchi, M., and Inoue Y. (1988) A new 4.8-kDa polypeptide intrinsic to the PS II reaction center, as revealed by modified SDS-PAGE with improved resolution of low-molecular-weight proteins. *Plant Cell Physiol* **29**: 1233-1239.
- Jansson, C., and Northen T. (2010) Calcifying cyanobacteria – the potential of biomineralization for carbon capture and storage. *Curr Op Biotech* **21**: 365-371.

Jensen, T.E., and Sicko L.M. (1973) Fine structure of cell wall of *Gloeocapsa alpicola*, a blue-green alga. *Cytobiologie* **6**: 439-446.

Kahlig, H., Kolarich D., Zayni S., Scheberl A., Kosma P., Schaffer C., and Messner P. (2005) N-acetylmuramic acid as capping element of α -D-Fucose-containing S-layer glycoprotein glycans from *Geobacillus tepidamans* GS5-97^T. *J Biol Chem* **280**: 20292-20299.

Kaneko, T., S. Sato, H. Kotani, A. Tanaka, E. Asamizu, Nakamura Y. *et al.* (1996) Sequence analysis of the genome of the unicellular cyanobacterium *Synechocystis* sp. strain PCC6803. II. Sequence determination of the entire genome and assignment of potential protein-coding regions. *DNA Res* **3**: 109-136.

Kern, J., and Schneewind O. (2010) BslA, the S-layer adhesin of *B. anthracis*, is a virulence factor for anthrax pathogenesis. *Mol Microbiol* **75**: 324-332.

Karlsson, B., Vaara T., Lounatmaa K., and Gyllenberg H. (1983) Three-dimensional structure of the regularly constructed surface layer from *Synechocystis* sp. strain CLII. *J Bacteriol* **156**: 1338-1343.

Kawai, E., Akatsuka H., Idei A., Shibatani T., and Omori K. (1998) *Serratia marcescens* S-layer protein is secreted extracellularly via an ATP-binding cassette exporter, the Lip system. *Mol Microbiol* **27**: 941-952.

McCarren, J., Heuser J., Roth R., Yamada N., Martone M., and Brahamsha B. (2005) Inactivation of SwmA results in the loss of an outer cell layer in a swimming *Synechococcus* strain. *J Bacteriol* **187**: 224-230.

Mescher, M.F., and Strominger J.L. (1976) Structural (shape-maintaining) role of the cell surface glycoprotein of *Halobacterium salinarium*. *Proc Natl Acad Sci USA* **73** :2687-2691.

Mohamed, H.E., van de Meene A.M.L., Roberson R.W., and Vermaas W.F.J. (2005) Myxoxanthophyll is required for normal cell wall structure and thylakoid organization in the cyanobacterium *Synechocystis* sp. strain PCC 6803. *J Bacteriol* **187**: 6883-6892.

Mrázek, J., Bhaya D., Grossman A.R., and Karlin S. (2001) Highly expressed and alien genes of the *Synechocystis* genome, *Nucleic Acids Res* **29**: 1590-1601.

Peters, J., Nitsch M., Kuhlorgen B., Golbik R., Lupas A., Kellermann J. *et al.* (1995) *Tetrabrachion*: a filamentous archaeobacterial surface protein assembly of unusual structure and extreme stability. *J Mol Biol* **245**: 385-401.

Rippka, R., Deruelles J., Waterbury J.B., Herdman M., and Stanier R.Y. (1979) Generic assignments, strain histories and properties of pure cultures of cyanobacteria. *J Gen Microbiol* **111**: 1-61.

Sakiyama, T., Ueno H., Homma H., Numata O., and Kuwabara T. (2006) Purification and characterization of a hemolysin-like protein, SII1951, a nontoxic member of the RTX

protein family from the cyanobacterium *Synechocystis* sp. strain PCC 6803. *J Bacteriol* **188**: 3535-3542.

Sato, T. (1967) A modified method for lead staining of thin sections. *J Electron Microscop* **16**: 133.

Schirmer, A., Rude M.A., Li X., Popova E., and del Cardayre S.B. (2010) Microbial biosynthesis of alkanes. *Science* **329**: 559-562

Schultze-Lam, S., and Beveridge T.J. (1994) Nucleation of celestite and strontianite on a bacterial S-layer. *Appl Env Microbiol* **60**: 447-453.

Simon, R.D. (1981) Gliding motility in *Aphanothece halophytica*: Analysis of wall proteins in *mot* Mutants. *J Bacteriol* **148**: 315-321.

Sleytr, U.B., and Messner P. (1983) Crystalline surface layers on bacteria. *Ann Rev Microbiol* **37**: 311-339.

Sleytr, U.B., Huber C., Ilk N., Pum D., Schuster B., and Egelseer E.M. (2007) S-layers as a tool kit for nanobiotechnological applications. *FEMS Microbiol Lett* **267**: 131-144.

Smarda, J., (2002) S-layers on cell walls of cyanobacteria. *Micron* **33**: 257-277.

Spurr, A.R. (1969) A low-viscosity epoxy resin embedding medium for electron microscopy. *J Ultrastruct Res* **26**: 31-43.

Thompson, S.A., Shedd O.L., Ray K.C., Beins M.H., Jorgensen J.P., and Blaser M.J. (1998) *Campylobacter fetus* surface layer proteins are transported by a type I secretion system. *J Bacteriol* **180**: 6450-6458.

Vermaas, W.F.J., Williams J.G.K., and Arntzen C.J. (1987) Sequencing and modification of PsbB, the gene encoding the CP-47 protein of photosystem II, in the cyanobacterium *Synechocystis* sp. PCC 6803. *Plant Mol Biol* **8**: 317-326.

Walker, S.G., Karunaratne D.N., Ravenscroft N., and Smit J. (1994) Characterization of mutants of *Caulobacter crescentus* defective in surface attachment of the paracrystalline surface layer. *J Bacteriol* **176**: 6312-6323.

Yu, N.Y., Wagner J.R., Laird M.R., Melli G., Rey S., Lo R., Dao P., Sahinalp S.C., Sleytr U.B., and Beveridge T.J. (1999) Bacterial S-layers. *Trends Microbiol* **7**: 253-260.

Zhang, L., Lib L. and Wu Q. (2007) Protective effects of mycosporine-like amino acids of *Synechocystis* sp. PCC 6803 and their partial characterization. *J Photochem Photobiol* **86**: 240-245.

Zhang, L.F., Yang H.M., Cui S. X., Hu J., Wang J., Kuang T.Y. *et al.* (2009) Proteomic analysis of plasma membranes of cyanobacterium *Synechocystis* sp. strain PCC 6803 in response to high pH stress. *J Proteome Res* **6**: 2892-2902.

CHAPTER IV. DELETION OF *SLR0941* PROMOTES THE DEVELOPMENT OF A CAROTENOID ACCUMULATING PHENOTYPE IN *SYNECHOCYSTIS*

Abstract

In this part of the work a *Synechocystis* mutant was created by disruption of a gene whose location on the genome is highly conserved immediately next to an essential carotenoid biosynthesis ORF in a wide variety of cyanobacteria. This unknown gene (*slr0941*) was presumed to play a role in carotenoid metabolism. A majority of the deletion mutants initially displayed extended doubling times by a factor of two to three but produced carotenoids equal to the wild-type strain. However, a few deletion mutants divided at rates similar to the wild type but accumulated carotenoid precursors, especially under low-light conditions. This alternative phenotype originated from an adaptive secondary mutation. The accumulating carotenoids were identified by preparative and analytical HPLC as well as MS and appeared to be mainly isomers of the regular biosynthetic pathway. The (photo)conversion of the isomers was monitored in a time-lapse experiment on cultures that were exposed to high-light intensities. Light-exposure seemed to ameliorate the carotenoid phenotype by assisting in the conversion of carotenoid isomers. By preparation of membranes from mutant strains it was found that the accumulating carotenoids were mainly located in the CM. Based on the results obtained, it was concluded that *slr0941* could have the function of a carotenoid binding/transport protein.

Introduction

In cyanobacteria carotenoids are important chromophores that assume roles in light harvesting, quenching of chlorophyll triplets and reactive oxygen species (Steiger *et al.*, 1999; Fraser *et al.*, 2001), prevention of lipid peroxidation (Steiger *et al.*, 1999; El-Agamey *et al.*, 2004) as well as the stabilization of membranes and proteins (Havaux, 1998). The biosynthetic pathway leading to the formation of the four major carotenoids in *Synechocystis* (β -carotene, echinenone, zeaxanthin and myxoxanthophyll) is well characterized. Briefly, dimethylallyldiphosphate (DMAPP), the C₅-backbone for the production of geranylgeranyldiphosphate (GGPP), is synthesized via the non-mevalonate 2C-methyl-D-erythritol 4-phosphate pathway that, in the case of *Synechocystis*, accepts pyruvate and sugar phosphates from glycolysis and the pentose phosphate cycle (Hunter, 2007; Ershov *et al.*, 2002). A pair of C₂₀-GGPP molecules are condensed head-to-head by phytoene synthase to phytoene, the C₄₀-carotenoid backbone (Fig. IV-1). Usually, phytoene, a colorless carotenoid with three conjugated double bonds, is then desaturated to lycopene, a red-colored carotenoid with an extended system of de-localized π -electrons spanning eleven conjugated double bonds (Fig. IV-2). These desaturation steps are catalyzed either by a single bacterial-type desaturase (CrtI) in fungi, animals and most bacteria (Giuliano *et al.*, 1986, Giraud *et al.*, 2004), or by two distinct plant-type desaturases (CrtP, CrtQ) in plants and cyanobacteria (Sandmann, 2002). While CrtI-type desaturases successively oxidize phytoene to neurosporene or lycopene (Harada *et al.*, 2001), the plant-type enzymes CrtP and CrtQ frequently produce partially desaturated carotenoid isomers, and are thus supported by carotenoid isomerases (Masamoto *et al.*, 2001; Chen *et al.*, 2010) to create valid substrates for further modifications of the polyene chain. Although the lack of enzyme-catalyzed isomerization is non-lethal, affected cells accumulate carotenoid isomers that are invalid substrates for downstream processes. This

effect can be ameliorated by exposure of cells to higher light intensities, which increases the rate of photoisomerization, whereas continuous growth in darkness results in a dramatic decrease of finalized carotenoids (Masamoto *et al.*, 2001).

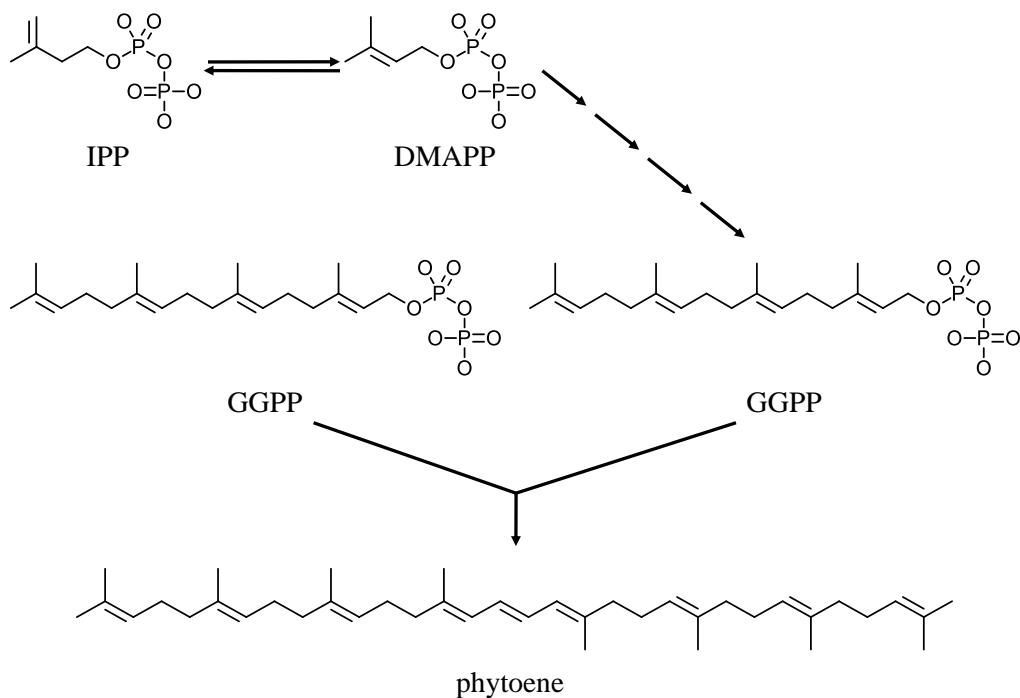


Fig. IV-1: Biosynthesis of phytoene from dimethylallylpyrophosphate (DMAPP) via geranylgeranylpyrophosphate (GGPP). Four molecules of DMAPP are successively condensed to form GGPP. In turn, two molecules of GGPP are condensed head-to-head, giving phytoene, the first carotenoid polyene.

In this work the effect of the deletion of a highly conserved cyanobacterial protein, Slr0941, was studied. Its deletion resulted in growth retardation and eventually the development of a carotenoid accumulation phenotype that was strikingly similar to the one of a carotenoid isomerase deficient strain as described by Masamoto *et al.*, (2001). Based on the experimental data and the analysis of the amino acid sequence of Slr0941, a role of this protein in carotenoid channeling between a carotenoid isomerase and other enzymes at the site of biosynthesis is proposed.

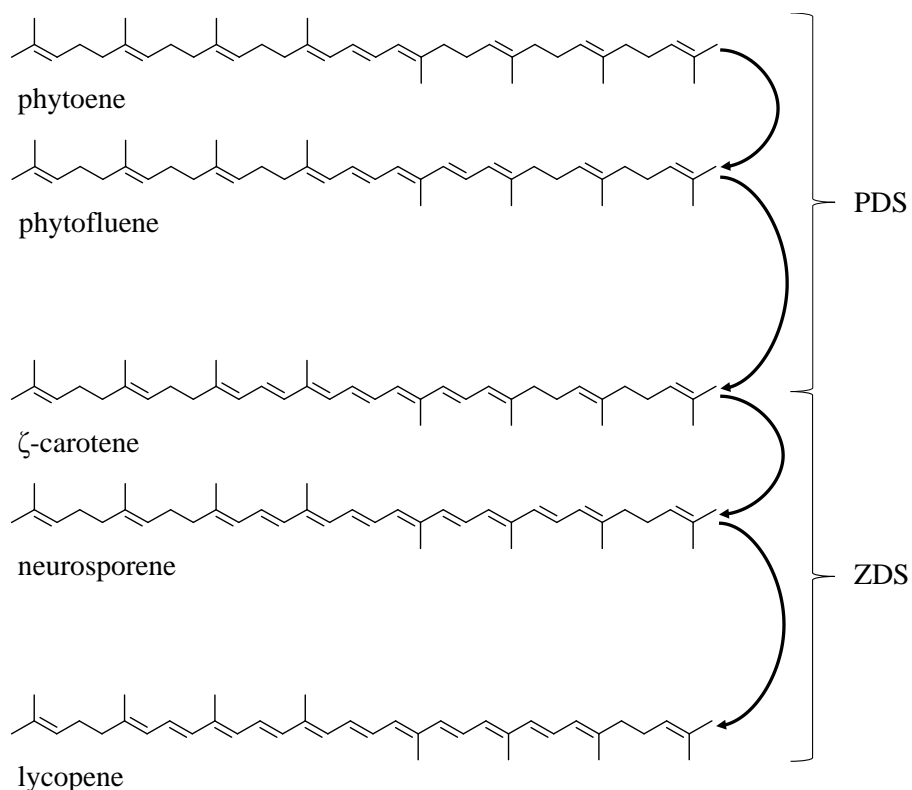


Fig. IV-2: Desaturation scheme of phytoene to lycopene in plants and cyanobacteria. The reactions are catalyzed by two distinct enzymes, phytoene desaturase (PDS) and ζ-carotene desaturase (ZDS).

Methods

Strains were prepared and grown as described in chapter III, page 37.

Analysis of carotenoid isomers

Preparative HPLC was performed as outlined in chapter III, page 42. Carotenoid isomers that could not be separated on the semipreparative column were collected at the time of elution (if necessary combined from multiple runs), the solvent evaporated in a speed-vac in darkness, and the pigments resuspended in 150 – 200 μl of methanol. The carotenoids were then loaded onto a Waters YMC carotenoid C₃₀-reversed phase column (3 μm, 4.5 × 250 mm) and separated with the solvents A (methanol/*tert*-butylmethyl ether/water = 80:15:5 (v/v/v)) and B (methanol/*tert*-butylmethyl ether/water = 6:90:4) in a 65 minute

gradient at a continuous flow rate of 1 ml/min: 100% A from 0 – 5 min, 100% - 30% A from 5 – 55 min, 30% - 0% A from 55 – 60 min, 0% A from 60 – 61 min, 0% - 100% A from 61 – 65 min.

Results

Analysis of the slr0941 coding region

The ORF *slr0941* is a highly conserved, 444 bp comprising coding region with orthologs in a variety of other cyanobacteria. At least 20 orthologs share a minimum amino acid identity of 50 percent throughout the entire coding length. Similar gene products are present in plants such as *Arabidopsis thaliana*, sharing 40 out of approximately 150 identical amino acids with Slr0941, and *Zea mays*. The *slr0941* gene as well as many orthologs of this ORF are often found in the immediate vicinity downstream of cyanobacterial ζ -carotene desaturase genes (Fig. IV-3). Many cyanobacterial orthologs have been annotated as “cyclase/dehydrase”, apparently without clear experimental support. According to a conserved domain query (Marchler-Bauer *et al.*, 2009) the Slr0941 protein belongs in the SRPBCC (START/RHO_alpha_C/PITP/Bet_v1/CoxG/CalC) domain superfamily that contains a deep hydrophobic ligand-binding pocket binding diverse ligands. Proteins in this family may be involved in lipid transfer, aromatase/cyclase reactions, etc. (Das and Khosla, 2009) or serve as a polyketide cyclase. In silico analysis also indicates probable water solubility and the absence of transmembrane regions. The *Arabidopsis* orthologs, of which at least three exist, code for ca. 70 additional amino acids at the 5'-end. This C-terminal region encodes a chloroplast targeting signal (Fig. IV-4). All *Arabidopsis* genes have predicted hydrophobic ligand binding sites.


```

S. PCC 6803 -----
AT1G02475 MSVVAIN-MNTINHLSKTCKTPNIQSPICFDR---KPFYSYSLIPLFPKTLNGFSSYSS-- 54
AT4G01883.1 MSATAILSVNNPKDLVTGFGNRTFHSRSNFAKPSRSLFPSSSSPMKPLTLA--SRFSP-- 56
AT1G02470.2 MSSIASGTVSTTRSTLCFRKIPKSATVLSMLHR-----SSSSSPRMLLLLLSSSSANSACL 55

S. PCC 6803 -----MANWLEHS-VQVEVDAPIELVWQLWSDLEQMPRWMKWIDSVK 41
AT1G02475 SVSRRSRFIIIPKRRRFSVSMWQDCS-VKMEVDVPVSVAYNFYLDRESFPKWMPPFISSVQ 113
AT4G01883.1 LISTNRSFKSSVFRFDTLMEWQECK-VKMKVEVPVSVAYGLYSERESIPKWMTFIISVK 115
AT1G02470.2 LNSNNGLLISSSPKFRPVMQVDVTRVKMVVDAPASVAYKLYADREMFPKWMPPFLSSVE 115
          :* : . *:: *:* * .::: :: : * :*:* :*:*:
S. PCC 6803 VLEDNPDLSRWKLAGS----SLEFTWLSRTKLSQQIIQWESVDGLPNRGAVRFYDR-H 96
AT1G02475 VLKDKPDLSRWSLKYNAFGQDIKYSWLARNLQPTPNQKIHWSLEGLPNKGSVRFPPKGP 173
AT4G01883.1 VLKDKPDLSRWTLKYKAFGQNLLEYAWLAKNLQPLPNQKIHWSLEGLPNKGTVRFFPLGP 175
AT1G02470.2 AMEGSPDLSRYLVKLESFGQNI EYHFLAKNLQPI PDRKIHWSIEGFENRGSVRFPPRGP 175
          .....*****: : : : : : : : : *:* *:* *:* *:* *:*
S. PCC 6803 GKSIVRLTIAYSVPGWLALLMDNFLGRVVESTIQADLERFREYINNLQAS 147
AT1G02475 SSCIVELTVSYEVPALLTPVASVLRP--FIESLLRGLLERFAALAKTT--- 219
AT4G01883.1 SSCDVELTFAYEVPLLLIPFAAALQP--LMQGLIKNSLEQFAEIAKSTKTT 224
AT1G02470.2 SSCLVEISFSYEVPNAPVAFAMKP--FMEKIIIRGGLERFAAFVKTI--- 221
          ... * .: : : * .** : . : : : : : : : : .**:* :.

```

Fig. IV-4: Alignment of *slr0941* with the three *A. thaliana* orthologs.

Segregation of $\Delta slr0941$ deletion strains

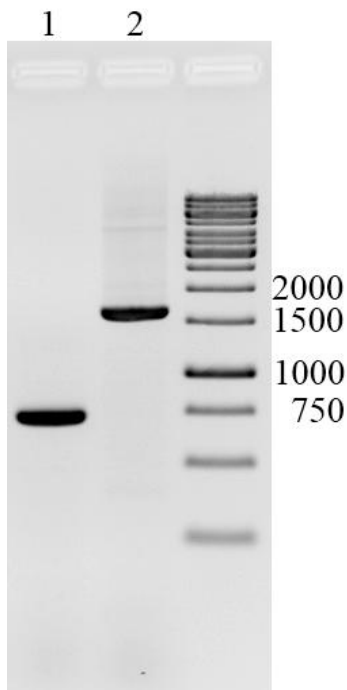


Fig. IV-5: 1% Agarose gel image of PCR fragments of the *slr0941* loci in the *Synechocystis* wild type strain (lane 1) and the fully segregated mutant $\Delta slr0941$ v2 (lane 2). The expected fragment lengths are 717 bp and 1641 bp for the wild-type locus and the locus interrupted with a kanamycin-resistance cassette, respectively.

Although during segregation strains were grown photomixotrophically under low light intensity conditions of $<5 \mu\text{mol photons m}^{-2} \text{s}^{-1}$, homozygosity was not reached for the $\Delta slr0941$ v1 strain with the Km cassette oriented anti-sense to the upstream located ζ -carotene desaturase, even at high selective pressure of 1.5 mg/ml kanamycin on plate. When maintained on plate at $2 \mu\text{mol photons m}^{-2} \text{s}^{-1}$ cultures of partially segregated $\Delta slr0941$ v1 secreted an uncharacterized yellow substance, an effect that could not be observed for cultures grown at $50 \mu\text{mol photons m}^{-2} \text{s}^{-1}$. Liquid cultures

of $\Delta slr0941$ v1 had a tendency to aggregate at $50 \mu\text{mol photons m}^{-2} \text{s}^{-1}$ while aggregation did not occur at $2 \mu\text{mol photons m}^{-2} \text{s}^{-1}$. Since both other strains reached complete segregation (Fig III-5, not shown for $\Delta slr094X$) the focus was shifted towards these strains. Initially, $\Delta slr0941$ v2 did not assume any carotenoid phenotype when grown under various light regime, However, doubling times of this mutant (24 ± 2 h) were increased by a factor of approximately two compared to the wild type strain (12 ± 1 h) under low intensities of 5 and three when grown at $50 \mu\text{mol photons m}^{-2} \text{s}^{-1}$ (Fig. IV-6, 7). Because of its slow growth this mutant was named $\Delta slr0941$ G. Curiously, certain mutants clones with the same gene deletion appeared to have shorter doubling times - these were named $\Delta slr0941$ C because they also developed a carotenoid phenotype.

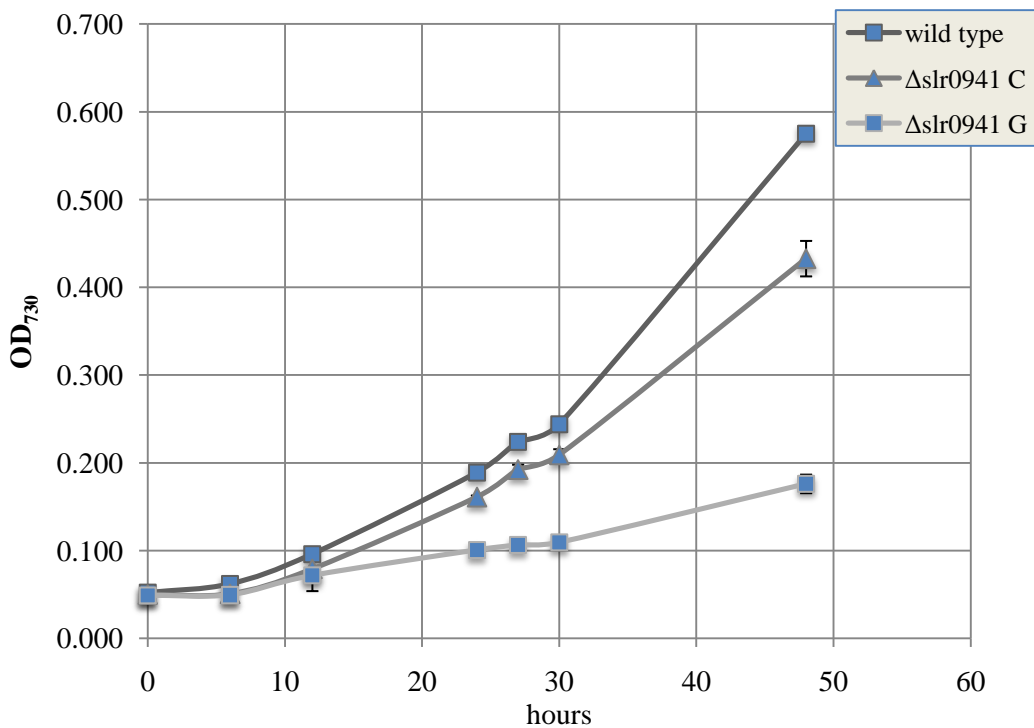


Fig. IV-6: Growth performance at $5 \mu\text{mol photons m}^{-2} \text{s}^{-1}$ of photomixotrophically grown strains of wild type (WT), carotenoid-phenotype mutant $\Delta slr0941$ C and slow-growth phenotype $\Delta slr0941$ G. Data of three independent experiments are shown.

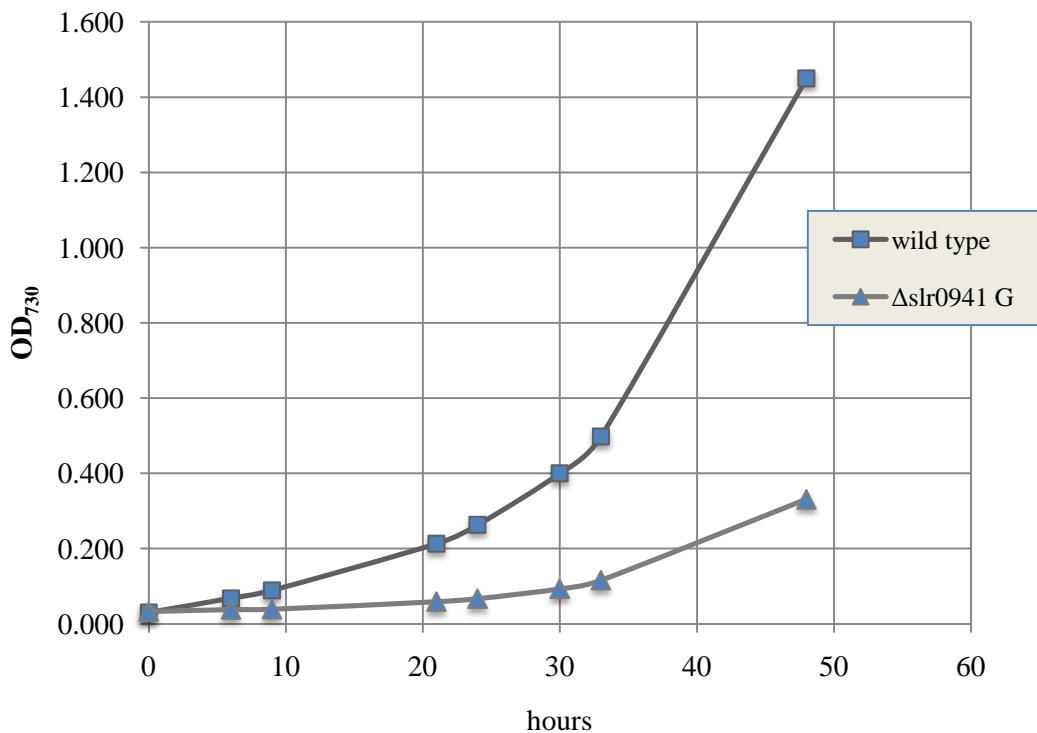


Fig. IV-7: Growth performance of photomixotrophically grown strains of wild type (WT), and slow-growth phenotype $\Delta slr0941$ G at $50 \mu\text{mol photons m}^{-2} \text{s}^{-1}$. Data from three different experiments are shown.

Pigment profiles of $\Delta slr0941$ deletion strains

The adjacency of *slr0941* to *slr0940*, the ζ -carotene desaturase gene, in *Synechocystis* that is conserved in many other cyanobacteria suggests a role of Slr0941 in carotenoid biosynthesis. This was analyzed by extraction of pigments from $\Delta slr0941$ with methanol and analysis thereof by HPLC. Even though the majority of $\Delta slr0941$ v2 segregants had pigment profiles that were qualitatively identical to the wild-type profile under a variety of light intensities tested (2 , 50 and $180 \mu\text{mol photons m}^{-2} \text{s}^{-1}$), two out of 10 segregants had developed a different profile when grown continuously at $5 \mu\text{mol photons m}^{-2} \text{s}^{-1}$, showing a significantly lower content of all native carotenoids while accumulating uncharacterized carotenoids in the more hydrophobic area between echinenone and β -

carotene (Fig. IV-8, Table III-1). Strains exhibiting this carotenoid phenotype had doubling times almost equal to the wild-type strain.

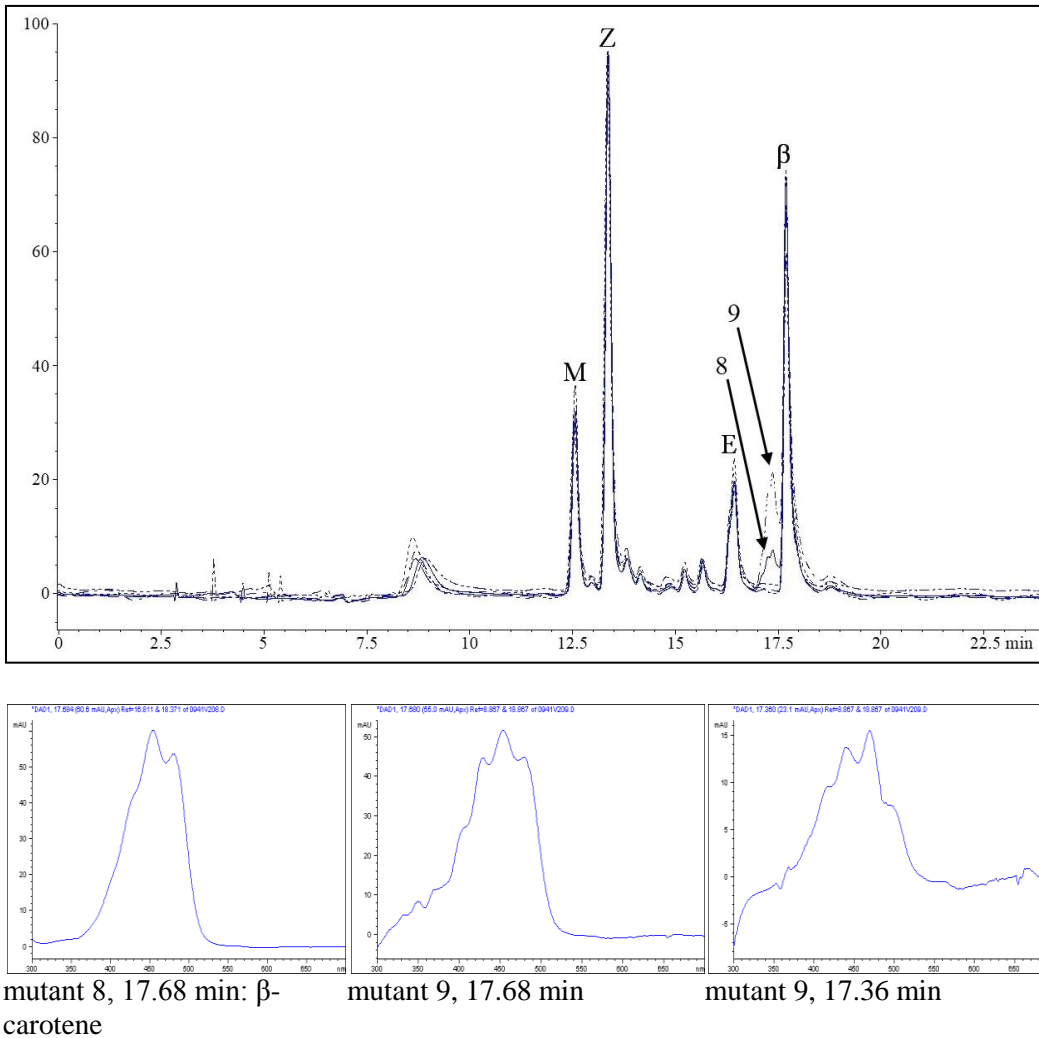


Fig. IV-8: Overlay of elution profiles monitored at 480 nm of methanol extracts from segregated $\Delta slr0941v2$ mutants grown at $5 \mu\text{mol photons m}^{-2} \text{s}^{-1}$. For the sake of clarity spectra of only five of the ten clones were combined, two of which were accumulating carotenoid precursors at an elution time of about 17.5 minutes (solid and dashed lines). Spectra of carotenoids eluting at specific time points from different segregants - mutant 8 exhibiting a slow-growth phenotype, mutant 9 exhibiting a carotenoid phenotype - at these time points are indicated in lower panels. *Synechocystis* native carotenoids are myxoxanthophyll (M), zeaxanthin (Z), echinenone (E) and β -carotene (β).

To assess a possible pseudoreversion, control experiments were performed in which *Synechocystis* wild-type cells were transformed with genomic DNA from $\Delta slr0941$ G, or

with genomic DNA from $\Delta slr0941$ C displaying the carotenoid phenotype (Fig. IV-9), respectively. Segregation of the transformants resulted in slow-growing strains with normal carotenoid profiles in both cases, suggesting that the carotenoid phenotype is the result of a pseudoreversion event.

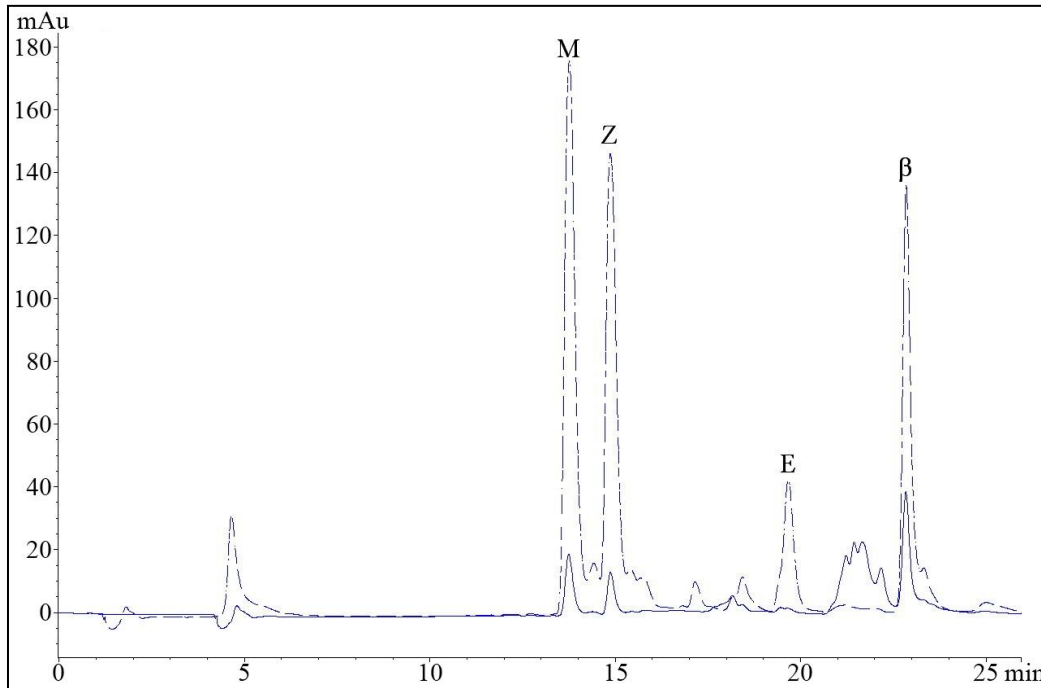


Fig. IV-9: Overlay of HPLC pigment elution profiles of wild type (dashed line) and $\Delta slr0941$ C (solid line) grown at $5 \mu\text{mol photons m}^{-2} \text{s}^{-1}$. Pigments extracted from equal amounts of cells were detected at 480 nm. Contents of myxoxanthophyll (M), zeaxanthin (Z), echinenone (E) and β -carotene (β) had dropped significantly in the mutant strain whereas various uncharacterized pigments eluted between minutes 21 and 22.5. Absorbance was normalized to chlorophyll levels at 665 nm.

Table IV-1: Peak intensities of pigments in the carotenoid accumulating mutant $\Delta slr0941$ C compared to the *Synechocystis* wild-type strain at their corresponding absorption wavelength maxima (myxoxanthophyll = 475 nm; zeaxanthin, echinenone and β -carotene = 453 nm; chlorophyll = 665 nm). Numbers in parenthesis are values not taken at maximum absorbance for this pigment.

	475 nm	453 nm	665 nm
myxoxanthophyll	8 %	(8 %)	n/a
zeaxanthin	(6 %)	6 %	n/a
echinenone	(4 %) ¹	16 % ¹	n/a
β -carotene	(22 %) ¹	49 % ¹	n/a
chlorophyll	n/a	(68 %)	65 %

⁽¹⁾ the β -carotene peak was not fully separated from other peaks

The assumption of a pseudoreversion was also supported by the colony-size heterogeneity that the $\Delta slr0941$ strain developed over time in plate cultures (Fig. IV-10), which was most likely due to shortened doubling times of cells in colonies carrying a secondary mutation.

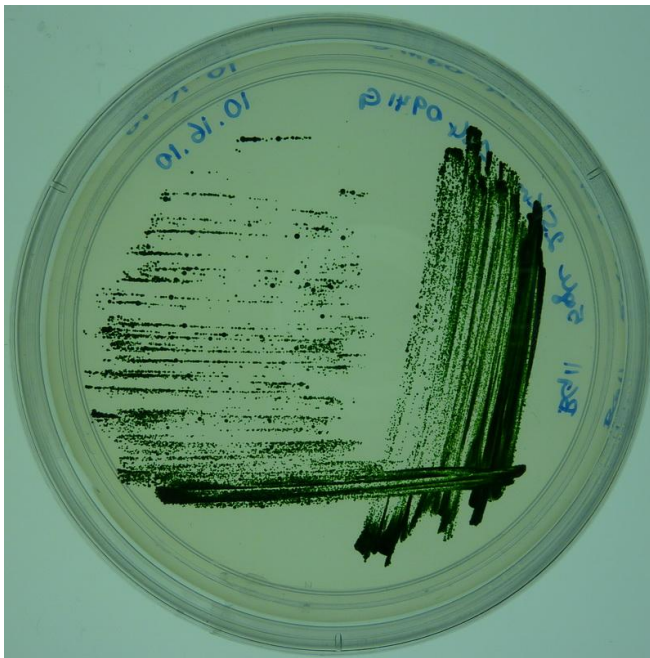


Fig. IV-10: A plate culture of slow-growing mutant $\Delta slr0941$ after several rounds of replating. The heterogenous appearance originates from faster growing cells that had presumably undergone pseudoreversion.

Based on these observations the two known *Synechocystis* carotenoid isomerase genes *slr0033* and *slr1599* were screened for mutations by sequencing and no mutations were found. Furthermore, an attempt was made to rescue the carotenoid phenotype of $\Delta slr0941$ C by transforming it with the subcloned native copy of *slr0941* on the plasmid *pslr0941*

His Sp. C-terminal His-tagging of *slr0941* with pslr0941 His Km did not produce a carotenoid phenotype in a wild-type strain and was therefore assumed not to interfere with *slr0941* expression (data not shown). Transformation of Δ *slr0941* C with pslr0941 His Sp replaced *slr0941* interrupted with a Km resistance cassette with the native, His-tagged gene followed by a Sp resistance cassette (Fig IV-11).

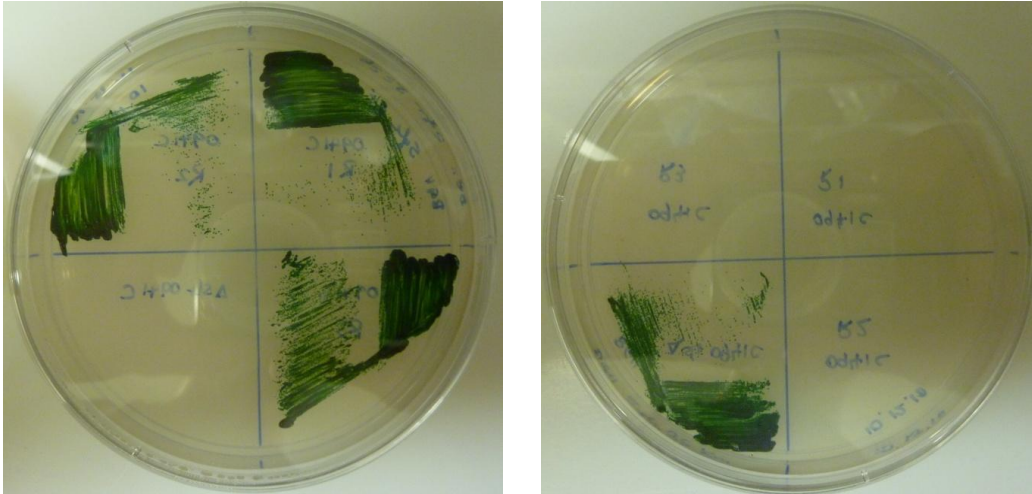


Fig. IV-11: Three clones of Δ *slr0941* that had been transformed with pslr0941 HIS Sp were plated in on the left plate (BG-11, 5 mM glucose, 25 µg/ml spectinomycin), and the right plate (BG-11, 5 mM glucose, 25 µg/ml kanamycin). Untransformed Δ *slr0941* was plated in the lower left corner of both plates.

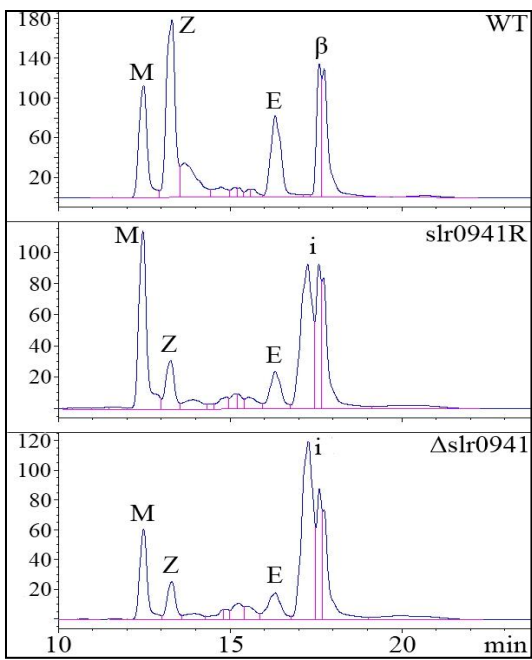


Fig. IV-12: HPLC absorption traces of wild type (WT), rescued Δ *slr0941* mutant (*slr0941R*) and Δ *slr0941* strains. *Synechocystis* native carotenoids myxoxanthophyll (M), zeaxanthin (Z), echinenone (E) and β -carotene (β) are present in all strains but reduced in *slr0941R* and Δ *slr0941*. Small amounts of β -carotene co-elute in rescued and mutant strains with carotenoid isomers (i).

Although the rescued strains were grown at high concentrations of Sp (>100 µg/ml) and had lost their resistance to Km, a rescue of the carotenoid phenotype was not observed (Fig. IV-12).

The segregated double-deletion strain $\Delta slr094X$ was highly light sensitive due to the absence of *slr0940*, the ζ -carotene desaturase gene (*CrtQ-2*) that catalyses the symmetric desaturation of ζ -carotene to lycopene via neurosporene (Breitenbach *et al.*, 1998; Sandmann, 2009). Therefore, the pigment profiles of $\Delta slr094X$ showed a complete absence of all native carotenoids and a significant accumulation of ζ -carotene (Fig. IV-13).

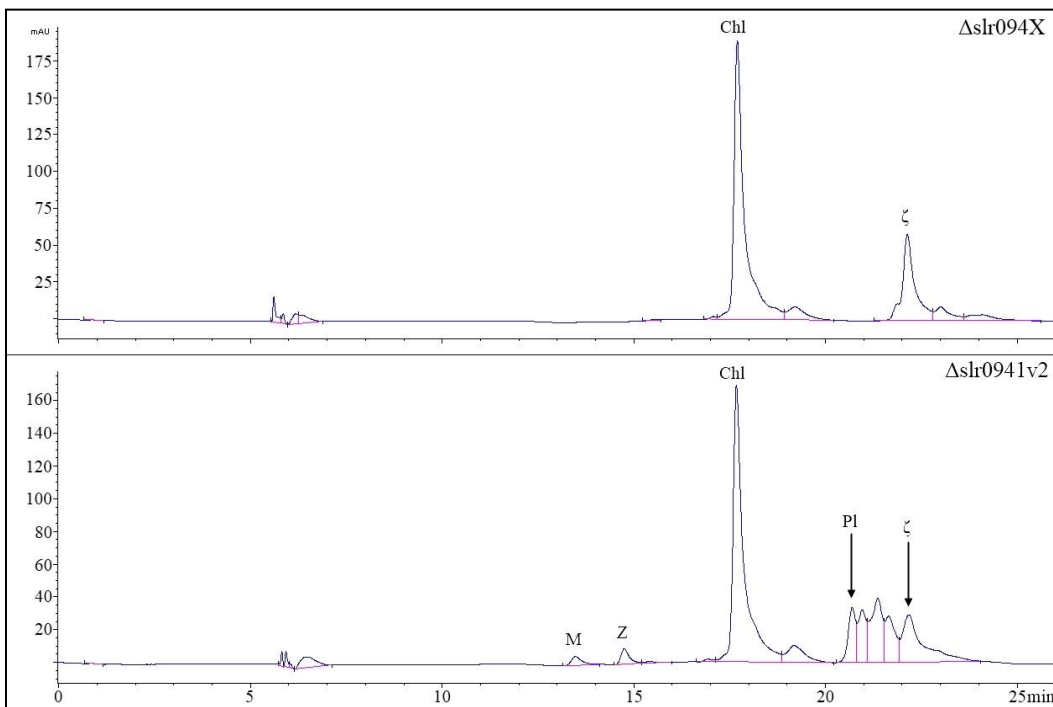


Fig. IV-13: HPLC spectra of pigment extracts from $\Delta slr094X$ (top) and $\Delta slr0941$ C (bottom) grown photomixotrophically at $0.4 \mu\text{mol photons m}^{-2} \text{s}^{-1}$. The absorption was monitored at 440 nm to indicate the presence and amount of chlorophyll (Chl) in both strains, as well as myxoxanthophyll and zeaxanthin (Z) peaks in the single mutant. $\Delta slr094X$ accumulated ζ -carotene (ζ), and small amounts of other partially unsaturated carotenoid precursors whereas the *slr0941* C single mutant accumulated prolycopene (PI, (7,9,7',9'-tetrakis lycopene; Zechmeister *et al.*, 1941) and a variety of unidentified carotenoids between 20.5 and 24 minutes.

When both $\Delta slr094X$ and $\Delta slr0941$ C were grown at only $0.4 \mu\text{mol photons m}^{-2} \text{s}^{-1}$, the $\Delta slr0941$ C single mutant was still able to produce small amounts of native carotenoids, indicating a dominance of ζ -carotene deletion (having resulted in a complete biosynthetic stop at the stage of ζ -carotene) over the $slr0941$ single gene deletion.

Since the pigments accumulating in $\Delta slr0941$ C could not be separated well enough on a semipreparative column for a more detailed analysis, they were collected and loaded onto an analytical YMC carotenoid column. Based on the shapes of the absorption spectra as well as their absorption maxima pigments were identified as various isomers of three major carotenoid intermediates: ζ -carotene, neurosporene and lycopene (Fig. IV-14).

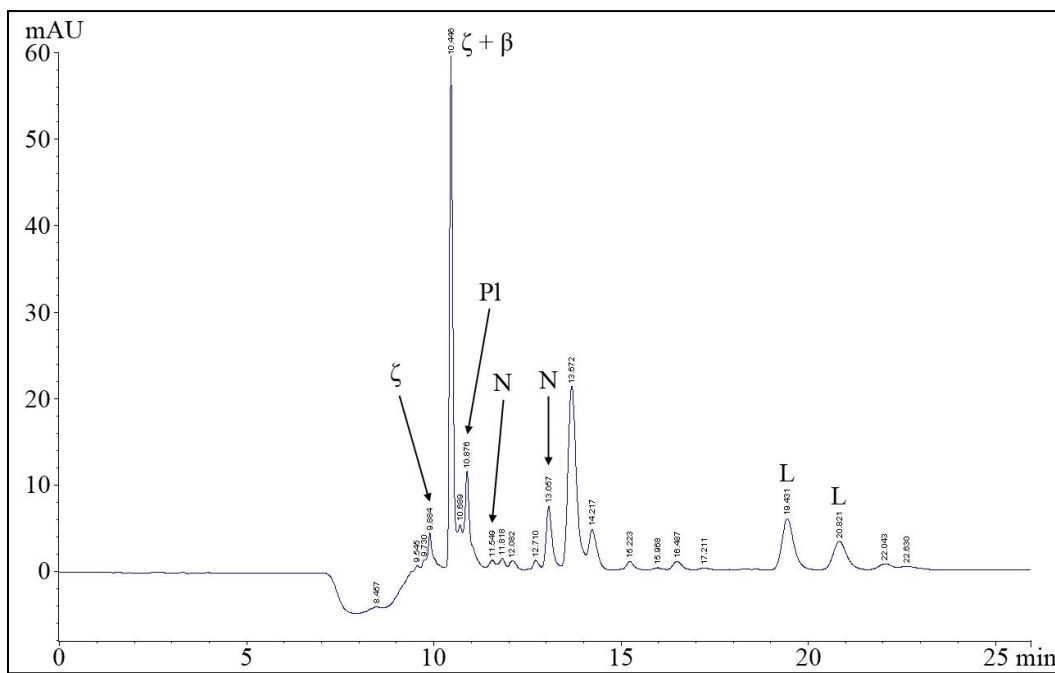


Fig. IV-14: HPLC spectrum of pigments accumulating in the mutant $\Delta slr0941$ C, separated by a 26-minute water/methanol/ethyl acetate gradient. Absorption for this spectrum was monitored at 480 nm. The peaks were identified by their spectra and absorption maxima. The major components present were different isomers of ζ -carotene (ζ ; 9.884), β -zeacarotene and ζ -carotene ($\zeta + \beta$; 10.446), polycopene (PI; 10.876), neurosporene isomers (N; 11.549, 13.057) and lycopene isomers (19.431, 20.821).

For a more detailed analysis with respect to compound masses, a mixture of carotenoid precursors that had been pre-purified on the semipreparative column was then subjected to mass spectroscopy.

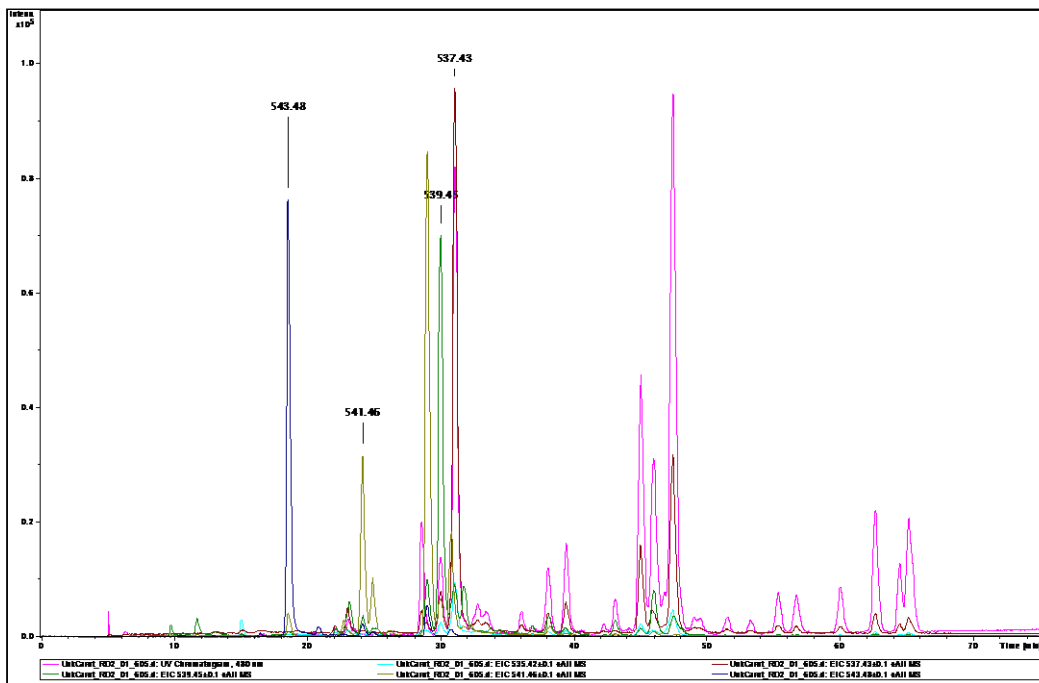


Fig. IV-15: Combined mass trace/absorption profile of carotenoid precursors accumulating in LAHG-grown $\Delta slr0941$ C. Accumulating pigments were separated on a YMC carotenoid column. Their absorption at 480 nm is shown in pink color. The masses of eluted pigments were analyzed by photoionization mass spectrometry. Abundances of carotenoid masses were combined with the absorption profile, time-corrected and overlaid. Different masses are indicated by differently colored peaks as labeled.

Comparison of mass abundances as indicated by different colors in Fig. IV-15 with the HPLC elution profile of the same sample (Fig. IV-14) confirmed the presence of carotenoid precursors, mainly polycopene, but also several isomers of ζ -carotene, neurosporene and lycopene. Minor amounts of phytofluene and β -carotene were identified by matching online spectra with their corresponding mass data. Due to a limitation of the HPLC system no absorption spectrum was obtained. However, phytofluene could be assigned based on its mass, its early appearance in the spectrum, and data from other experiments (Table IV-2). Of the mixture of ζ -carotenes the

dominant isomer appeared to be the *dicis*-form because of its absorption properties and III/II-peak ratios (being ~100 %) as *tricis*-isomers are often hypsochromically shifted (Breitenbach and Sandmann, 2005; Chen *et al.*, 2010). The structures of carotenoids eluted after 32 minutes are less clear.

Table IV-2: Identification of carotenoids with respect to elution times, mass and online spectra.

carotenoid	elution time	λ peaks (nm)	abundance	matching spectrum	mass
phytofluene isomer	19.501	-	+	(none)	542
ζ -carotene isomer	24.167	(360:)379:400:424	(trace)	ζ -carotene	540
dihydro-zeacarotene	24.641	(358:)376:395:420	(trace)	β -zeacarotene	540
ζ -carotene	27.415	(360:)380:401:426	+	ζ -carotene	²
ζ -carotene isomer	27.670	(360:)380:402:426	(trace)	ζ -carotene	540
neurosporene isomer	27.913	(389:)410:433(:459)	++	(multiple)	538
prolycopene	28.478	417:439:465	+++	prolycopene	536
¹	32.598	(421:)443:469			536/538 ³
¹	33.343	(417:)440:465			536
¹	34.887	(439:)462:489	(trace)		536
¹	35.331	420:440:469	+		540
β -carotene isomer	36.224	(423:)447:468	++	β -carotene	536
all-trans neurosporene	36.900	(418:)443:468(:493)	+		538
¹	37.463	(422:)448:471	+		536
¹	39.515	440:465:494	(trace)		536
all-trans lycopene	43.555	(444:)471:497	+	lycopene	536
¹	44.905	(450:)471:501	+		536

- (1) Compounds that produced a peak in the HPLC profile but could not be identified due to a missing spectrum match are indicated with their elution times.
- (2) The reported mass for ζ -carotene was inconclusive but the online spectrum indicated the presence of this carotenoid.
- (3) Mass traces for this unidentified carotenoid overlapped.

Masses of 538 and 536 indicate the presence of at least nine double bonds, and correspond to those of isomers of neurosporene and lycopene, respectively. The presence of a large number of carotenoid isomers is similar to what was observed in a carotenoid isomerase deficient strain ($\Delta sll0033$) that has been described previously (Breitenbach *et al.*, 2001; Masamoto *et al.*, 2001). Although the mutant analyzed here was a second-site mutant, sequencing of *sll0033* and *slr1599* in this strain confirmed the absence of mutations in these ORFs, suggesting a different cause for the accumulation of carotenoids.

In an experiment without a light-sensitizer, exposure of carotenoid precursors extracted from the LAHG-grown mutant strain $\Delta slr0941$ to high light intensities did not obviously change the isomerization states of these pigments (data not shown). However, in intact cells a transition from LAHG-growth to regular ($50 \mu\text{mol photons m}^{-2} \text{ s}^{-1}$, not shown because the effect was more dramatic on exposure to higher light intensity) or light intensities of $140 \mu\text{mol photons m}^{-2} \text{ s}^{-1}$, (Fig. IV-16, 17, 18) resulted in significantly different carotenoid profiles. After 6 hours of exposure to $140 \mu\text{mol photons m}^{-2} \text{ s}^{-1}$ only small amounts of myxoxanthophyll, zeaxanthin and echinenone had formed, when compared to the residual presence of prolycopene. These native pigments were virtually absent at the zero time point while levels of β -carotene were barely detectable. Upon light exposure the β -carotene content rose quickly to an intermediate level as shown in Fig. IV-16, 480 nm trace (elution time for β -carotene was 17.6 min) and remained almost constant between 2.5 and 6 hours of illumination. Carotenoid precursors still contributed the strongest signals after 6 hours of illumination, and their signal had only slightly dropped after 20 hours of exposure to $140 \mu\text{mol photons m}^{-2} \text{ s}^{-1}$ (data not shown), at which β -carotene was present as a dominant peak among a variety of carotenoid isomers such as lycopene at minute 17 on the HPLC spectrum. All other native carotenoids

showed a strong presence after 6 hours of illumination. Changes in pigment composition between hours 6 and 28 were minimal, mainly with a further reduction on carotenoid precursors (data not shown).

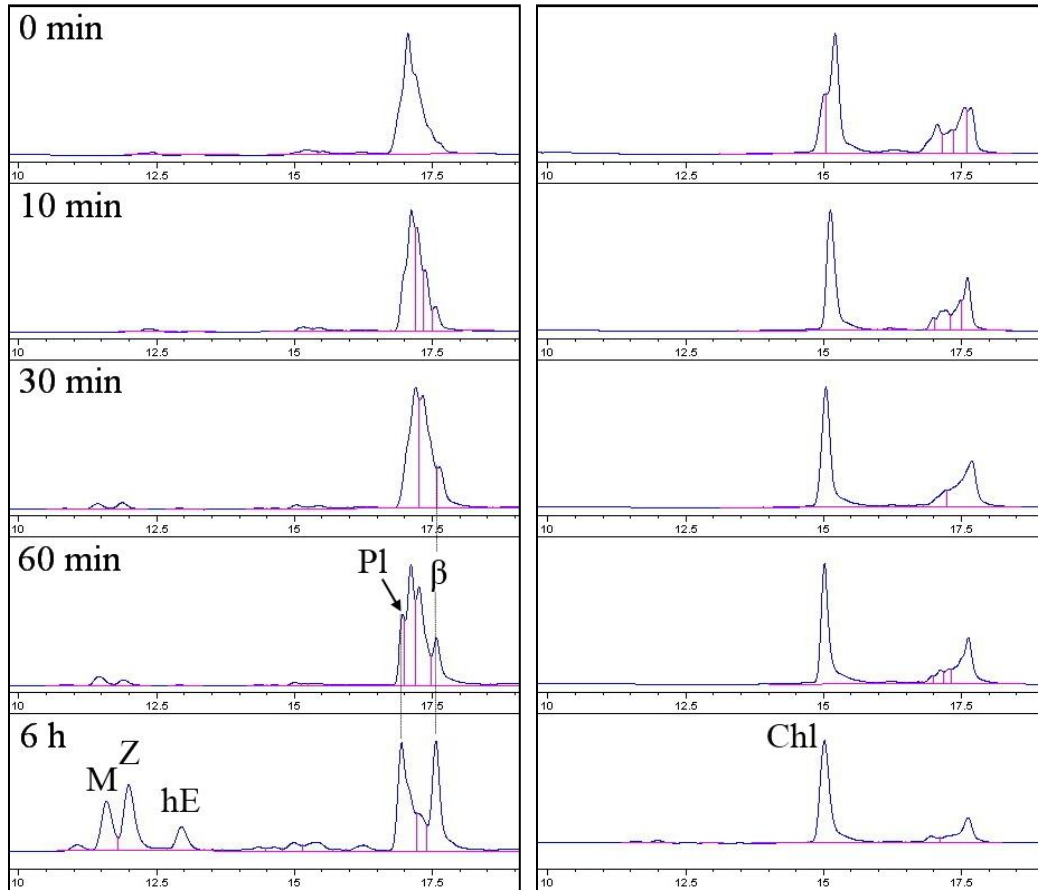


Fig. IV-16: HPLC spectra of carotenoid precursors from $\Delta slr0941$ after increasing times of exposure of cells to $140 \mu\text{mol photons m}^{-2} \text{s}^{-1}$. Native carotenoids myxoxanthophyll (M), zeaxanthin (Z), hydroxyechinenone (hE) eluted between 11.5 and 13 minutes were mostly absent until 30 minutes of illumination. Light-catalyzed changes in carotenoid composition are reflected in significant changes of the absorption trace between elution time 16.5 and 18 min as can be seen at both absorption wavelengths of 480 nm (left) and 350 nm (right). P1 = prolycopene, β = β -carotene, Chl = chlorophyll.

The exposure to $140 \mu\text{mol photons m}^{-2} \text{s}^{-1}$ accelerated the photo-conversion process: Traces of myxoxanthophyll and zeaxanthin were detectable after 30 min of illumination while after 6 hours, when carotenoid precursors were still present, all native carotenoids were prevalent in the HPLC spectrum. Since the semipreparative column could not

separate the carotenoid precursors, they were collected and loaded onto the YMC analytical carotenoid column. The absorption trace at 350 nm (Fig. IV-17) indicated significant presence of phytofluene and ζ -carotene. Although prolonged illumination did not result in disappearance of these compounds, photoisomerization occurred and changed the structural properties of the pigments. A variety of different ζ -carotene isomers had formed after 6 hours of exposure to $140 \mu\text{mol photons m}^{-2} \text{s}^{-1}$ eluting between minutes 25 and 32. However, ζ -carotene was present at very low abundance. β -carotene was also present among these peaks.

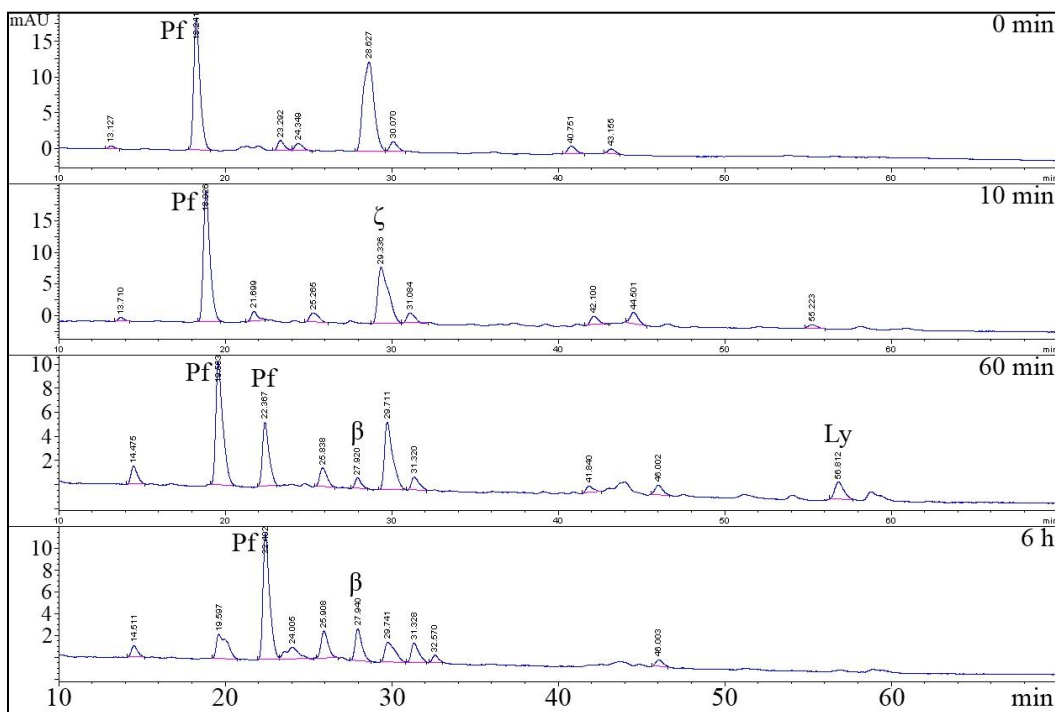


Fig. IV-17: 350 nm absorption trace of carotenoids purified between 16.5 and 18.5 min (Fig. IV-13) of an LAHG-adapted culture of $\Delta\text{slr0941 C}$ after 0, 10, 60 and 360 min (top to bottom) of illumination at $140 \mu\text{mol photons m}^{-2} \text{s}^{-1}$. Phytofluene (Pf) was one of the major carotenoids present throughout all times of detection. Photoisomerization produced different isomers of ζ -carotene (ζ) as well as a small amount of β -carotene (β) via a temporary lycopene (Ly) intermediate that was detected after 60 min of light exposure. Only the peaks that could be unequivocally assigned according to their spectra were labeled. The slight shift in elution time was most likely due a compression of the matrix of the YMC carotenoid column after multiple runs.

The initially dominating phytofluene peak had almost disappeared and a different, slightly more hydrophobic isomer had formed on the HPLC spectrum. The appearance of additional phytofluene- and ζ -carotene peaks was presumably due to a *cis*-to-*trans* isomerization of the precursors that had accumulated during LAHG-growth and higher degree of *trans*-configuration generally increased the hydrophobicity of the compound.

Prolycopene was the major component detected at 480 nm before light exposure while neurosporene was present in smaller amounts (Fig. IV-18). Various isomers of neurosporene had emerged after 10 minutes of light exposure and they dominated the chromatogram between minutes 40 and 65. Prolycopene had almost completely disappeared after 60 minutes of illumination whereas significant amounts of lycopene and later β -carotene had formed. Lycopene (isomer) peaks had completely replaced the strong presence of neurosporene after 60 minutes of illumination at elution times between 50 and 60 minutes. After 6 hours of $140 \mu\text{mol photons m}^{-2} \text{s}^{-1}$ the dominant carotenoid absorbing at 480 nm was β -carotene. Small amounts of lycopene (and isomers) were still present and were eluted between minutes 55 and 60.

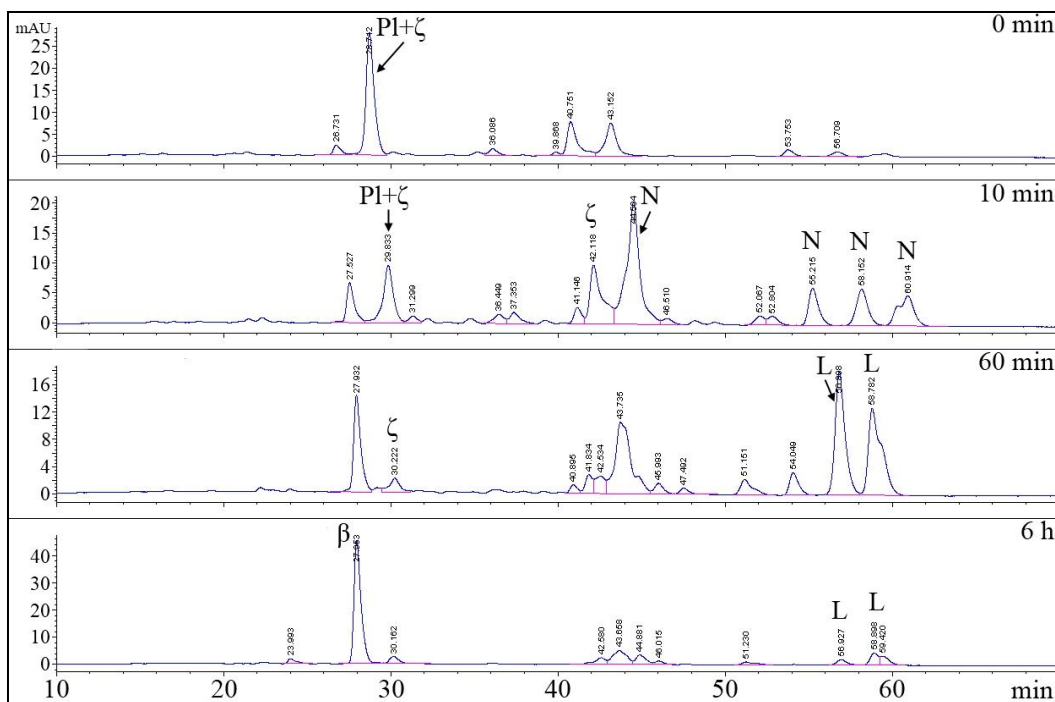


Fig. IV-18: Absorption trace from the same experiment as in Fig. IV-17 but monitored at 480 nm to detect pigments that absorbed at higher wavelength. At time zero (no illumination, top panel) the major carotenoid present in this extract was prolycopene (PI) at 28.7 minutes. Prolycopene co-eluted with a ζ -carotene isomer. Upon illumination of cells for 10 minutes before extraction, various isomers of neurosporene (N) appeared at 44.6, 55.2, 58.2, 60.3 and 60.9 minutes while at the same time the isomer of ζ -carotene that was predominant before illumination (29.83 minutes) had been converted into different compounds. After 60 minutes of light exposure, lycopene was present on the absorption trace with two major peaks at 56.9 and 58.8 minutes. Neurosporene and ζ -carotene contributed small peaks between 40 and 48 minutes. 6 hours of exposure to $140 \mu\text{mol photons m}^{-2} \text{s}^{-1}$ resulted in β -carotene (β) being the dominant peak on the chromatogram (minute 27.9) with traces of lycopene left.

Differences between *Synechocystis* wild type, *Δslr0941 C* and *Δslr0941 G*

To analyze a possible transition state between the *Synechocystis* wild type, the slow growing strain *Δslr0941 G*, the strain that apparently was the primary transformant, and *Δslr0941 C*, the strain displaying the carotenoid phenotype, a differential comparison of all these was performed. For this experiment all strains were grown at $5 \mu\text{mol photons m}^{-2} \text{s}^{-1}$, and their pigments were extracted and pre-purified on the semipreparative column. Pigments eluting between echinenone and β -carotene were collected and separated on the YMC carotenoid column. As expected, the HPLC profiles of the wild type- and *Δslr0941 G* strain were similar whereas *Δslr0941 C* was largely different from the other strains (Fig. IV-19). Apparently, *Δslr0941 C* accumulated a significant amount of phytofluene, a carotenoid intermediate produced by phytoene desaturase by desaturation of phytoene to ζ -carotene (Sandmann, 2009). Interestingly, this intermediate was absent in *Δslr0941 G*.

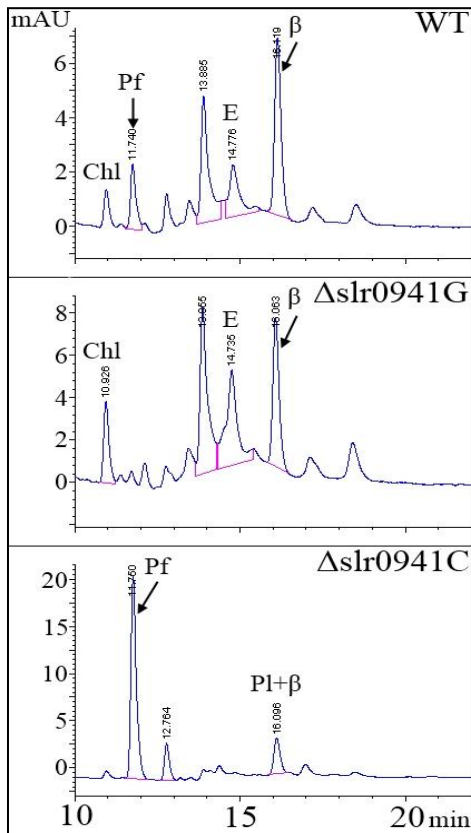


Fig. IV-19: Comparison of pigment profiles of *Synechocystis* wild type (top), *Δslr0941 G* (middle) and *Δslr0941 C* (bottom) strains. Pigments were detected at 350 nm. Phytofluene (~11.7) was absent in *Δslr0941 G* but present in the other strains. Peaks that were not present in *Δslr0941 C* were β -carotene and echinenone (16.1, 14.7 min). The peak at ~16.1 min in the bottom strain originated mainly from polycopene. The pigment at ~13.9 min could not be identified – its absorption properties were similar to that of β -carotene with maxima of II-452 nm and III-472 nm. The presence of different amounts of chlorophyll at ~10.9 min was adventitious and due to the manual collection of pigments. Its peak height is not representative of the chlorophyll content of these strains.

Comparison of $\Delta slr0941$ with a carotenoid isomerase-less ($\Delta sll0033$) strain

Because of the strikingly similar carotenoid phenotypes of $\Delta slr0941$ and a carotenoid isomerase deficient strain $\Delta sll0033$ (Masamoto *et al.* 2001), additional mutants were created lacking the known isomerase gene *sll0033* and a double-deletion strain, deficient in both, *slr0941* and *sll0033*.

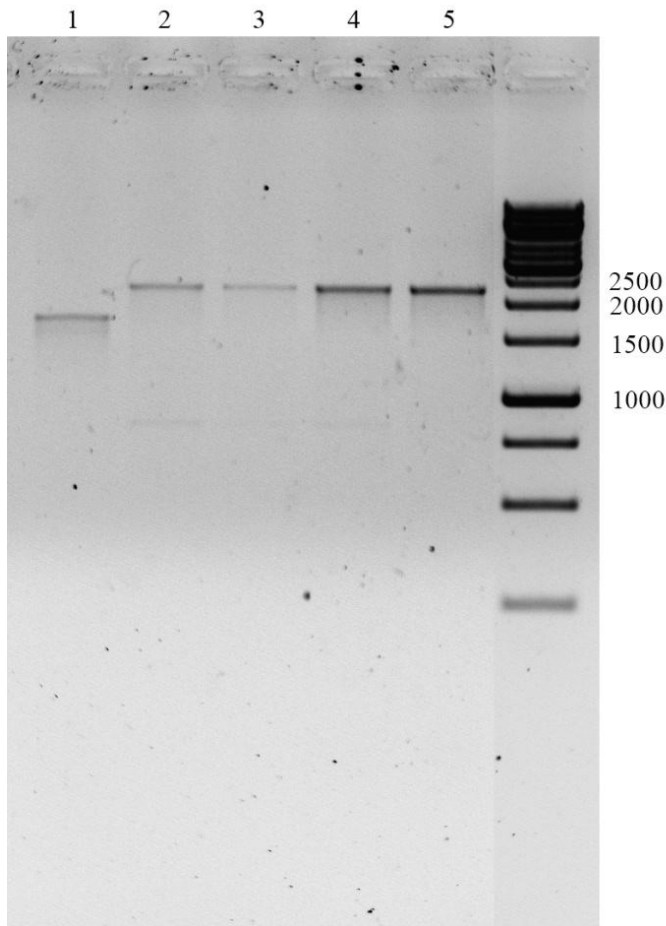


Fig. IV-20: 1% agarose gel of PCR products of the *Synechocystis* wild type (lane 1), and the mutant strains $\Delta sll0033$ (lanes 2, 3) and $\Delta sll0033/\Delta slr0941$ (lanes 4, 5), respectively, grown on plates supplemented with 10 $\mu\text{g/ml}$ chloramphenicol (lanes 2 and 3) or in liquid cultures supplemented with 66 $\mu\text{g/ml}$ chloramphenicol. In the mutants, *sll0033* loci were interrupted with a chloramphenicol acetyl transferase resistance cassette, resulting in a PCR product of 2194 bp. The wild-type locus spans 1697 bp.

Both carotenoid isomerase mutants were segregated readily (Fig. IV-20). Photomixotrophically grown ($15 \mu\text{mol photons m}^{-2} \text{ s}^{-1}$) isomerase mutant strains had doubling times similar to the *Synechocystis* wild type strain (Fig. IV-21). Unlike the wild type, however, the mutants quickly developed a very obvious carotenoid phenotype, accumulating various uncharacterized isomers.

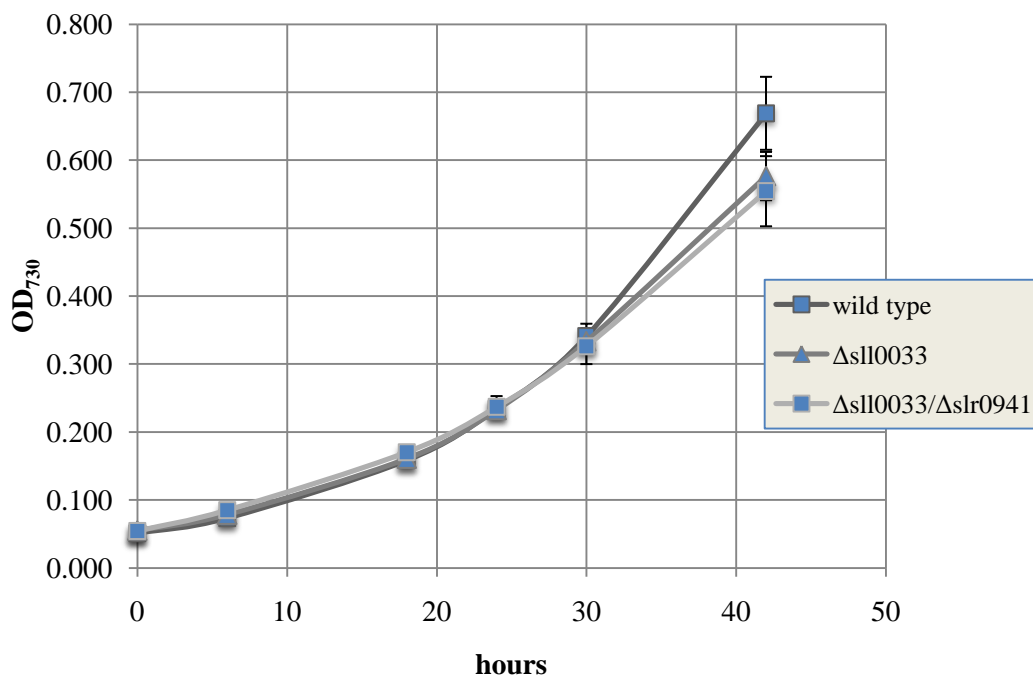


Fig. IV-21: Growth performance of wild type, carotenoid isomerase mutant $\Delta sll0033$ and the double mutant $\Delta sll0033/\Delta slr0941$. Strains were photomixotrophically grown at $15 \mu\text{mol photons m}^{-2} \text{s}^{-1}$. Data of three independent experiments are shown.

Localization of accumulating carotenoids

In *Synechocystis* three different types of membranes are present: The outer membrane (OM), the cytoplasmic membrane (CM) and thylakoid membrane (TM). Carotenoids, due to their low solubility in aqueous environment, are most likely assembled by membrane-associated (or -anchored) enzyme complexes. To date it is still uncertain where carotenoid biosynthesis takes place, it was therefore of particular interest to pinpoint the accumulation of the carotenoid isomers in the mutant strains.

A separation of different membrane types from the *Synechocystis* wild type and the $\Delta sll0033/\Delta slr0941$ double-deletion mutant was performed by sucrose density gradient centrifugation of cell extracts. Only the CM and TM fractions were abundant and pure enough for pigment analysis.

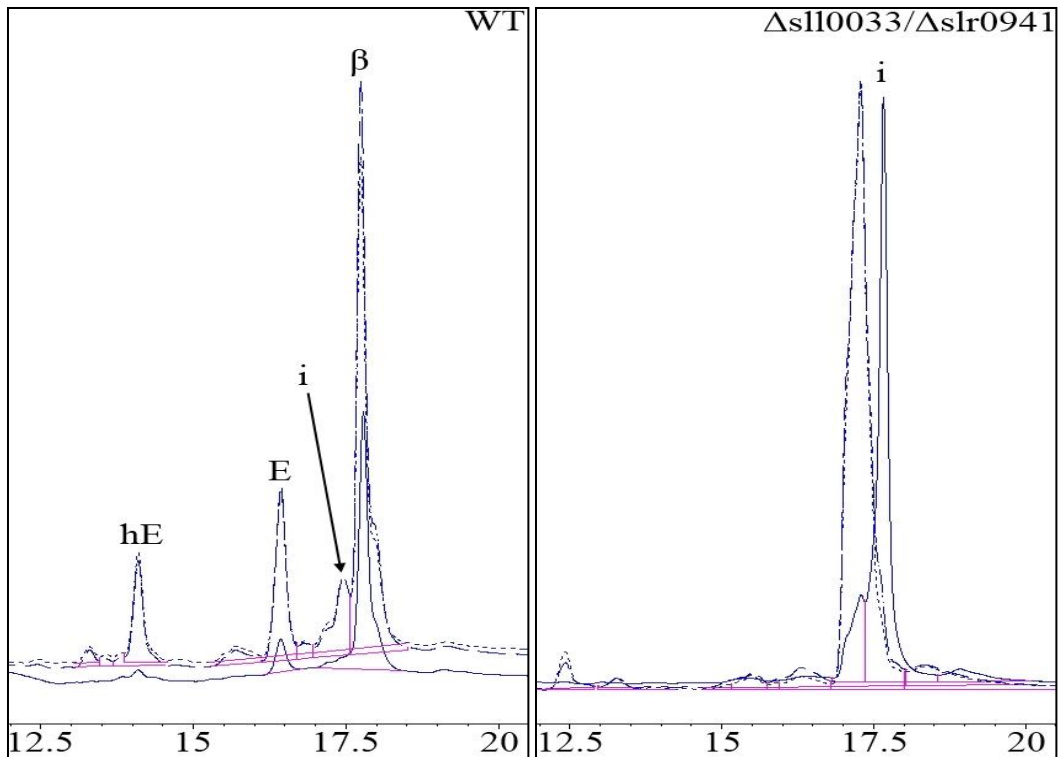


Fig. IV-22: Pigments isolated from CM fractions of the *Synechocystis* wild type and the $\Delta slI0033/\Delta slr0941$ double deletion mutant grown photomixotrophically at $5 \mu\text{mol photons m}^{-2} \text{s}^{-1}$. Absorption was detected at the wavelengths 350 (solid line), 453 (dashed), 475 (broken) and 665 nm (dotted), and the signals were overlaid. As expected, chlorophyll was absent in the CM fractions. The wild type CM fraction (left) contained hydroxyechinenone (hE), echinenone (E) and β -carotene (β), as well as small amounts of carotenoid isomers (i). In the double mutant (right) only large amounts of carotenoid isomers were detected. X-axis - elution time in minutes, Y-axis - absorbance.

Carotenoids were isolated from CM and TM of both strains and analyzed by HPLC. Chlorophyll was absent in the top (<10% sucrose), yellow-colored CM fractions of both strains. While the double mutant accumulated large amounts of carotenoid isomers, the major carotenoids present in wild type cells were β -carotene, echinenone and hydroxyechinenone (Fig. IV-22). Even though the accumulating carotenoids in $\Delta slI0033/\Delta slr0941$ double deletion mutant could not be separated in this experiment, the absorption characteristics of the isomers match with those of the isomers characterized in previous experiments (Fig. IV-16, 17, 18). Hence they most likely represent

combinations of lycopene, prolycopene, neurosporene and β -carotene in the 475 nm trace, as well as phytofluene in the 350 nm trace. Interestingly, small amounts of uncharacterized carotenoid isomers were also present in the wild-type strain (Fig. IV-22). In the TM the *Synechocystis* native carotenoids myxoxanthophyll, zeaxanthin and echinenone could barely be detected in the mutant strain, whereas chlorophyll contributed a major peak to the chromatogram. Small amounts of myxoxanthophyll and echinenone were present in the wild type TM; the predominant pigments in the TM of wild type were chlorophyll, zeaxanthin and β -carotene (Fig. IV-23).

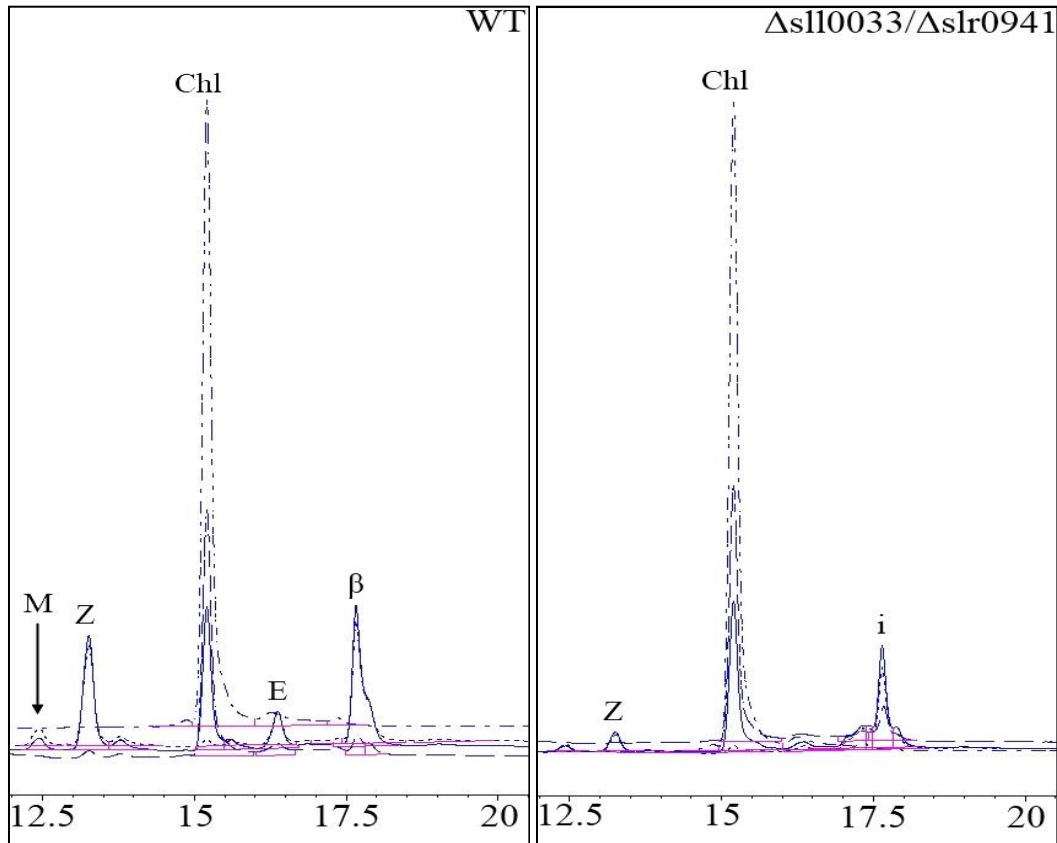


Fig. IV-23: Pigments isolated TM of wild type and $\Delta sl10033/\Delta slr0941$ double deletion strains from the same experiment as in Fig. IV-19. Native carotenoids were mostly absent in the mutant strain and a low amount of isomers had accumulated. In the wild type β -carotene (β) and zeaxanthin (Z) had the strongest presence in the thylakoid membrane while only small amounts of echinenone (E) and myxoxanthophyll (M) were detected. Chlorophyll (Chl) content was similar in both strains. Absorptions at 350 (broken line), 453 (solid), 475 (dotted) and 665 nm (dashed) were combined into one chromatogram. X-axis - elution time in minutes, Y-axis - absorbance.

Expression levels of slr0941

The promoter region of *slr0941* was analyzed in silico and its transcript levels were assessed in a tiling array approach. For the *slr0941* coding region there are no predicted (BPROM, SoftBerry Inc., NY) promoter elements present. Since the *slr0941* ORF is located 24 bp downstream and transcribed in sense of the ζ -carotene desaturase gene *slr0940* a co-transcription of both genes is likely.

Analysis of the transcript abundances of the *slr0940/slr0941* locus revealed low, but similar transcript levels for both genes (Fig. IV-24, experimental data, courtesy of Dr. Hongliang Wang, included here not as part but in support of this work).

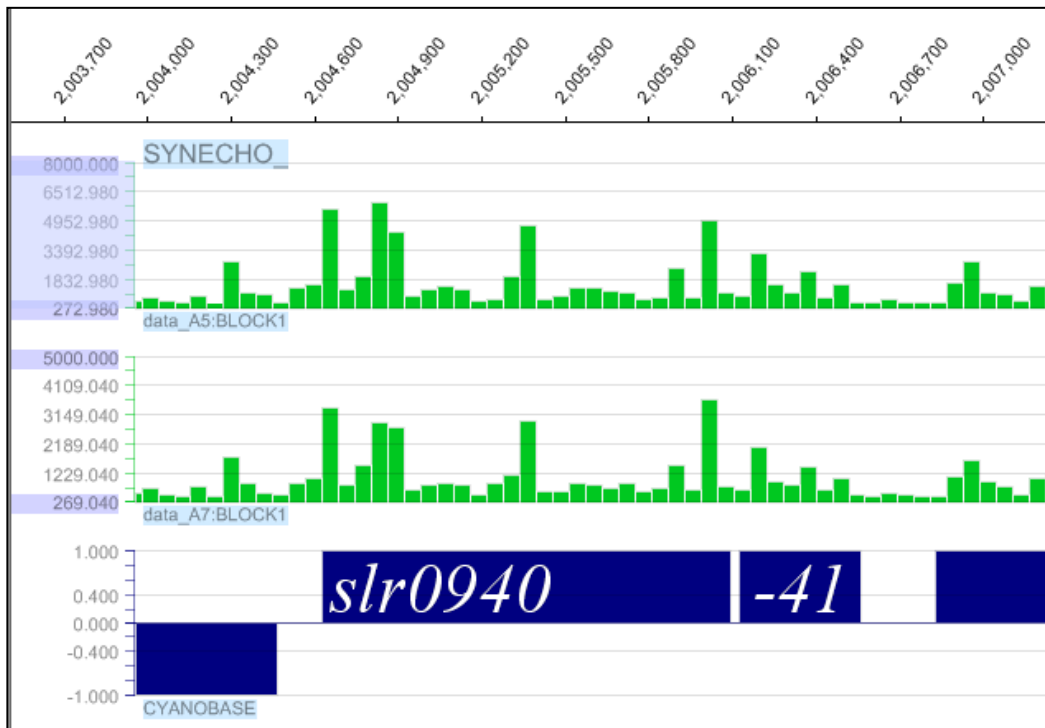


Fig. IV-24: Tiling array data showing RNA probe abundances for the *slr0940/slr0941* locus including truncated up- and downstream ORFs in exponential growth phase (top) and linear growth phase (middle). The bars represent individual 60 bp probes.

Discussion

Carotenoids are essential pigments in a wide variety of phototrophic eukaryotes and prokaryotes. One part of this work was to elucidate the function of a *Synechocystis* protein potentially involved in carotenoid processing, Slr0941. Orthologs of *slr0941* are present not only in cyanobacteria but also in plants such as *A. thaliana* and *Z. mays* as well as the green alga *Chlamydomonas reinhardtii*. Another reason for choosing *slr0941* as a candidate gene was its conserved location downstream of ζ -carotene desaturase genes (*slr0940* in *Synechocystis*) in many cyanobacteria. *Synechococcus* sp. PCC 7002 and *Microcystis aeruginosa* NIES-843, both cyanobacteria that encode CrtQb-type ζ -carotene desaturases, are rare exceptions whose *slr0941* orthologs are not within several kb of their ζ -carotene desaturase genes. *Gloeobacter violaceus* PCC 7421 which produces an eubacterial CrtI-type ζ -carotene desaturase (Giuliano *et al.*, 1986; Tsuchiya *et al.*, 2005) does not appear to have an *slr0941* ortholog. This CrtI-type enzyme catalyzes all desaturation steps from phytoene to lycopene (Fig. IV-2) without producing partially desaturated carotenoid isomers, thus eliminating the need for additional carotenoid isomerases in this organism (Steiger *et al.*, 2005). The amino acid sequence of Slr0941 has significant similarity to the weakly characterized SRPBCC (START/RHO α C/PITP/Bet v1/CoxG/CalC) domain superfamily, commonly featuring binding pockets for a variety of hydrophobic ligands such as lipids, steroids, plant cytokinins (Pasternak *et al.*, 2006), and oligo-/polyketide antibiotics (Sultana *et al.*, 2004), which is in agreement with the predicted secondary structure for Slr0941: β - α - β ₆- α (Fig. IV-3). In this organization the antiparallel β -sheets associate with the α -helix joined perpendicularly to a Hotdog-fold (Dillon and Bateman, 2004) to form a large pocket. Data on the molecular mechanism of oligo-/polyketide cyclases have emerged recently and suggest a role in holding and positioning a substrate molecule (Ames *et al.*, 2008).

Interestingly, ectopic expression of a *Streptomyces* polyketide synthase lacking the cyclase function in *E. coli* resulted in wide variety of unspecifically cyclized products (Shen *et al.*, 1999).

Strains of $\Delta slr0941$ have markedly extended doubling times

A combined deletion of the *slr0940/slr0941* locus resulted in a severe carotenoid phenotype and the highly light-sensitive $\Delta slr0941X$ mutant accumulated large amounts of ζ -carotene. The effects of a ζ -carotene desaturation deficiency have been described before (Conti *et al.*, 2004; Bautista *et al.* 2005; Dong *et al.*, 2007). In contrast to the double-deletion strain, the single-deletion strain $\Delta slr0941$ first developed a transient phenotype of about a three-fold reduced growth rate while keeping a carotenoid profile that was largely identical to that of the wild-type strain except for the accumulation of phytofluene. Due to the presence of all native carotenoids the $\Delta slr0941$ mutant was not sensitive to varying light intensities. However, its doubling time was increased by a factor of approximately two to three under all growth conditions tested (Fig. IV-6, 7). Although the deletion of *slr0941* did not produce a carotenoid phenotype that could be detected by quantitative HPLC, an analysis of carotenoids eluting between echinenone and β -carotene demonstrated reduced amounts of phytofluene in the slow growing mutant (Fig. IV-19). Phytofluene (7,8,11,12,7',8'-hexahydro- ψ,ψ -carotene) is the asymmetrically desaturated carotenoid intermediate produced by PDS upon dehydrogenation of phytoene at the C11-C12 position (Fig. IV-2). Phytofluene is therefore expected to be present in small amounts under normal physiological growth conditions. Previous studies on dark-adapted *Scenedesmus obliquus* have shown a rapid increase of phytofluene levels on illumination followed by a steady decline of the carotenoid after about 30 minutes (Powls and Britton, 1977). Limited availability of carotenoid intermediates could have adverse

effects on growth performance. Possible reasons for the lack of phytofluene in slow-growing $\Delta slr0941$ could be a lowered activity of phytoene desaturase, i.e. by feedback inhibition in the mutant strain, or an increased rate of downstream processes, leading to a faster turnover of carotenoid intermediates. In the latter case desaturation of phytoene (or any other upstream process) would be a rate-limiting step.

$\Delta slr0941$ is prone to a secondary mutation leading to the accumulation of carotenoid isomers

Continued subculturing over several generations after complete segregation eventually led to an adaptation of the mutant strain, an almost completely restored growth performance, but also an altered carotenoid composition relative to the wild type during light-limited growth (Fig. IV-8, 9). Parallel segregation of ten individually picked colonies transformed with $pslr0941v2$ demonstrated that two out of ten clones were in the process of developing a carotenoid phenotype towards the end of the segregation (Fig. IV-8).

A more detailed inspection of the accumulating carotenoids by analytical HPLC (Fig. IV-14) complemented by mass spectroscopy (Fig. IV-15, Table 2), resulted in the identification of various carotenoid isomers of lycopene such as prolycopene, neurosporene, ζ -carotene and phytofluene. In fact, phytofluene now seemed to be even more abundant than in the wild-type strain (Fig. IV-19). All-*trans* isomers of carotenoids were present as well, although only in small amounts. Curiously, the accumulation of the carotenoid precursors was much more severe at $<0.4 \mu\text{mol photons m}^{-2} \text{s}^{-1}$ and under LAHG conditions. This result suggests an impaired ability of strain $\Delta slr0941$ to ultimately synthesize all-*trans* lycopene (and from it β -carotene or myxoxanthophyll) due to a limitation of this strain to isomerize carotenoids. The isomerization of carotenoids is

either photo-catalyzed (Cunningham and Schiff, 1985) or enzyme-catalyzed. In *Synechocystis* a carotenoid isomerase (Sll0033) had previously been identified and characterized (Breitenbach *et al.*, 2001a; Masamoto *et al.*, 2001). This enzyme converts prolycopene, a dominant product created by ζ -carotene desaturase, into all-*trans* lycopene. Additionally, a probable 9,15,9'-*tricus* ζ -carotene isomerase had recently been identified in maize (Chen *et al.*, 2010), with an ortholog gene present in the *Synechocystis* genome: *slr1599*. Similar to prolycopene, 9,15,9'-*tricus* ζ -carotene is the major carotenoid product created by the desaturation of phytoene by phytoene desaturase. Formally, phytoene desaturase possesses isomerization activity as well since this enzyme preferentially produces the aforementioned *tricus* ζ -carotene isomer during the desaturation of phytoene by rotation of the 9,10,9',10'-double bonds (Qureshi *et al.*, 1974). Two of the three main sources for carotenoid isomers, the genes *sll0033* and *slr1599* were sequenced in the mutant strain and no point mutations could be found. It was therefore concluded that a thus far unidentified secondary mutation had caused the carotenoid phenotype of Δ *slr0941*. This was confirmed by the complementation of Δ *slr0941* with its native gene *slr0941* which did not rescue the carotenoid phenotype (Fig. IV-11, 12), and by transformation of the *Synechocystis* wild type with genomic DNA from the slow growing or the carotenoid phenotype strain, both of which did not develop a carotenoid phenotype upon reaching complete segregation.

The lack of enzyme-catalyzed isomerization leads to a wide variety of carotenoid isomers generated mainly by the desaturation of intermediates (Masamoto *et al.*, 2001; Breitenbach and Sandmann, 2005). Heterologous expression of the *Synechocystis* ζ -carotene desaturase CrtQ-2 in *E. coli* resulted in two neurosporene isomers and at least eight different lycopene isomers (Breitenbach *et al.*, 2001b). Of these, however, only all-*trans* lycopene, which is produced in small amounts is a valid substrate for cyclization by

lycopene cyclase. To date no data are available for the *Synechocystis* phytoene desaturase but similar observations were made for the enzyme ortholog from *Capsicum annuum*, which produces at least six different ζ -carotene isomers (mostly of the *dicis*- and *tricis*-type) as well as two phytofluene isomers.

Presence of functional isomerase genes in $\Delta slr0941$ suggest a structural role of Slr0941 at the stage of carotenoid isomerization

In this work the turnover of carotenoids isolated from an LAHG-grown $\Delta slr0941$ mutant was monitored in vitro prior to and until after six hours of exposure to $140 \mu\text{mol photons m}^{-2} \text{ s}^{-1}$ (Fig. IV-16, 17, 18). As expected, light exposure significantly accelerated the conversion of isomers, and mono- and di-cyclic carotenoids were detected after 30 minutes of illumination. Interestingly, the 350 nm YMC trace showed a persistent presence of phytofluene, which, after six hours of light exposure, eluted at a slightly different position, indicating more hydrophobic properties (Fig. IV-17, 19). As an asymmetric pentaene intermediate produced directly by phytoene desaturase, this carotenoid must already have undergone isomerization prior to being accepted as a substrate for desaturation, and is usually processed further to ζ -carotene. Low levels of ζ -carotene could be detected even after six hours of illumination, which is unusual considering the presence of functional ζ -carotene desaturase and polycopene isomerase at high-light intensity (Fig. IV-17, 18). These findings suggest a biosynthetic block at the stage of phytofluene conversion. It is possible that Slr0941 is a missing substrate channel or substrate transporter to phytoene desaturase as part of a multienzyme complex located in the cell membrane (Fig. IV-22) consisting of both carotenoid isomerases as well as the ζ -carotene desaturase. This is supported by the predicted secondary structure of Slr0941 and its apparent lack of catalytic sites. A channelling/transport role of Slr0941 would also

explain the initial slow-growth phenotype of $\Delta slr0941$ strains: The possible carotenoid binding pocket formed by Slr0941 could hold (a) carotenoid precursor(s) and make them available to a set of enzymes in this multienzyme complex, presumably the isomerases. Even though the absence of such a binding pocket may not be lethal to the cell, it may result in a slowed carotenoid turnover and the limited availability of carotenoids would increase the doubling times of the mutant. Furthermore, carotenoid depletion would put the mutant under considerable selective pressure. Masamoto *et al.* (2004) have shown that β -carotene is essential for the assembly of photosystem II. Lack of zeaxanthin resulted in a significant drop in oxygen evolution of the affected mutant strain in a different study (Schäfer *et al.*, 2005), and loss of myxoxanthophyll led to a disruption of thylakoid organization and an altered cell wall (Mohamed *et al.*, 2005).

The restored doubling time of the $\Delta slr0941$ C mutant hints a secondary mutation

Continued subculturing of the $\Delta slr0941$ G strain resulted in heterogenous plate cultures (Fig. IV-11), shortened doubling times and the described carotenoid phenotype. A possible explanation of the restored growth performance that comes at the expense of a carotenoid profile equal to that of the wild type strain would be a structural change (or changes) in the carotenoid processing enzymes, enabling a higher rate of pigment biosynthesis. The accumulation of isomers could be due to “leakage” of these precursors from such a structurally altered enzyme complex, which appeared to be located in the CM (Fig. IV-22). Despite all membrane fractions were largely depleted of finalized carotenoids in the $\Delta slr0941$ C strain the chlorophyll content in thylakoid membranes retained wild type levels (Fig. IV-23). Thus, the level of β -carotene produced by the mutant was probably enough for the assembly of both photosystems. In the case of a pseudoreversion that results in severe changes in the carotenoid metabolism, it is unlikely

that a rescue attempt such as the one performed here (Fig. IV-11, 12) would completely (or even partially) restore the wild-type situation.

The data presented here suggest a role of Slr0941 in binding or positioning of carotenoid precursors. Further experiments would be necessary for a better characterization of this protein, for example isolation and purification of Slr0941, followed by an assessment of its probable pigment binding capabilities. Since certain precursors such as phytofluene persist in $\Delta slr0941$, a detailed comparison of carotenoid lifetimes in the *Synechocystis* wild type, the $\Delta slr0941$ mutant, and other carotenoid accumulating mutants ($\Delta sll0033$, $\Delta slr1599$) could shed light on the fate of these carotenoids.

References

- Ames, B.D., Korman T.P., Zhang W., Smith P., Vu T., Tang Y., and Tsai S.C. (2008) Crystal structure and functional analysis of tetraacenomycin ARO/CYC: implications for cyclization specificity of aromatic polyketides. *Proc Natl Acad Sci USA* **105**: 5349-5354.
- Bautista, J.A., Rappaport F., Guergova-Kuras M., Cohen R.O., Golbeck J.H., Wang J.Y., et al. (2005) Biochemical and biophysical characterization of photosystem I from phytoene desaturase and zeta-carotene desaturase deletion mutants of *Synechocystis* sp. PCC 6803: evidence for PsaA- and PsaB-side electron transport in cyanobacteria. *J Biol Chem* **280**: 20030-20041.
- Breitenbach, J.B., Fernandez-Gonzalez B., Vioque A., and Sandmann G. (1998) A higher-plant type carotene desaturase in the cyanobacterium *Synechocystis* PCC6803. *Plant Mol Biol* **36**: 725-732.
- Breitenbach, J., Vioque A., and Sandmann G. (2001a) Gene sll0033 from *Synechocystis* 6803 encodes a carotene isomerase involved in the biosynthesis of all-E lycopene. *Zeitschrift für Naturforschung* **56**: 915-917.
- Breitenbach, J., Braun G., Steiger S., and Sandmann G. (2001b) Chromatographic performance on a C30-ounded stationary phase of monohydroxycarotenoids with variable chain length or degree of desaturation and of lycopene isomers synthesized by various carotene desaturases. *J Chromatogr A* **936**: 59-69.
- Breitenbach, J., and Sandmann G. (2005) ζ -carotene cis isomers as products and substrates in the plant poly-cis carotenoid biosynthetic pathway to lycopene. *Planta* **220**: 785-793.

- Chen, Y., Li F., and Wurtzel E.T. (2010) Isolation and characterization of the Z-ISO gene encoding a missing component of carotenoid biosynthesis in plants. *Plant Physiol* **153**: 66-79.
- Conti, A., Pancaldi S., Fambrini M., Michelotti V., Bonora A., Salvini M., and Pugliesi C. (2004) A deficiency at the gene coding for ζ -carotene desaturase characterizes the sunflower non dormant-1 mutant. *Plant Cell Physiol* **45**: 445-455.
- Cunningham, Jr. F.X., and Schiff J.A. (1985) Photoisomerization of ζ -carotene stereoisomers in cells of *Euglena gracilis* mutant W₃BUL and in solution. *Photochem Photobiol* **42**: 295-307.
- Das, A., and Khosla C. (2009) Biosynthesis of aromatic polyketides in bacteria. *Acc Chem Res* **42**: 631-639.
- Dillon, S.C., and Bateman A. (2004) The Hotdog fold: wrapping up a superfamily of thioesterases and dehydratases. *BMC Bioinformatics* **5**: 109-123.
- Dong, H., Deng Y., Mu J., Lu Q., Wang Y., Xu Y., Chu C., Chong K., Lu C., and Zuo J. (2007) The *Arabidopsis Spontaneous Cell Death1* gene, encoding a ζ -carotene desaturase essential for carotenoid biosynthesis, is involved in chloroplast development, photoprotection and retrograde signaling. *Cell Res* **17**: 458-470.
- El-Agamey, A., Lowe G.M., McGarvey D.J., Mortensen A. Phillip D.M., Truscott G.T., and Young A.J. (2004) Carotenoid radical chemistry and antioxidant/pro-oxidant properties. *Arch Biochem Biophys* **430**: 37-48.
- Ershov, Y.V., Gantt R.R., F.X. Cunningham, Jr., and Gantt E. (2002) Isoprenoid biosynthesis in *Synechocystis* sp. strain PCC6803 is stimulated by compounds of the pentose phosphate cycle but not by pyruvate or deoxyxylulose-5-phosphate. *J Bacteriol* **184**: 5045-5051.
- Fraser, N.J., Hashimoto H., and Cogdell R.J. (2001) Carotenoids and bacterial photosynthesis: The story so far... *Photosyn Res* **70**: 249-256.
- Giraud, E., Hannibal L., Fardoux J., Jaubert M., Jourand P., Dreyfus B, *et al.* (2004) Two distinct crt gene clusters for two different functional classes of carotenoid in *Bradyrhizobium*. *J Biol Chem* **279**: 15076-15083.
- Giuliano, G., Pollock D., and Scolnik P.A. (1986) The gene CrtI mediates the conversion of phytoene into colored carotenoids in *Rhodospseudomonas capsulata*. *J Biol Chem* **261**: 12925-12929.
- Harada, J., Nagashima K.V.P., Takaichi S., Misawa N., Matsuura K., and K. Shimada. (2001) Phytoene desaturase, CrtI, of the purple photosynthetic bacterium, *Rubrivivax gelatinosus*, produces both neurosporene and lycopene. *Plant Cell Physiol* **42**: 1112-1118.

- Havaux, M. (1998) Carotenoids as membrane stabilizers in chloroplasts. *Trends Plant Sci* **3**: 147-151.
- Hunter, W.N. (2007) The non-mevalonate pathway of isoprenoid precursor biosynthesis. *J Biol Chem* **282**: 21573-21577.
- Marchler-Bauer, A., Anderson J.B., Chitsaz F., Derbyshire M.K., DeWeese-Scott C., *et al.* (2009) CDD: specific functional annotation with the Conserved Domain Database. *Nucleic Acids Res* **37**: 205-210.
- Masamoto, K., Wada H., Kaneko T., and Takaichi S. (2001) Identification of a gene required for cis-to-trans carotene isomerization in carotenogenesis of the cyanobacterium *Synechocystis* sp PCC 6803. *Plant Cell Physiol* **42**: 1398-1402.
- Masamoto, K., Hisatomi S., Sakurai I., Gambos Z., and Wada H. (2004) Requirement of carotene isomerization for the assembly of photosystem II in *Synechocystis* sp. PCC 6803. *Plant Cell Physiol* **45**: 1325-1329.
- Mohamed, H.E., van de Meene A.M.L., Roberson R.W., and Vermaas W.F.J. (2005) Myxoxanthophyll is required for normal cell wall structure and thylakoid organization in the cyanobacterium, *Synechocystis* sp strain PCC 6803. *J Bacteriol* **187**: 6883-6892.
- Pasternak, O., Bujacz G.D., Fujimoto Y., Hashimoto Y., Jelen F., Otlewski J., Sikorski M.M., and Jaskolski M. (2006) Crystal structure of *Vigna radiata* cytokinin-specific binding protein in complex with zeatin. *Plant Cell* **18**: 2622-2634.
- Powls, R., and Britton G. (1977) The roles of isomers of phytoene, phytofluene and ζ -carotene in carotenoid biosynthesis by a mutant strain of *Scenedesmus obliquus*. *Arch Microbiol* **115**: 175-179.
- Qureshi, A.A., Andrewes A.G., Qureshi N., and Porter J.W. (1974) The enzymatic conversion of *cis*-¹⁴C-phytofluene, *trans*-¹⁴C-phytofluene, and *trans*- ζ -¹⁴C-carotene to more unsaturated acyclic, monocyclic, and dicyclic carotenes by a cell-free preparation of red tomato fruits. *Arch Biochem Biophys* **162**: 93-107.
- Sandmann, G., (2002) Molecular evolution of carotenoid biosynthesis from bacteria to plants. *Physiol Plant* **116**: 431-440.
- Sandmann, G., (2009) Evolution of carotene desaturation: The complication of a simple pathway. *Arch Biochem Biophys* **483**: 169-174.
- Schäfer, L., Vioque A., and Sandmann G. (2005) Functional in situ evaluation of photo synthesis-protecting carotenoids in mutants of the cyanobacterium *Synechocystis* PCC6803. *J Photochem Photobiol B, Biol* **78**: 195-201.
- Shen, Y., Yoon P., Yu T.W., Floss H.G., Hopwood D., and Moore B.S. (1999) Ectopic expression of the minimal whiE polyketide synthase generates a library of aromatic polyketides of diverse sizes and shapes. *Proc Natl Acad Sci USA* **96**: 3622-3627.

Steiger, S., Schäfer L., and Sandmann G. (1999) High-light-dependent upregulation of carotenoids and their antioxidative properties in the cyanobacterium *Synechocystis* PCC 6803. *J Photochem Photobiol* **52**: 14-18.

Steiger, S., Jackisch Y., and Sandmann G. (2005) Carotenoid biosynthesis in *Gloeobacter violaceus* PCC4721 involves a single CrtI-type phytoene desaturase instead of typical cyanobacterial enzymes. *Arch Microbiol* **184**: 207-214.

Sultana, A., Kallio P., Jansson A., Wang J.S., Niemi J., Mäntsälä P., *et al.* (2004) Structure of the polyketide cyclase SnoaL reveals a novel mechanism for enzymatic aldol condensation. *EMBO J* **23**: 1911-1921.

Tsuchiya, T., Takaichi S., Misawa N., Maoka T., Miyashita H., and Mimuro M. (2005) The cyanobacterium *Gloeobacter violaceus* PCC 7421 uses bacterial-type phytoene desaturase in carotenoid biosynthesis. *FEBS Lett* **579**: 2125-2129.

Zechmeister, L., LeRosen A.L., Went F.W., and Pauling L. (1941) Prolycopene, a naturally occurring stereoisomer of lycopene. *Proc Natl Acad Sci USA* **27**: 468-474.

CHAPTER V. SLR1648 AND SLL1541 ARE PUTATIVE CAROTENOID CLEAVAGE
DI-OXYGENASES OF *SYNECHOCYSTIS*

Abstract

The last chapter of this work was focused on the turnover of carotenoids in *Synechocystis*. Mutants were constructed with disruptions in the putative carotenoid cleavage dioxygenase genes *sll1541*, *slr1648* as well as both genes. Sll1541 and Slr1648 are presumed to bind and cleave carotenoids with a chain length of less than 40 carbon atoms (apo-carotenoids). All mutants could be segregated to homozygosity. The pigment profiles of these strains that had been grown under various light regimes were analyzed by HPLC. Neither the wild-type nor the mutant strains produced or accumulated any detectable carotenoid breakdown products. Chlorophyll contents as well as fluorescence emission of photosystems of the mutant strains were altered when compared to the wild type: High-light exposure resulted in a significant drop of chlorophyll levels and lowered PS II to PS I ratios. Although electron microscopy on the dioxygenase mutants showed subcellular organizations that were very similar to the wild type, cells of $\Delta slr1648$ and the double mutant displayed highly electron-dense inclusion that were absent in the other strains. ^{13}C -labeling of carotenoids in all strains under photoheterotrophic conditions demonstrated equal turnover rates in all strains. The data obtained in this work suggest a minimal contribution of Sll1541 and Slr1648 to the turnover of carotenoids under high-light intensity.

Introduction

In the previous two chapters of this work various aspects of *Synechocystis* carotenoids such as their role and localization in a Surface-layer less mutant, as well as their accumulation in a strain lacking a protein potentially involved in carotenoid binding were studied.

Quite possibly all aerobic phototrophic organisms are capable of producing carotenoids because of their versatile photochemical abilities to quench various reactive oxygen species (ROS) such as singlet oxygen ($^1\text{O}_2$), frequently formed from chlorophyll triplets (^3Chl) (Triantaphylidès and Havaux, 2009), but also highly reactive radicals such as the hydroxyl radical ($\text{HO}\cdot$) and the superoxide anion (O_2^-) (Imlay, 2003). Moreover, carotenoids will readily react with peroxide species such as hydrogen peroxide (H_2O_2) and, more importantly, lipid peroxide (ROOH) (Burton and Ingold, 1984). Although superoxide is normally dismutated to H_2O_2 by superoxide dismutase (SOD), which in turn is reduced to water by catalase-peroxidase enzymes, the H_2O_2 intermediate in the presence of ferrous ion can initiate a Fenton reaction, leading to the formation of $\text{HO}\cdot$ (Fenton, 1894).

ROS are commonly generated in chemical reactions involving single electron transfers, e.g., some reactions of the respiratory or photosynthetic chains, by autoxidation of participating enzyme complexes (Massey, 1994). To cope with the formation of different types of oxidative stress most aerobic organisms employ a wide spectrum of defenses against harmful ROS, which are either enzymatic such as the aforementioned SOD (Carlioz and Touati, 1986; Fridovich, 1997) and various types of peroxidases, for instance, ascorbate- or glutathione peroxidases as well as H_2O_2 -specific catalases (Chelikani *et al.*, 2004), or non-enzymatic such as carotenoids and some vitamins (Latifi *et al.*, 2009). The high density of delocalized π -electrons along the polyene chain of

carotenoids increases the reactivity of these pigments and makes them particularly efficient scavengers of ROS. Quenching of triplet chlorophyll or singlet oxygen by carotenoids is often achieved in a catalytical process either by internal conversion, intersystem crossing or fluorescence, all of which are non-destructive. In contrast, the reaction with radicals or peroxides usually re-arranges the covalent bonds of the carotenoid molecule and disrupts the conjugated polyene chain. Such a destabilization frequently causes the formation of carotenoid endoperoxides or apo-carotenoids by a shortening of the carotene backbone (Stratton *et al.*, 1993, Walter *et al.*, 2010). In plants and certain animals apo-carotenoids are created purposely by a variety of enzymes and such carotenoid cleavage products assume biologically important roles as signaling molecules (Schwartz *et al.*, 2004), aroma compounds (Rodríguez-Bustamante and Sánchez, 2007), and rhodopsin chromophores (von Lintig and Vogt, 2000). Interestingly, cyanobacteria and other single-celled organisms possess carotenoid cleavage enzymes as well (Jüttner and Höflacher, 1985; Ruch *et al.*, 2005; Marasco *et al.*, 2006). The chemical nature of the conjugated double bonds in carotenoids makes them accessible to unspecific cleavage by various enzymes including phenoloxidases, peroxidases, lipoxygenases and xanthine oxidase (Bouvier *et al.* 2005). Specific cleavage is catalyzed by carotenoid (di-)oxygenases such as nine-*cis*-epoxy carotenoid dioxygenase (NCED, Fig. V-1A), carotenoid cleavage dioxygenases (CCD, Fig. V-1B), as well as zeaxanthin- and lycopene cleavage dioxygenases (ZCD, LCD). It is assumed that these enzymes recognize electron densities and/or functional groups of their carotenoid substrate. Although reports on cyanobacterial carotenoid cleavage have emerged (Ruch *et al.*, 2005; Marasco *et al.*, 2006; Scherzinger and Al-Babili, 2008), the functions of carotenoid cleavage products in these organisms remain a mystery. In this work strains of *Synechocystis* were constructed that lack one or both of the putative CCD genes *slI1541*, and *slr1648*. The data obtained

suggest a minimal (if any) contribution of these enzymes to processing or turnover of (apo-) carotenoids in *Synechocystis* under the conditions tested.

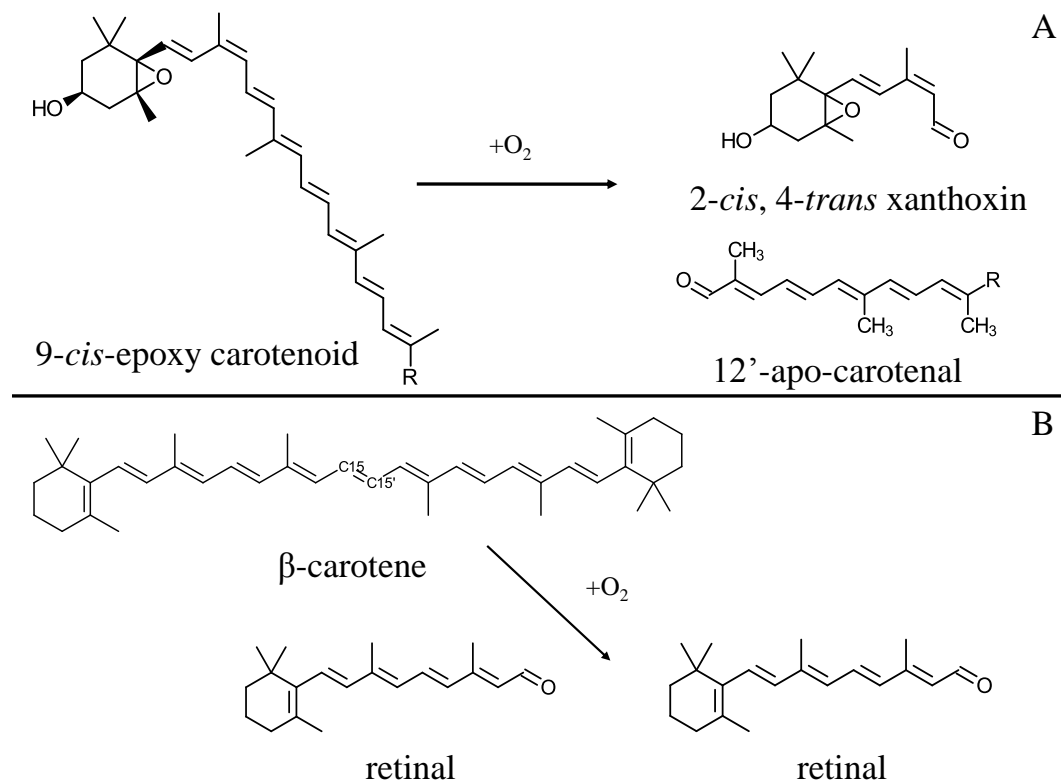


Fig. V-1: Cleavage of carotenoids by 9-*cis*-epoxy carotenoid dioxygenase (A) and by 15-15'-carotenoid dioxygenase (B).

Methods

Labeling of carotenoids with ¹³C-glucose

To assess the turnover of carotenoids in *Synechocystis*, strains were initially grown photomixotrophically at 50 or 125 μmol photons m⁻² s⁻¹ supplemented with 5 mM glucose, their OD₇₃₀ was measured and then old growth medium was removed by centrifugation. About 3.5 – 6 × 10⁷ cells were harvested and snap-frozen in liquid nitrogen prior to labeling. The remaining cells were then resuspended in BG-11, in which Na₂CO₃ had been replaced by an aequimolar amount of NaCl, to an OD₇₃₀ between 0.10 – 0.15, and universally ¹³C-labeled D-glucose (Cambridge Isotope Laboratories, Andover,

MA) was added to a final concentration of 1 mM. To prevent the introduction of unlabeled carbon through the Calvin cycle, atrazine was added to a final concentration of 20 μ M. Mutant strains were grown supplemented with antibiotics to a final concentration of 25 μ g/ml. Depending on the experiment, cultures were incubated at different light intensities at 30 °C and 150 rpm on a rotary shaker. Labeling was performed over time periods of 48 to 72 hours total. Growth was monitored every 12 hours, and $3.5 - 6 \times 10^7$ cells were harvested by centrifugation, frozen in liquid nitrogen and stored at -80 °C. Remaining cultures were supplemented with 1 mM 13 C-labeled glucose before the incubation was continued. To keep cultures from entering stationary phase, they were subcultured to OD₇₃₀ between 0.10 and 0.15 once they had reached densities greater than 0.600. Pigments of harvested cells were extracted three times with methanol (500, 300 and 200 μ l) under dimmed light conditions.

Pigments were analyzed either manually by collecting HPLC fractions of eluted carotenoids, followed by MALDI-TOF (Matrix Assisted Laser Desorption/Ionization – Time Of Flight), or by HPLC-Pi-MS (HPLC – Photoionization) Mass Spectrometry. For the former, 100 μ l aliquots of the extracts were loaded onto a semi-preparative column and individual peaks of carotenoids were collected, which were then dried in the speed-vac and stored at -80 °C until MS. MALDI-TOF was performed on an Applied Biosystems Voyager-DE Biospectrometry Work Station (Foster City, CA), equipped with a nitrogen laser. Pigments were resuspended in 5 μ l dichloromethane containing 10 % (w/v) terthiophene matrix, and 1 – 2 μ l of dissolved pigment was pipetted onto a single spot of a stainless steel plate and left to dry for a few minutes before loading. The carotenoids were ionized by 50 laser shots of intensities from 1800 – 2250 (arbitrary units) at a rate of 3 Hz in reflector 1300 mode.

The detected mass range was limited to 500 – 1800 Da. Obtained spectra of 200 – 550 laser shots total were accumulated and averaged to reduce noise.

Fluorescence emission spectroscopy

Cells were grown photomixotrophically at either at regular light intensity (50 $\mu\text{mol photons m}^{-2} \text{ s}^{-1}$) or high light intensity (200 $\mu\text{mol photons m}^{-2} \text{ s}^{-1}$), harvested in the clinical centrifuge at 1200 rpm and then OD-adjusted to approximately 0.3. Cell suspensions were snap-frozen in liquid nitrogen and 77 K emission spectra were taken on a Fluorolog 2 spectrometer (Spex Industries, Metuchen, NJ) at an excitation wavelength of 435 nm. The instrument was set to a slit width of 1 mm (excitation) and 0.25 mm (emission), respectively. Emission spectra of three scans per sample were recorded from 625 to 755 nm and averaged. The obtained data were normalized to the emission of PS II.

Electron microscopy

Transmission electron microscopy (TEM) was performed with cells that had been harvested during exponential growth (at approximately $\text{OD}_{730} = 0.5$) under photoautotrophic conditions. The cells were washed once in BG-11 supplemented with ammonium and then resuspended in 100 mM phosphate buffer (PB) (pH 7.2). Chemical fixation in 2% freshly prepared glutaraldehyde was carried out at 4 °C for 90 minutes. After fixation the cell suspensions were concentrated from 1.5 ml to 300 μl and pre-embedded in 1% (w/v, final concentration (f.c.)) ionagar #2 (Consolidated Labs. Inc., Chicago, IL) at 4 °C for a few minutes. The gel blocks were cut with a spatula edge and washed twice for 10 min with PB. Cells were stored overnight at 4 °C in PB. After removal of the PB, the fixation was resumed with 2% OsO_4 (w/v, f.c.) and the samples were incubated at 4 °C for 2 h. The specimens were washed three times with Barnstead

water for 10 minutes each, and the cells were stained with 0.5% uranyl acetate overnight at 4 °C. The gel blocks were rinsed with Barnstead water three times and then gradually dehydrated in 3 – 4 ml of 10%, 20%, 40%, 60%, 80% and 100% (twice) of ethanol for 10 minutes, followed by two additional dehydration steps in acetone. Infiltration of the specimen with Spurr's resin (Spurr, 1969) was achieved in four steps of increasing resin concentrations from 25% to 50%, 75% and finally 100% resin (v/v) in acetone. For each step the specimens were placed on a rotary wheel and incubated at RT for 9 – 16 h. The gel cubes were then transferred into plastic molds, the molds filled with resin and incubated in a convection oven for 24 h at 60 °C. Resin blocks were pre-trimmed, and sections were cut on a Leica Ultracut R microtome (Leica, Vienna, Austria). Thin sections were post stained with Sato's lead citrate for 6 minutes and electron micrographs were taken on a Philips CM12S transmission electron microscope (Philips Electronic Instruments, Co., Mahwah, NJ) equipped with a Gatan 791 CCD 1,024- by 1,024-pixel-area digital camera (Gatan, Inc., Pleasanton, CA) using Gatan Digital Micrograph 3.9.1 software, at 80 kV.

Preparation of membrane profiles on sucrose density gradients

For membrane preparations, 150 ml cultures were grown photoautotrophically under continuous aeration to a density of approximately 1.5 (early stationary phase). The cells were harvested and then re-suspended in 1 ml thylakoid buffer. In seven 30-second break cycles in a Minibead-beater (BioSpec Products, Bartlesville, OK) the cells were broken. The samples were cooled on ice for two minutes between the cycles. After a four-hour incubation on ice, the material was loaded on top of sucrose gradients that had been prepared as follows: 2 ml of 55%, 3 ml of 35%, 3 ml of 25% and 3 ml of 10% sucrose (w/v), all supplemented with protease inhibitor cocktail (1 mM phenylmethanesulfonyl

fluoride, 1 mM benzamidine, 1 mM ϵ -amino caproic acid). Membranes were separated by ultracentrifugation in a Beckman SW-41 rotor for 16 h at 4 °C and $\sim 120,000 \times g$.

Calculation of chlorophyll contents of cells

The procedure was performed with sample triplicates. Cells were harvested from cultures in exponential growth phase and the equivalent of approximately 1.2×10^8 cells (~ 1 ml of $OD_{730} = 1$) was pelleted for 20 min at $16,000 \times g$. The pellet was extracted with 3 times with 1 ml of methanol and the absorption was measured at 665 nm. Chlorophyll contents were calculated according to the following formula:

$$\text{mg/ml} = 3 \times OD_{663} / 82$$

Preparative analysis of pigments by HPLC

Pigments were extracted three times from cell pellets of 5 ODU with 500, 300 and then 200 μl of methanol, and then separated on an HP-1100 Chemstation using a 24-min gradient of acetone in water/methanol, with an initial water content of 10%, continuously decreasing to 0% to the third minute. The content of acetone was continuously added to the methanol mobile phase to create a concentration gradient of 0 to 70% from minutes 3 to 11, then from 70% to 100% until the 21st minute. The elution of carotenoids was recorded at wavelengths as indicated in the figures/text.

A concentrated retinal standard was prepared from all-*trans*-retinal (Sigma-Aldrich, St. Louis, MO) by dissolving 25 mg of powder in 50 ml of methanol containing 0.5 mg/ml butylated hydroxytoluene (BHT) under dim-light conditions. After taking aliquots for analysis, the standard was wrapped in aluminum foil and stored at -80 °C.

Results

Segregation of the mutants

$\Delta slr1648$ was the first strain of three putative dioxygenase deletion strains to reach complete segregation. This strain required a Sp concentration of 200 $\mu\text{g/ml}$ on plate, at which no wild type sequence could be detected by PCR (Fig. V-2). However, to ensure complete segregation, $\Delta slr1648$ was streaked repeatedly on plates containing 500 $\mu\text{g/ml}$

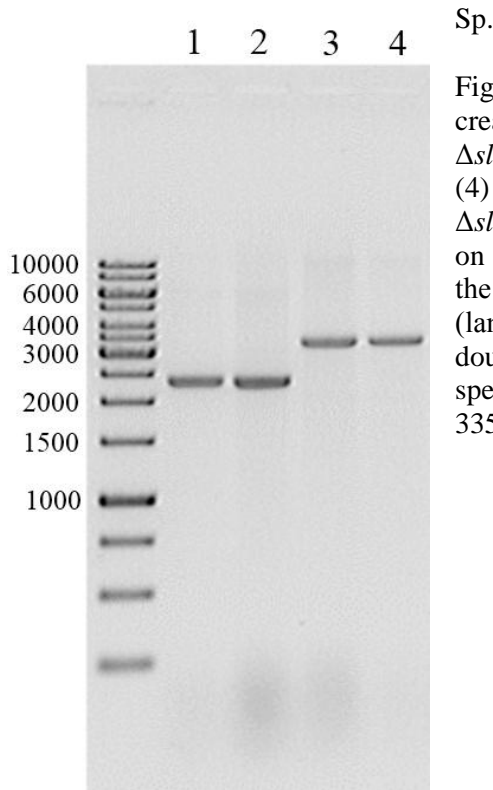


Fig. V-2: 1% agarose gel image of PCR products created from genomic DNA of wild type (lane 1), $\Delta sll1541$ (2), $\Delta slr1648$ (3), and $\Delta sll1541/\Delta slr1648$ (4) to confirm the complete segregation of $\Delta slr1648$. The primers span a distance of 2399 bp on the native *slr1648* locus which was present in the WT (lane 2) as well as the $\Delta sll1541$ mutant (lane 3) whereas the loci of $\Delta slr1648$ and the double mutant had been interrupted by the spectinomycin cassette (lanes 3, 4) and consists of 3357 bp.

$\Delta sll1541$ was created by transforming the wild type strain with *pslr1541*, and the double mutant $\Delta sll1541/\Delta slr1648$ was created by transforming the fully segregated $\Delta slr1648$ with the plasmid *pslr1541*. Homozygosity of $\Delta sll1541$ as well as $\Delta sll1541/\Delta slr1648$ was achieved at an antibiotic concentration of about 300 $\mu\text{g/ml}$ Km on plate, and confirmed by PCR using external and internal primers (Fig. V-2, 3).

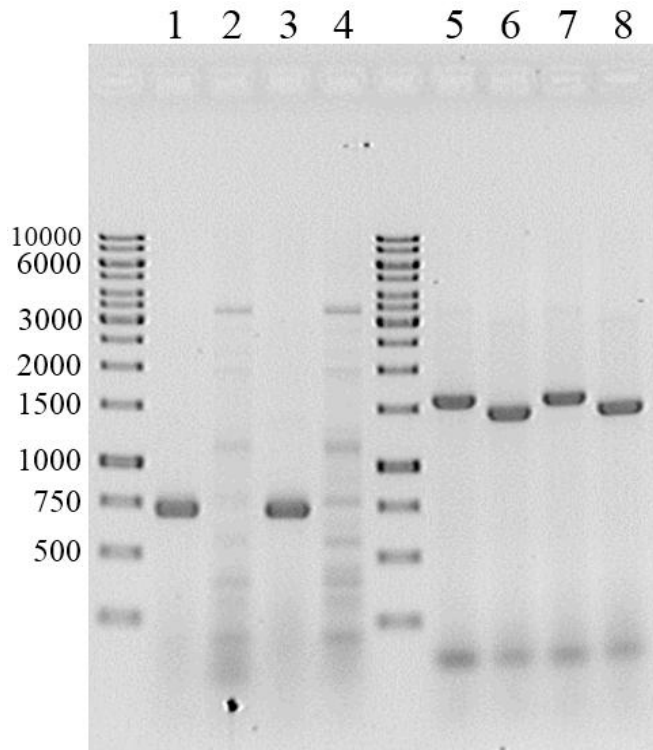


Fig. V-3: 1% agarose gel image of PCR products from wild type as well as mutants deficient in *sll1541*, *slr1648* and both genes. The *sll1541* locus was amplified using internal and external primers (lanes 1 – 4), and external primers only (lanes 5 – 8). Samples loaded were of wild type (1, 5), $\Delta sll1541$ (2, 6), $\Delta slr1648$ (3, 7), and $\Delta sll1541/\Delta slr1648$ (4, 8). The segregated $\Delta sll1541$ single- and double mutants lacked binding sites for the *sll1541* gene-internal primers and produced no PCR fragments (lanes 2 and 4). As shown in lanes 5 to 8 the *sll1541* native locus is 1564 bp whereas the mutated locus is 1365 bp.

Description of the fully segregated mutants

Even though complete segregation was achieved in all three mutants, none of them displayed a visible phenotype when grown photo- or mixotrophically at 50 $\mu\text{mol photons m}^{-2} \text{ s}^{-1}$ on BG-11 plates or in liquid cultures. Adaptation to certain growth conditions such as high/low light intensity, treatment with atrazine and varying concentrations of glucose in the medium generally took longer for the mutant strains. Without these extended periods of adaptation to high light ($>200 \mu\text{mol photons m}^{-2} \text{ s}^{-1}$) the mutant strains $\Delta slr1648$ as well as $\Delta sll1541/\Delta slr1648$ often did not show any growth at all, whereas adapted mutant strains grew with a doubling time very similar to the wild type at light intensities up to 330 $\mu\text{mol photons m}^{-2} \text{ s}^{-1}$.

Plate cultures of all three mutant strains looked identical to the wild type strain with no visible difference in pigmentation or colony morphology. Colonies were also formed by the mutant strains at rates similar to the wild-type strain.

Analysis of the carotenoids of the Synechocystis wild-type strain and the dioxygenase mutants

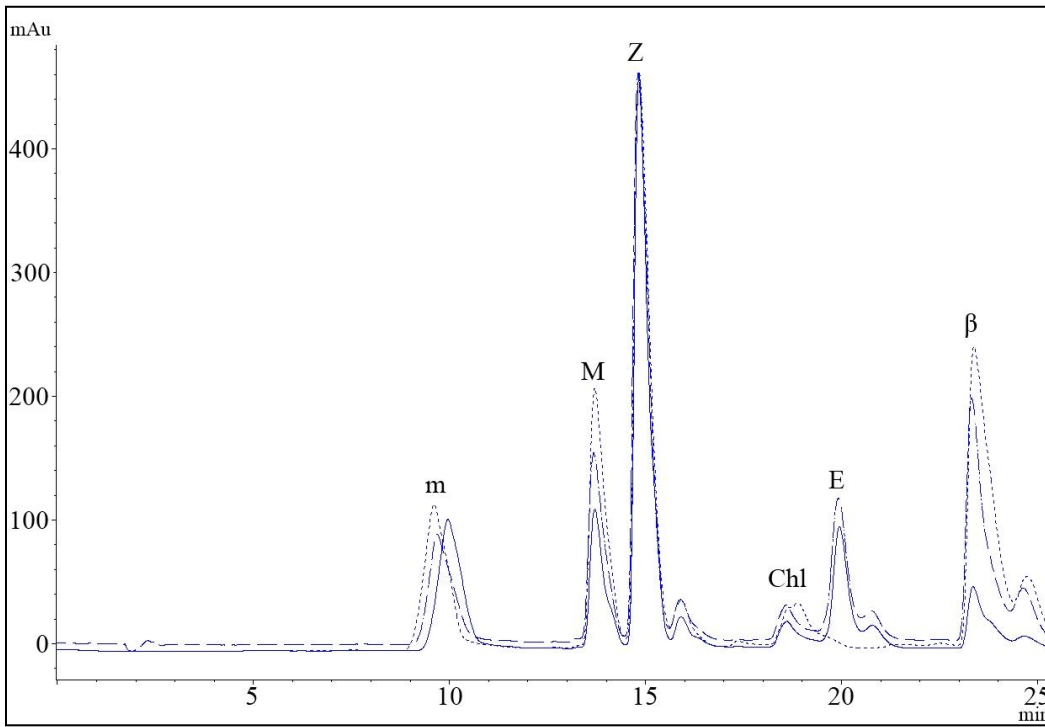


Fig. V-4: Combined HPLC spectra of strains grown at $5 \mu\text{mol photons m}^{-2} \text{s}^{-1}$ – normalized to zeaxanthin – of *Synechocystis* wild type (solid) and the mutant strains $\Delta sl11648$ (dashed) and $\Delta sl11541/\Delta slr1648$ (dotted). Absorption was detected at 480 nm and pigments were eluted on a semipreparative column with a water/methanol/acetone gradient. Eluted pigments are myxol (m), myxoxanthophyll (M), zeaxanthin (Z), echinenone (E), β -carotene (β) and chlorophyll (Chl). The spectra of myxol (m) were identical in all strains, the slight shift in the wild-type trace was probably due to compression of the column matrix.

The pigment content and profiles of all strains were analyzed by HPLC. Individual pigments were identified by their online spectra as well as by mass spectrometry. Absorption traces of pigments were monitored at the following wavelengths: 665 nm for

chlorophyll, 480 and 440 nm for carotenoids, and 350 nm for retinoids. Chlorophyll, as well as all *Synechocystis* native carotenoids, β -carotene, echinenone, zeaxanthin and myxoxanthophyll were present in the mutant strains. Depending on the growth conditions, the abundance of pigments varied slightly when compared to the wild-type strain. Mutant cultures that had been growth-adapted to $5 \mu\text{mol photons m}^{-2} \text{s}^{-1}$ for several generations showed increased levels of β -carotene and slightly increased levels of zeaxanthin whereas echinenone levels had dropped to very low levels in the case of the $\Delta\text{sl}11541$ and $\Delta\text{sl}11541/\Delta\text{slr}1648$ mutants (Fig. V-4). Although myxoxanthophyll levels were generally elevated in all strains grown at higher light intensities ($180 \mu\text{mol photons m}^{-2} \text{s}^{-1}$) its content was even higher in the mutants than it was in the wild type strain.

To evaluate possible changes in pigment production of the wild type strain and $\Delta\text{sl}11541/\Delta\text{slr}1648$, both strains were initially grown at $7 \mu\text{mol photons m}^{-2} \text{s}^{-1}$, then exposed to $150 \mu\text{mol photons m}^{-2} \text{s}^{-1}$, and pigments were analyzed after 10 min, 2 h, 5 h (not shown), 21 h and 29 h of exposure (Fig. V-5, 6). Ten minutes after exposure to higher light intensity the pigment content was virtually identical in both strains. However, with increasing times of light exposure the double mutant showed increased levels of chlorophyll and myxoxanthophyll but decreased levels of zeaxanthin (Fig. V-6).

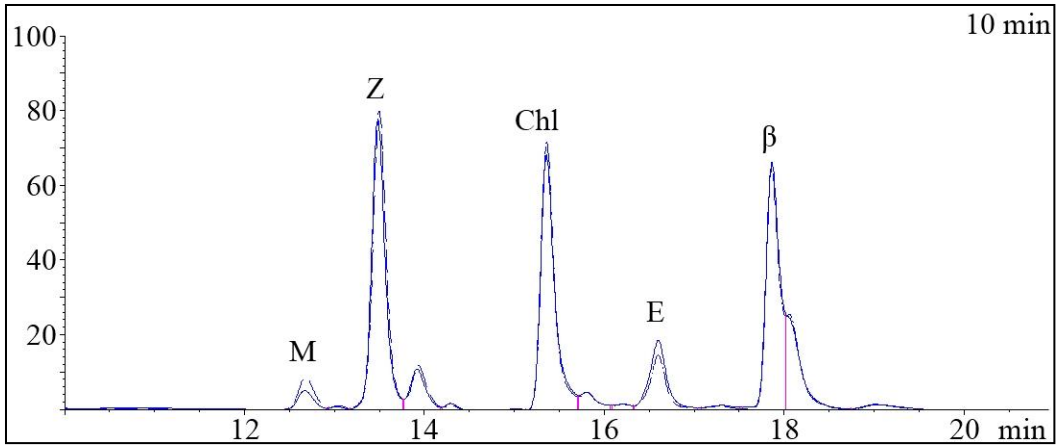


Fig. V-5: combined pigment profiles of low-light adapted wild type (solid line) and $\Delta sl11541/\Delta slr1648$ strains (dashed) after 10-minute exposure to $150 \mu\text{mol photons m}^{-2} \text{s}^{-1}$. Pigments are myxoxanthophyll (M), zeaxanthin (Z), unidentified carotenoid isomer at 13.9 min. elution time, hydroxyechinenone at 14.3 min., chlorophyll (Chl), echinenone (E) and β -carotene (β). Pigments were detected at 453 nm.

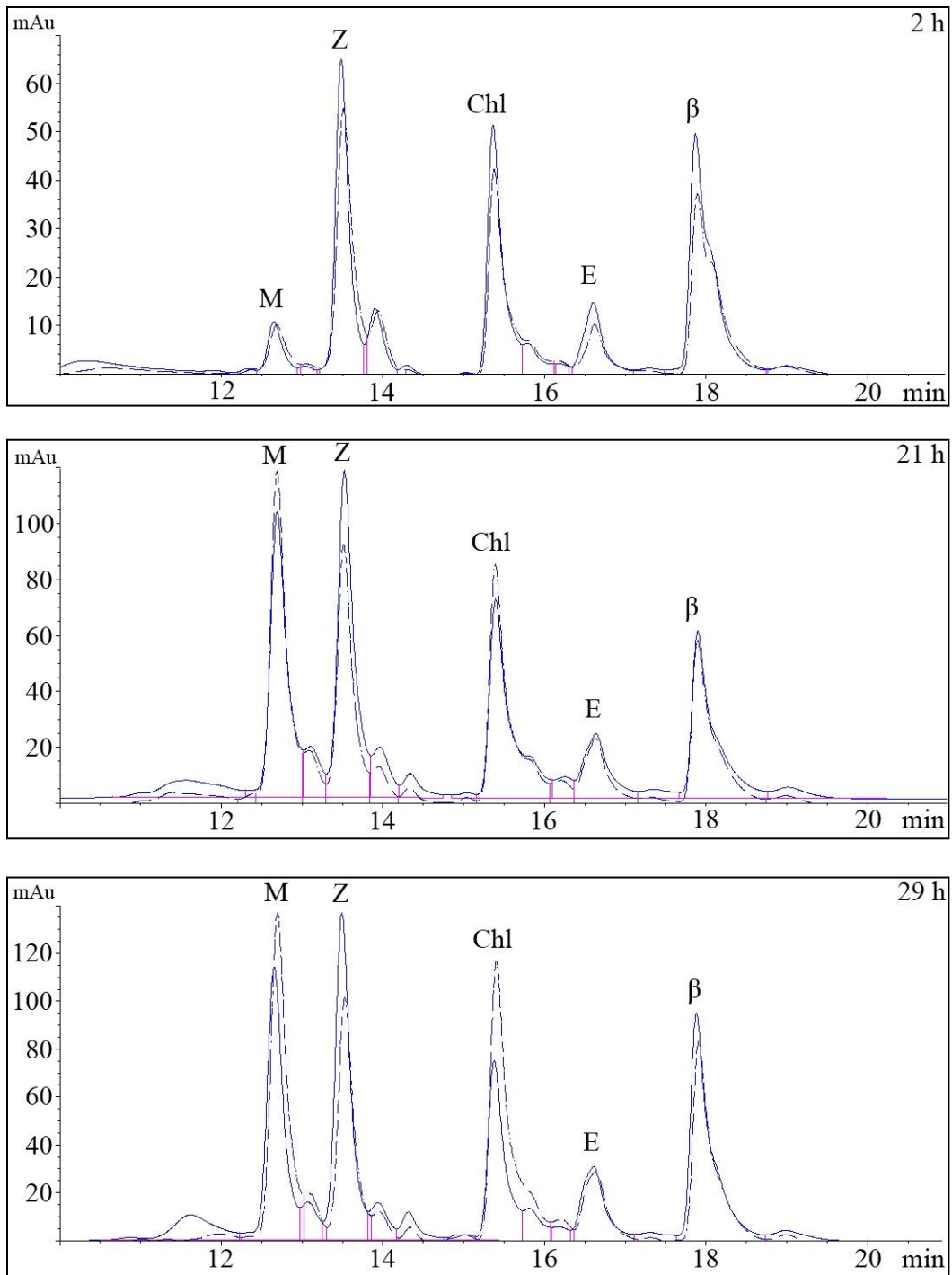


Fig. V-6: Combined pigment profiles of wild type (solid line) and the double mutant *Δslr1541/Δslr1648* (dashed) after 2 h (top), 21 h (middle) and 29 h (bottom) of exposure to $180 \mu\text{mol photons m}^{-2} \text{s}^{-1}$. Exposure to high light intensity resulted in only slightly different pigment profiles and a changed myxoxanthophyll (M)-zeaxanthin (Z)-chlorophyll (Chl) ratio in the mutant. Pigments were detected at 453 nm.

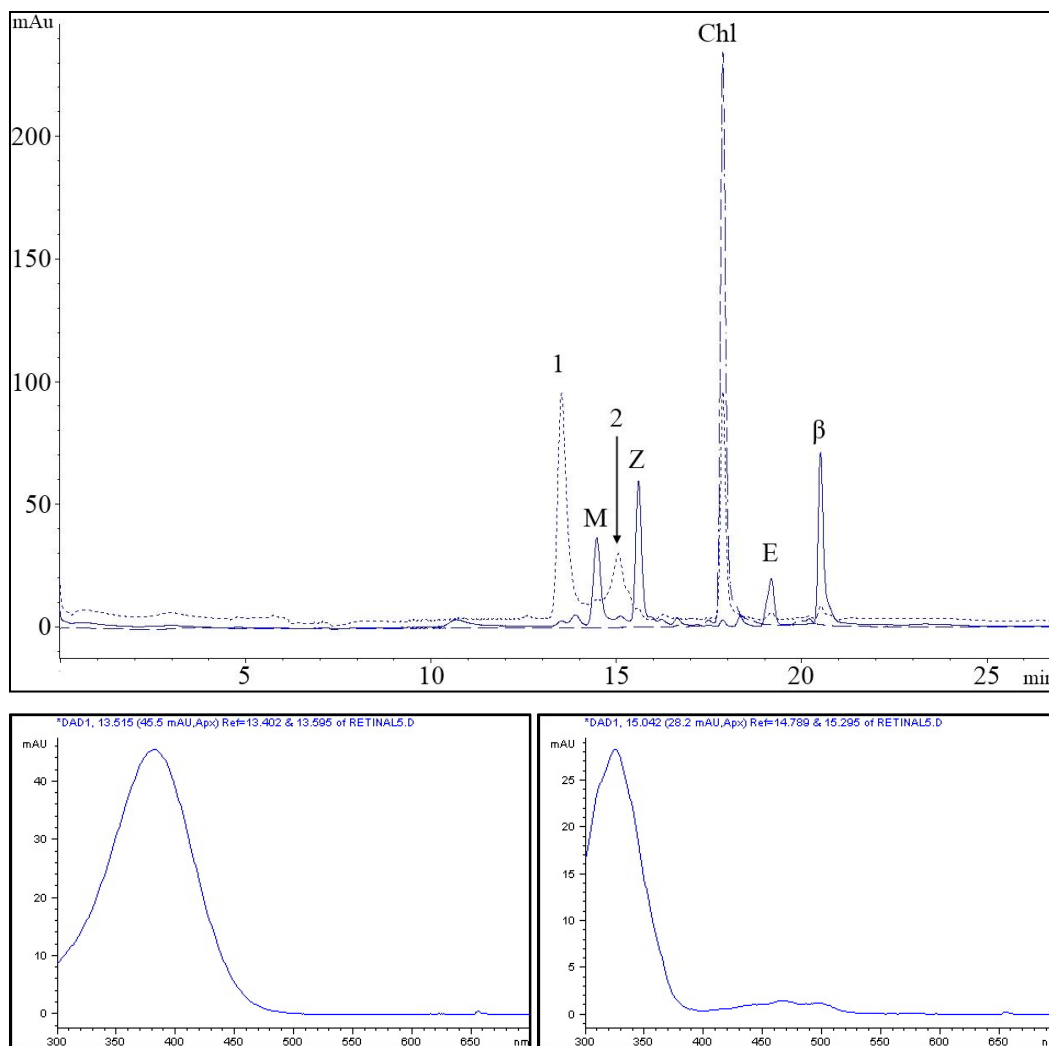


Fig. V-7: HPLC trace of pigments from the *Synechocystis* wild type (solid) combined with 1 μg of retinal standard (dotted). Retinal (compound 1, lower left spectrum) was eluted immediately before myxoxanthophyll (M) after 13.4 minutes whereas retinol (2, lower right spectrum) was eluted after 15 minutes between myxoxanthophyll and zeaxanthin (Z). Retinoids were detected together at 350 nm, carotenoids were detected at 480 nm and chlorophyll (Chl, dashed trace) (18 min), which also absorbs at 350 nm, was detected at 665 nm.

Absence of detectable retinoids in the Synechocystis wild-type strain

Ruch *et al.* (2005) reported retinoid-forming activity for Sll1541 under *in vitro* conditions with substrate specificity for apo-carotenals and apo-carotenols lacking one β -ionone ring. According to the authors, the enzyme did not process C_{40} -carotenoids. The experimental setup used in this dissertation to analyze the pigments of all strains of

Synechocystis constructed in this work was capable of detecting a retinal standard (see Fig. V-7). Even though retinoids are possible carotenoid breakdown products, the HPLC profiles of neither the *Synechocystis* wild type nor any other *Synechocystis* strain, regardless of the growth conditions, indicated the presence of these pigments, or any other pigments whose online spectrum would match the known spectra of retinoids.

The ratios of PS II to PS I were assessed in all strains under different growth conditions. When compared to the wild type strain, the content of chlorophyll was lower in the mutant strain (Table V-1). Photomixotrophic growth at $50 \mu\text{mol photons m}^{-2} \text{s}^{-1}$ resulted in a PS II:PS I ratio of 1:2.8 for the wild type, whereas the ratio was only 1:2 in the mutant strains $\Delta\text{sl}1541$ and $\Delta\text{sl}1541/\Delta\text{sl}r1648$ (Fig. V-8).

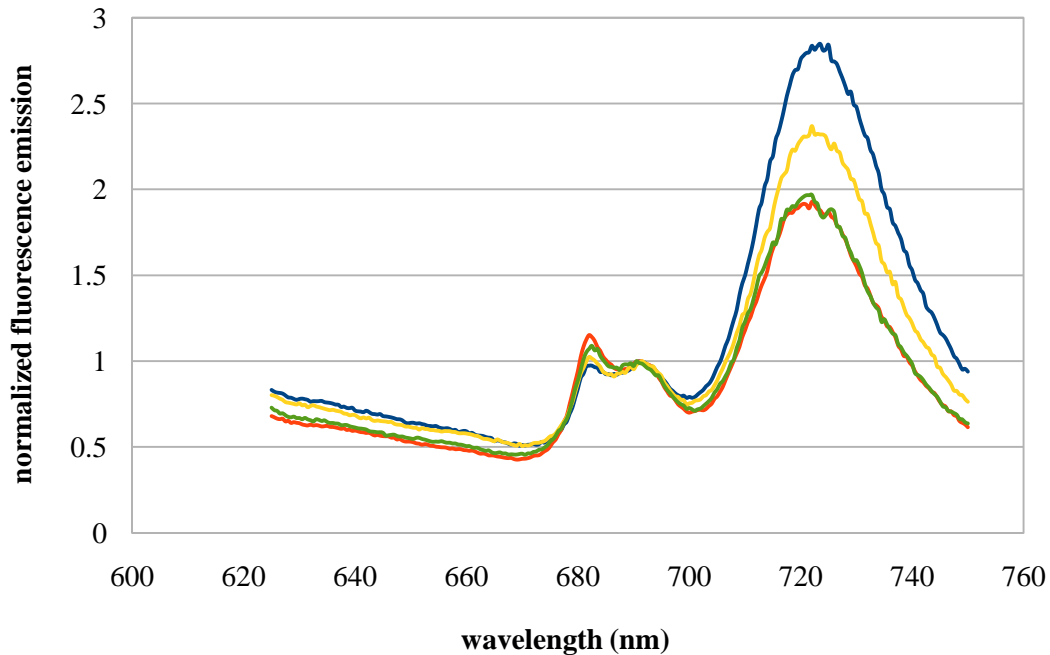


Fig. V-8: Fluorescence emission of the *Synechocystis* wild type (blue line), $\Delta\text{sl}1541$ (red), $\Delta\text{sl}r1648$ (yellow), and the double mutant (green) at an excitation wavelength of 435 nm. All strains were grown at $50 \mu\text{mol photons m}^{-2} \text{s}^{-1}$. Data are shown from three scans per strain and averaged. The peak intensities were normalized to the absorption maximum of PS II.

Table V-1: Chlorophyll (chl) contents of strains grown photomixotrophically at 200 $\mu\text{mol photons m}^{-2} \text{s}^{-1}$, supplemented with 20 μM atrazine.

strain	wild type	$\Delta\text{sll1541}$	$\Delta\text{slr1648}$	$\Delta\text{sll1541}/\Delta\text{slr1648}$
$\mu\text{g/ml chl}$	2.5 ± 0.5	2.4 ± 0.1	1.8 ± 0.3	1.6 ± 0.3

A more dramatic change in the PS II to PS I ratio was observed in all strains upon exposure to increased light intensities and carbon-limitation, increasing to a ratio of about 1 to 1 at 200 $\mu\text{mol photons m}^{-2} \text{s}^{-1}$ in $\Delta\text{slr1648}$ and the double mutant. Under these conditions, which were growth-limiting to the double mutant, the wild-type strain retained full viability and maintained a 1:1.5 ratio, the ratio of $\Delta\text{sll1541}$ was lower than that of the wild type but higher than in the other mutants (1:1.3) (Fig. V-9).

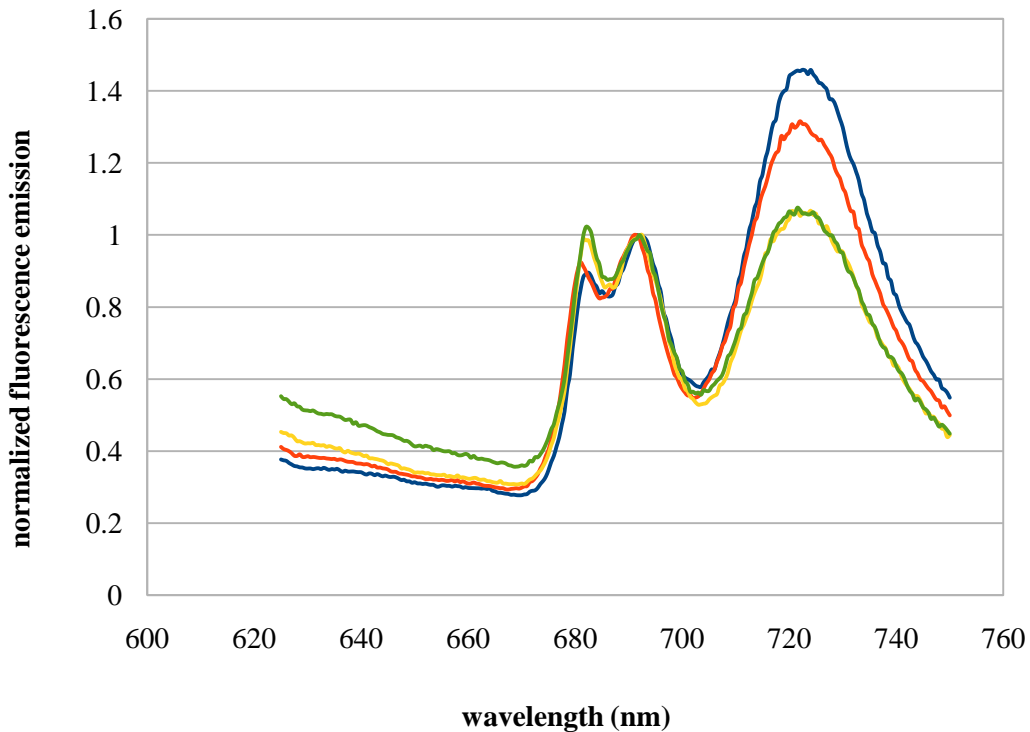


Fig. V-9: Photosystem ratios of all strains grown under high-light (200 $\mu\text{mol photons m}^{-2} \text{s}^{-1}$) and supplemented with 1 mM glucose. Emission is shown for wild type (blue line), $\Delta\text{sll1541}$ (red), $\Delta\text{slr1648}$ (yellow line) and the double mutant (green). Data are shown from three scans per strain and averaged. The peak intensities were normalized to the absorption maximum of PS II.

Electron microscopy of the Synechocystis wild type and dioxygenase mutants

To compare the (sub-)cellular organization of the *Synechocystis* wild type to those of the created dioxygenase mutants transmission electron microscopy was performed on all strains. Micrographs were taken of different sections of all strains (Fig. V-10 - 13). Variations among the *Synechocystis* wild type and the three mutant strains were minimal as all strains showed the subcellular structures of the wild type. S-layer, outer membrane, the peptidoglycan sacculus as well as the cytoplasmic membrane were clearly visible in wild type (Fig. V-10) and $\Delta sl1541$ (Fig. V-11) but appeared to be missing on the other mutants (Fig. V-12, 13). Thylakoid membranes appeared properly structured and were located close to the cytoplasmic membrane in stacks of three to four double-membrane bilayers. Carboxysomes were also present in all strains in similar amounts and sizes. No significant changes in cell sizes or shapes were observed in the mutant strains. However, some of the mutant cells seemed to accumulate highly electron dense inclusions of unknown origin (Fig. V-11). Even though these inclusions as well as loss of the S-layer could have been artifacts from the specimen preparation, additional experiments were performed to analyze the subcellular contents of all strains.

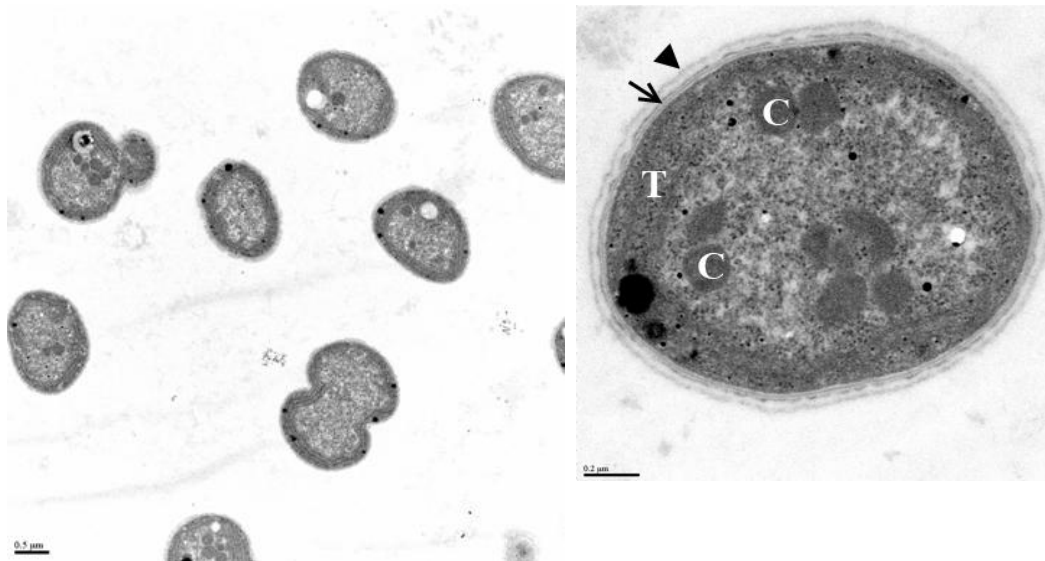


Fig. V-10: Low- (left) and high magnification (right) images of photoautotrophically grown, chemically fixed *Synechocystis* wild-type cells. S-layer (triangle), peptidoglycan (arrow) thylakoids (T) and carboxysomes (C) are indicated. Scale bars are 0.5 μm and 0.2 μm respectively.

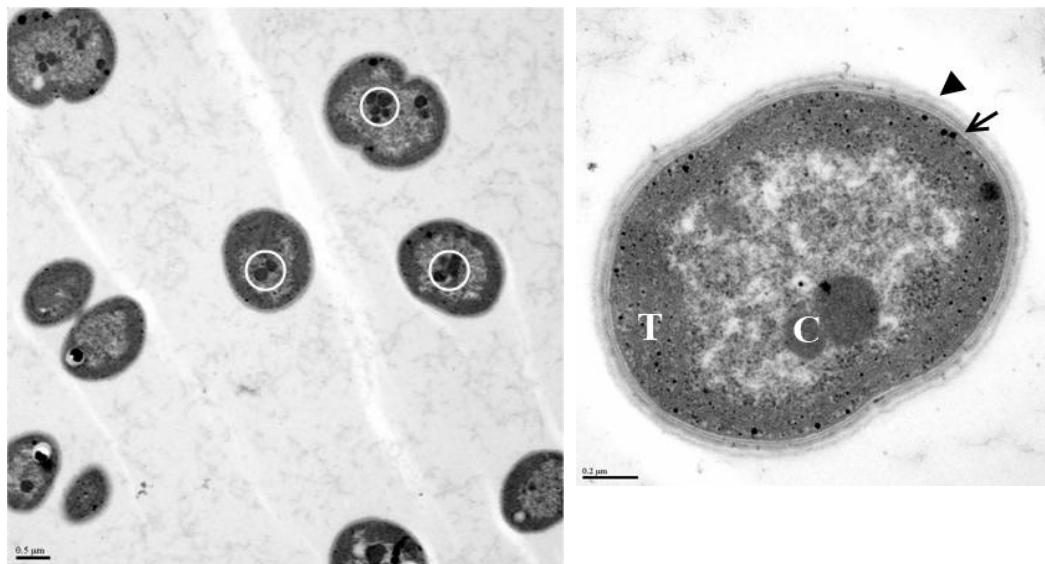


Fig. V-11: Low- (left) and high magnification (right) TEM images of cells of $\Delta sll1541$, prepared like the wild type cells. Some cells appeared to have highly electron dense inclusions which (white circles, absent in the high magnification image) were not present in the wild type strain. S-layer (triangle), peptidoglycan (arrow) thylakoids (T) and carboxysomes (C) are indicated. Scale bars are 0.5 μm and 0.2 μm respectively.

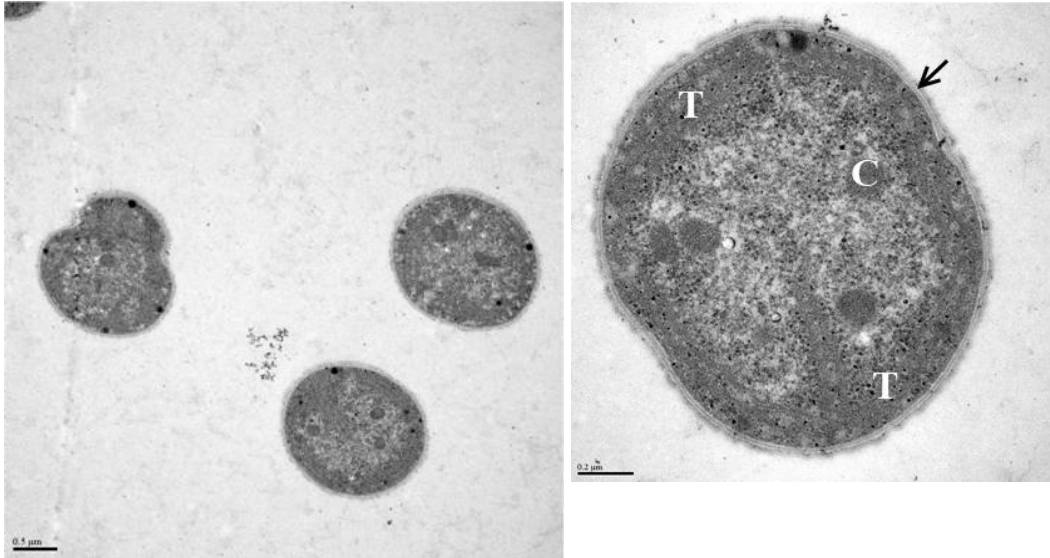


Fig. V-12: Cells of $\Delta slr1648$. The S-layer appeared to be absent in this strain. However, the subcellular structure was almost identical to the wild type cells. Peptidoglycan (arrow), thylakoids (T) and carboxysomes (C) are indicated. Scale bars are 0.5 μm for the low magnification (left) and 0.2 μm for the high magnification image (right).

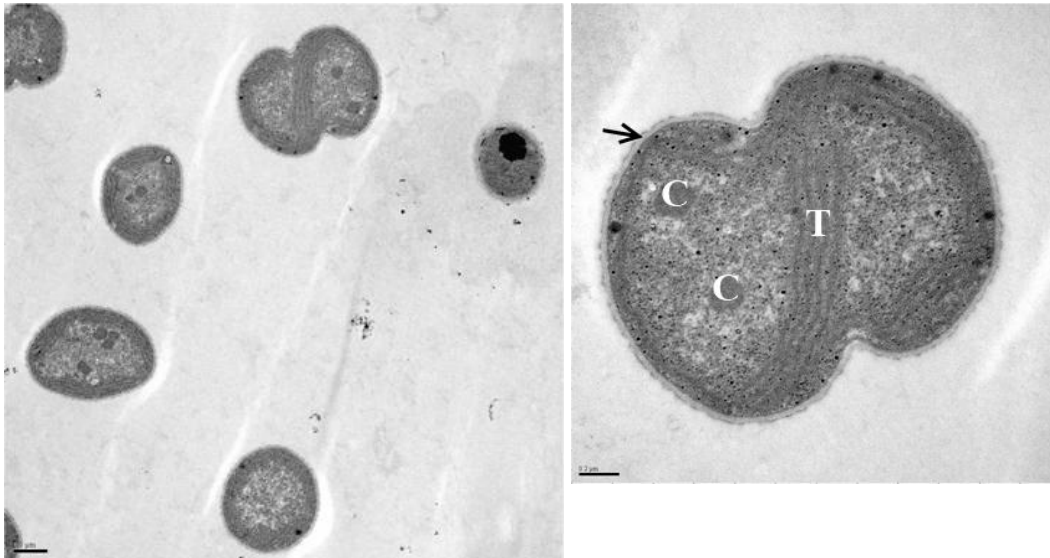


Fig. V-13: The $\Delta sll1541/\Delta slr1648$ double mutant. Highly electron-dense inclusions were infrequently present in this strain as well. The periphery of these cells looked similar to the $\Delta slr1648$ mutant with an absence of the S-layer. Scale bars are 0.5 μm for the low magnification (left) and 0.2 μm for the high magnification image (right).

Membrane profiles of the Synechocystis wild type and dioxygenase mutants

Based on the results obtained from electron microscopy, sucrose gradient membrane density profiles of all strains were prepared in order to study the role of the inclusions found in the EM micrographs. The inclusions could have been the results of compounds accumulating in the mutant strains. The discontinuous sucrose gradients used in these experiments separated the different fractions of cytoplasmic membrane, phycobilisomes, thylakoid membrane and cell wall according to their density (Fig. V-14). The membrane/protein profiles of the mutants obtained from this fractionation were almost identical to the *Synechocystis* wild-type profile – the inclusions observed in the electron micrographs obviously did not have any effect on the appearance of the membrane/protein profiles of the mutant strains. This was also confirmed by illumination of the gradients with UV-light, which could have revealed the presence of UV-absorbing compounds, i.e., carotenoid breakdown products. (Fig. V-15).

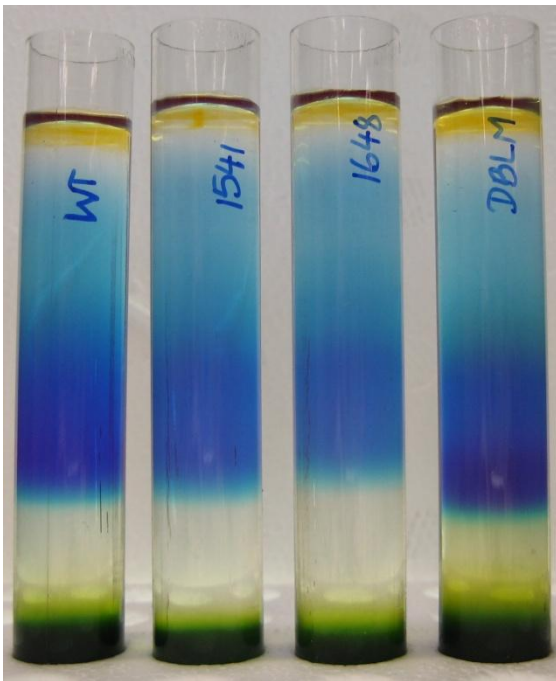


Fig. V-14: Sucrose gradients of the *Synechocystis* wild type (WT) and all mutant strains ($\Delta slr1541$, $\Delta slr1648$ and the double mutant). The low-density cell membrane fraction is located on top of the gradients, phycobilisomes are distributed in 10 to 35 % sucrose whereas thylakoid membranes as well as unbroken cells accumulate in/at 55 % sucrose.

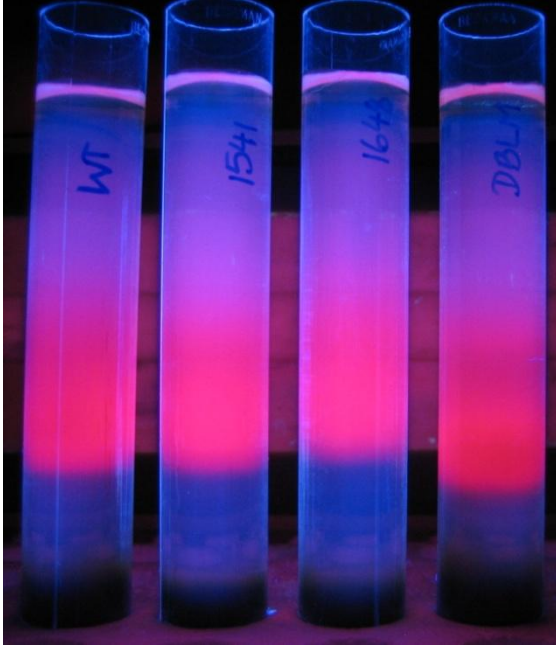


Fig. V-15: Illumination of the gradients from Fig. V-14 with UV-light. Membrane profiles of all strains were very similar. Differences in coloration originated from slightly different amounts of material loaded.

*Turnover of carotenoids in the *Synechocystis* wild type and carotenoid dioxygenase mutants monitored by ^{13}C -labeling*

To monitor the incorporation of ^{13}C into carotenoids, labeling was performed with 1 mM ^{13}C -glucose (99% purity) on the *Synechocystis* wild type and all dioxygenase mutants under photoheterotrophic growth conditions (carbon fixation by the Calvin cycle was blocked by atrazine). Experiments were conducted at different light intensities of 50 and 125 $\mu\text{mol photons m}^{-2} \text{s}^{-1}$ (data shown only for the high light experiment). Being the only carbon source, ^{13}C was most quickly incorporated into the “pool”-carotenoid β -carotene, whose natural isotopomer had disappeared completely 24 hours after the addition of labeled glucose. Fully labeled pigments had masses increased by ~40 Da, compared to their average monoisotopic mass. The same rate of labeling was observed for all dioxygenase mutants and the *Synechocystis* wild-type strain (Fig. V-16 and 18). As expected, turnover of carotenoids other than β -carotene took longer but again occurred at virtually identical rates in all strains. The majority of unlabeled isotopomers had

disappeared after 24 hours of labeling, and after 48 hours unlabeled pigments could not be detected by MS (data shown only for echinenone, Fig. V-17 and 19). All strains had very similar doubling times throughout the experiments.

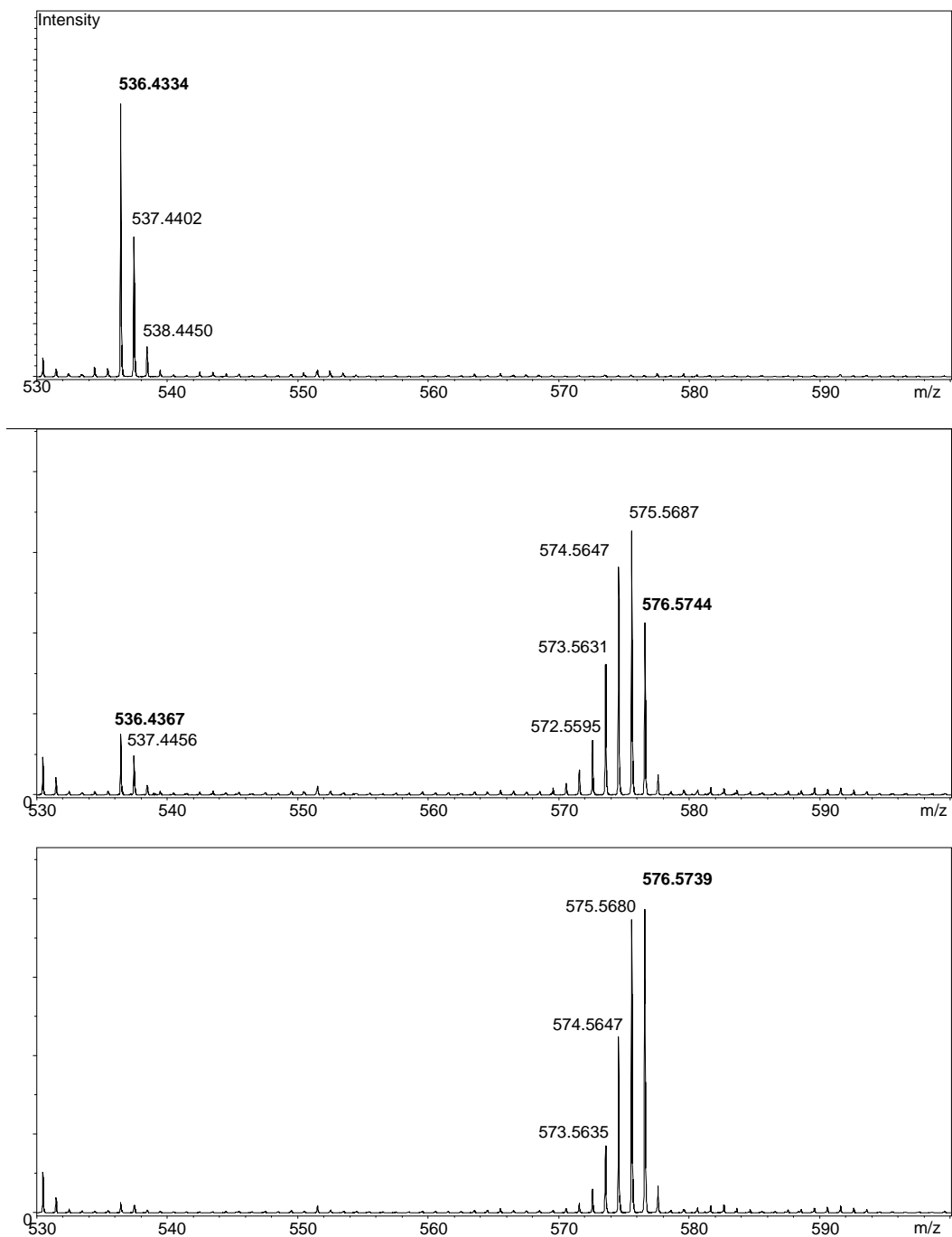


Fig. V-16: Mass spectra of β -carotene in wild type, a carotene with a monoisotopic mass of 536.8846 Da. The top spectrum represents the unlabeled (time 0) pigment. After 12 hours of labeling with ^{13}C -glucose (middle) under photoheterotrophic growth conditions a significant portion of β -carotene was fully labeled and masses were increased by 40 (576.5740). After 24 hours of labeling (bottom) unlabeled β -carotene was virtually absent. Fully labeled/unlabeled masses are indicated in bold.

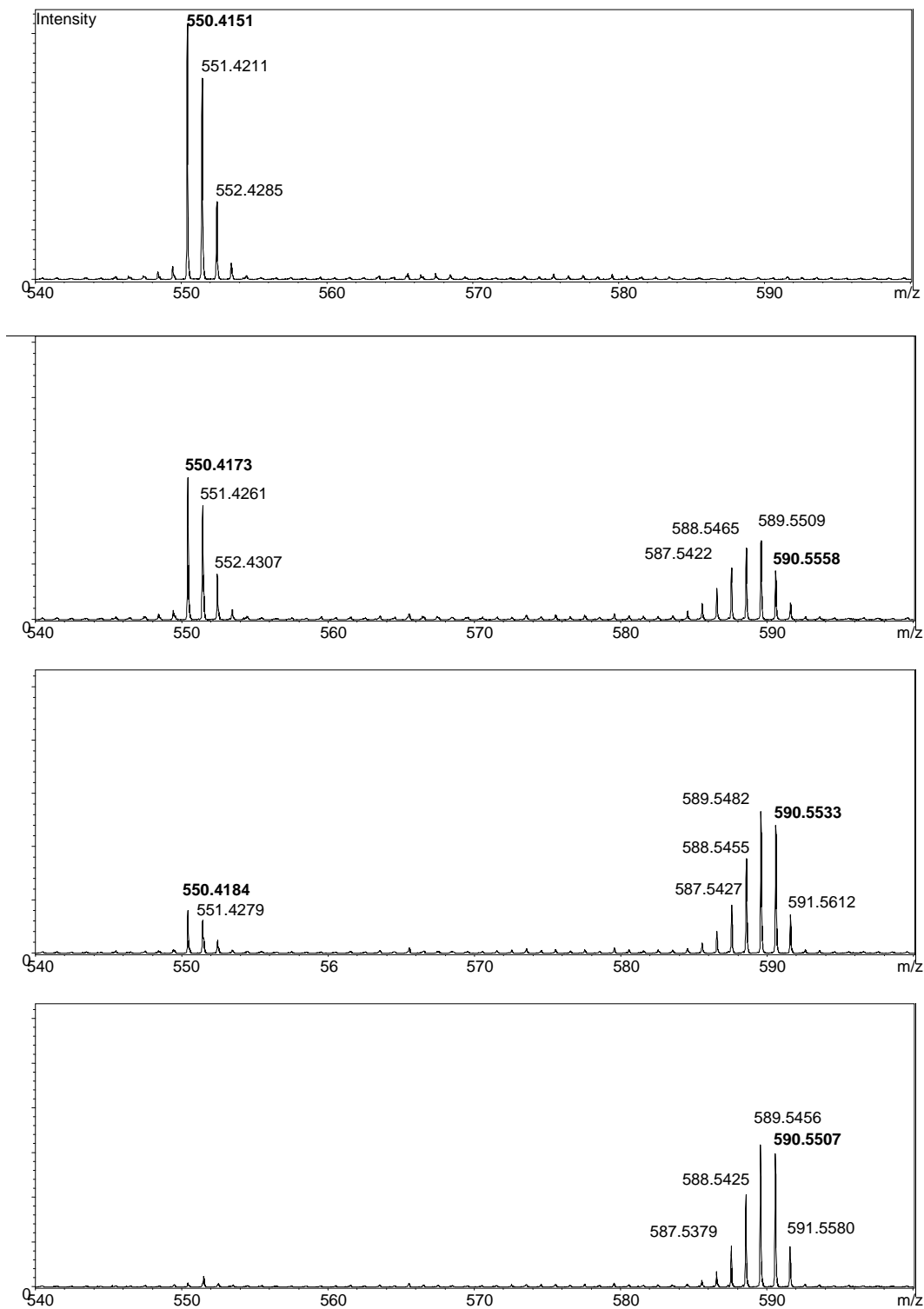


Fig. V-17: Mass spectra of echinenone of the wild type, a carotene with a monoisotopic mass of 550.8562 Da. Spectra from top to bottom were after 0, 12, 24 and 48 hours of labeling.

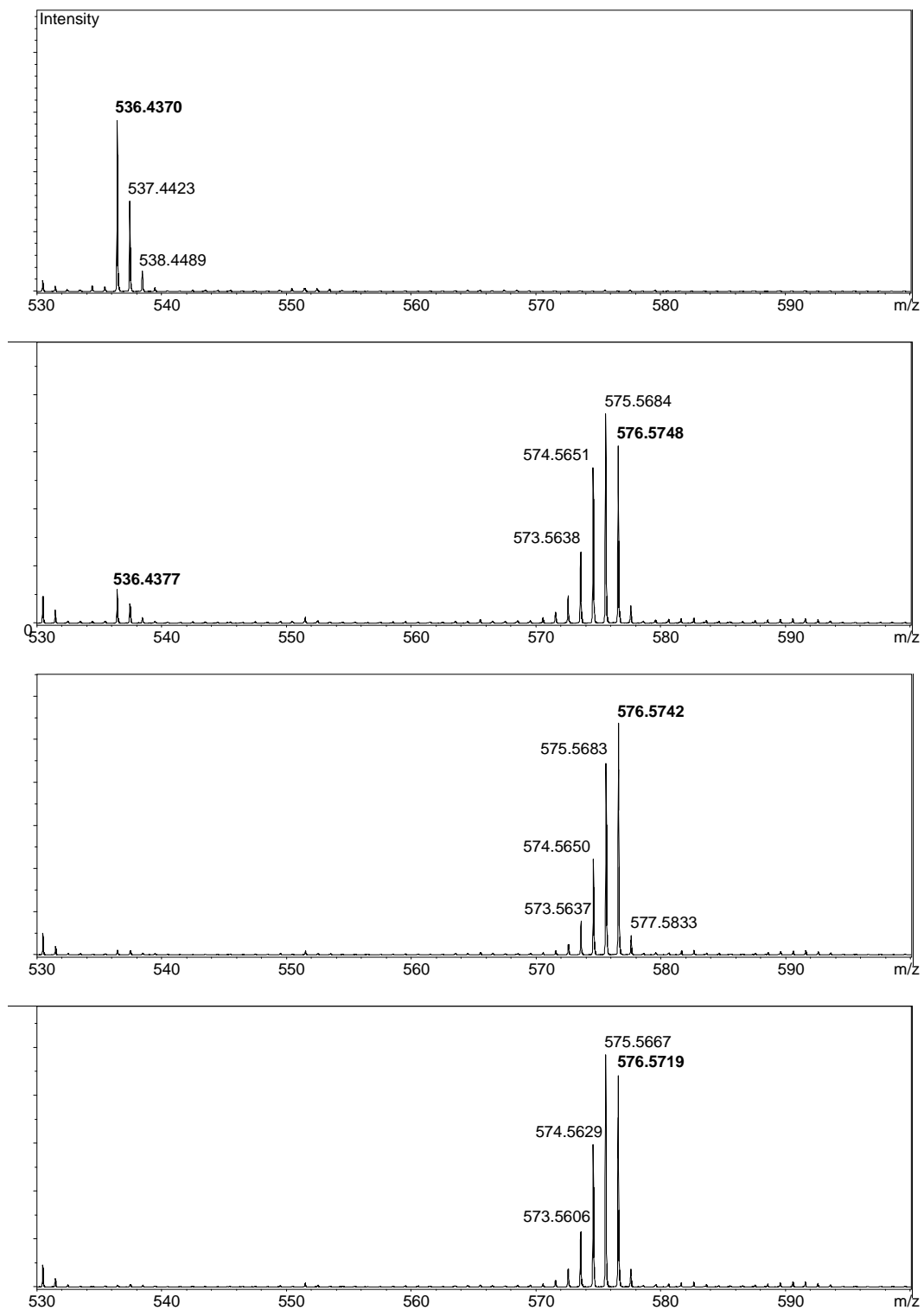


Fig. V-18: Labeling of β -carotene in the double mutant $\Delta sll1541/\Delta slr1648$. Sampling time points were 0, 12, 24 and 36 hours of labeling. Unlabeled pigments disappeared at a rate very similar to the wild type.

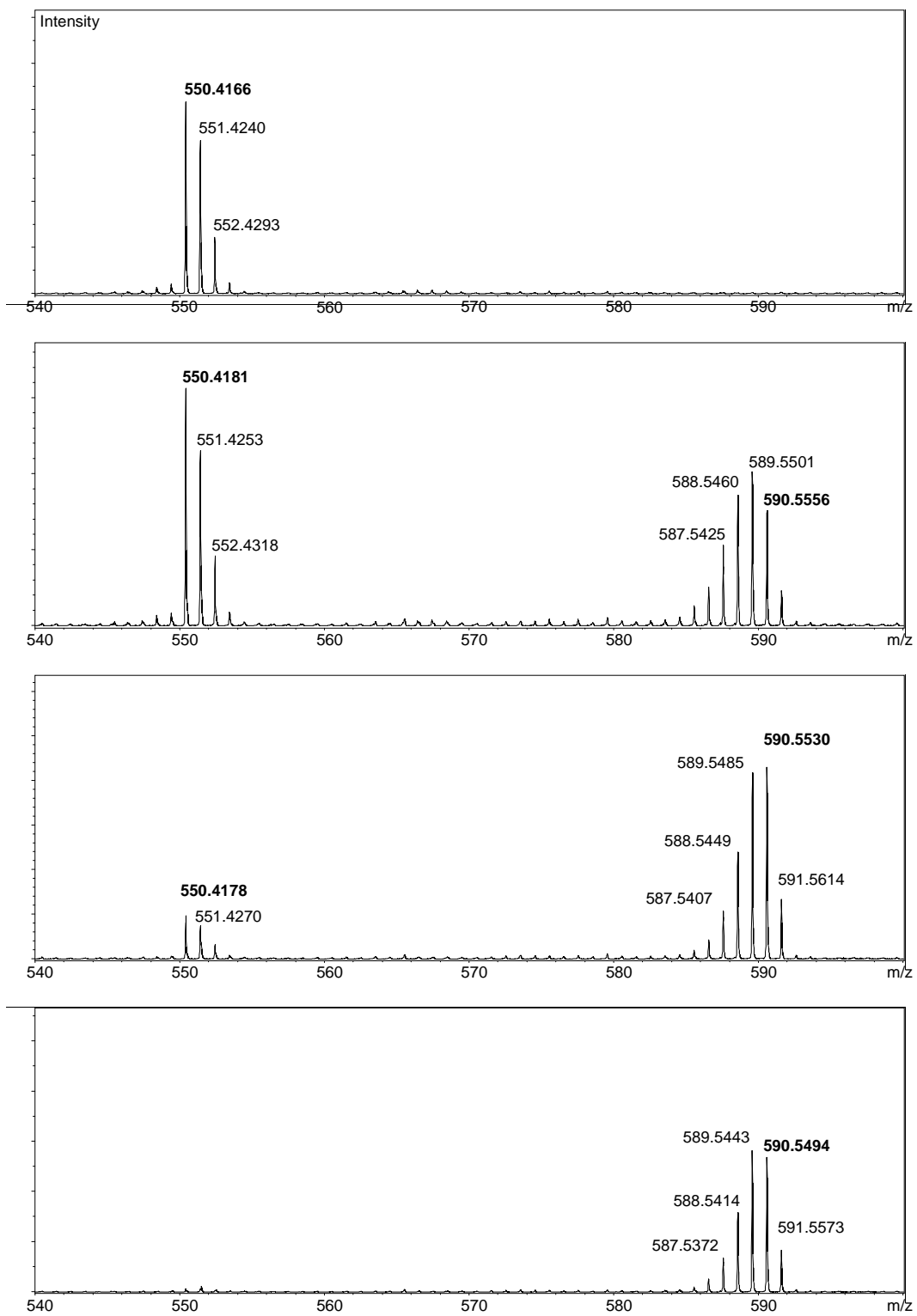


Fig. V-19: Masses of echinenone in the double mutant $\Delta sll1541/\Delta slr1648$ after 0, 12, 24 and 48 hours of labeling. The rates of turnover were very similar to those observed for the wild type.

Discussion

While most of the carotenoid biosynthesis mechanisms have been studied in detail, almost nothing is known about lifetimes and turnover of these pigments in cyanobacteria, whose primary functions are to harvest light, quench reactive oxygen species as well as stabilize membranes and protein complexes. During destructive events such as lipid peroxidation, carotenoids may be damaged and their polyene chain shortened. In this work mutants were created that lack one or two genes that can potentially process carotenoids with shortened carbon backbones. Ruch *et al.* (2005) have reported apo-carotenoid di-oxygenase activity of Sll1541 when tested with a variety of apo-carotenoids as substrates. Based on their findings *Synechocystis* single- and double deletion mutants lacking not only *sll1541* but also its close homolog *slr1648*, an ORF sharing a similar length with *sll1541* of 480 and 490 amino acids, respectively, as well as 158 (33%) identical and 234 (50%) related amino acids, were constructed and analyzed.

Pigment profiles of dioxygenase strains

All mutants created could be segregated under moderately high selective pressure (Fig. V-2, 3) and neither of these displayed an obvious phenotype different from the wild type strain when grown under different light regimes or carbon-limited conditions. Strains that are at least partially deficient in their ability to metabolize carotenoid breakdown products may accumulate such compounds. Curiously, despite using an HPLC setup to detect the presence of polyenes and carotenoids with decreased chain lengths or lower degrees of desaturation, as demonstrated with the retinal standard (Fig. V-7), the pigment profiles of the mutant strains were strikingly similar to those of the wild type strain (Fig. V-4, 5). The only differences observed were with slight variations in pigment quantities, which do not appear to be significant and could have originated from the preparation

procedure (Fig. V-6). Pigments with shortened (<40) carbon chains and fewer conjugated double bonds would therefore exhibit dramatically blue-shifted absorption maxima in the spectral range, most likely below 450 nm. Examples of such carotenoid breakdown products are given in Fig. V-20. However, no compounds were detected at 380 (retinal), 350 (general retinoids) or 285 nm.

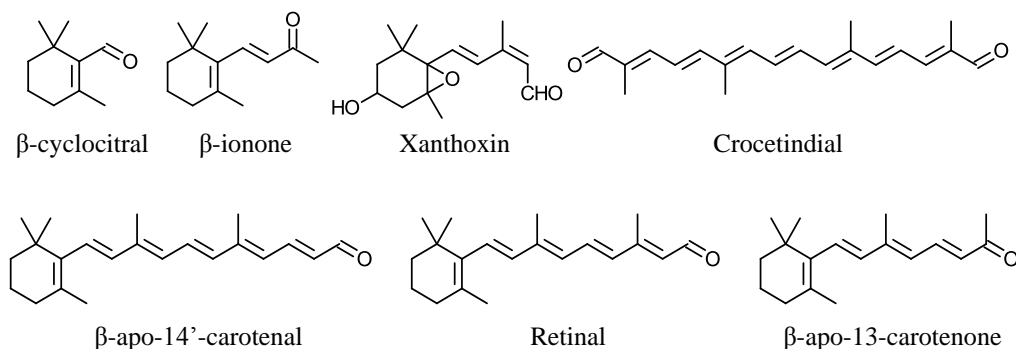


Fig. V-20: Examples of carotenoid breakdown products.

Effects of environmental stress on dioxygenase mutants

Exposure of all strains to $\sim 300 \mu\text{mol photons m}^{-2} \text{ s}^{-1}$ did not result in the formation of pigment breakdown products on any of the strains, including the wild type, that were detectable by HPLC. Under increasingly stressful conditions, e.g., exposure to higher light intensities, photoheterotrophic growth and carbon limitation, growth of the mutant strains became more unstable, and PS I to PS II ratios as well as chlorophyll contents dropped when compared to the wild type strain (Fig. V-8, 9; Table 1). This could indicate a generally lower amount of active photosystems in the dioxygenase strains and a more significant drop thereof under high-light stress.

Even though fully adapted strains did grow at up to $330 \mu\text{mol photons m}^{-2} \text{ s}^{-1}$ with doubling times similar to the wild type, the mutant strains sometimes did not grow at all after sudden changes to different conditions, suggesting a reduced ability of the

dioxygenase mutants to adapt to environmental changes. Upon adaptation from low- to high light intensity, the double mutant increased the concentrations of myxoxanthophyll and zeaxanthin at rates very similar to the wild (Fig. V-6) in spite of markedly changed photosystem ratios and chlorophyll contents. Apparently, the mutant strains are capable of maintaining the required steady-state level of these pigments while keeping the number of photosystems (and possibly other sources for the production of ROS) at a lower level than the *Synechocystis* wild type.

Electron microscopy and membrane profiles of dioxygenase mutants

TEM was carried out with photoautotrophically grown strains of the dioxygenase mutants and the *Synechocystis* wild type to compare the subcellular organization and visualize possible accumulating pigments or metabolic products that would not have been detected by the HPLC analysis. Although the mutant cells were of similar size (~1.5 μm) and shared all the structural details of the wild type cells (Fig. V-10 - 13), they occasionally displayed highly electron dense, circular inclusions of varying sizes that were predominantly present in $\Delta slr1541$ and the double mutant (Fig. V- 11, 13). Besides, the strains $\Delta slr1648$ and the double mutant appeared to have lost their surface layer (Fig. V- 12, 13). Even though in chemically fixed specimen of *Synechocystis* the S-layer protein is much less preserved than in an HPF approach (see EM micrographs in chapter III, p. 52, 53), it must be noted that all specimens were prepared for EM at the same time and under the same conditions, and the S-layer remained intact in the wild type and $\Delta slr1648$ strains.

Inclusions are frequently observed on (photo-)mixotrophically grown cells of *Synechocystis* due to the formation of storage granules, e.g., polyhydroxyalkanoates (PHA), but not expected to a degree found in the dioxygenase mutants.

Therefore, membranes/proteins were isolated of all strains and analyzed on sucrose density step gradients (Fig. V-14). Since these gradients looked virtually identical for all strains an inclusion-forming phenotype of the dioxygenase mutants was excluded.

*¹³C-labeling of carotenoids in the *Synechocystis* wild type and the dioxygenase mutants*

The deletion of putative CCDs could have resulted in altered carotenoid lifetimes in the affected mutants and therefore ¹³C-labeling was performed on all strains. Interestingly, the turnover of carotenoids in the mutant strains was equal to the *Synechocystis* wild-type strain. This result confirms the data from other groups (Ruch *et al.*, 2005; Marasco *et al.*, 2006) who reported no catalytic activity of either Sll1541 or Slr1648 on native carotenoids of *Synechocystis*. Moreover, a possible accumulation of substrates (which were not detected) for these enzymes had no effect on the carotenoid metabolism of the deletion strains, indicating a role of Sll1541 and Slr1648 presumably either under different conditions than the ones tested here, or with a different group of substrates. Interaction with an entirely different class of substrates, however, is unlikely at least for Sll1541 since Kloer *et al.* (2005) have shown binding of apo-carotenoid substrates to Sll1541 used for determining its the crystal structure.

Contribution of Sll1541 and Slr1648 to carotenoid turnover is negligible under high light conditions

As a whole the data obtained in this work on *Synechocystis* mutants lacking the two putative carotenoid cleavage dioxygenases Sll1541 and Slr1648 suggest a minimal (if any) contribution of these enzymes to the turnover of carotenoids in this cyanobacterium. This is in agreement with reports from other authors (Ruch *et al.*, 2005; Marasco *et al.*,

2006): In a biochemical study with purified Slr1541, Ruch's group demonstrated enzymatic activity of this protein on apo-carotenoids, mainly apo-carotenals and apo-carotenols of various chain lengths but also apo-lycopenals. In their study the central C15-C15' double bond appeared to be the recognized cleavage site for Sll1541 (Fig. V-1B). However, for the substrates tested the authors reported relatively low conversion rates. Furthermore, native full-length carotenoids of *Synechocystis* were not cleaved by Sll1541. In a different study by Marasco *et al.* (2006) the authors expressed both Sll1541 and Slr1648 heterologously in *E. coli* strains producing β -carotene, zeaxanthin, torulene, lycopene or diapocarotenodial. Again, no activity was detected for either of the two enzymes in this color-based assay.

The plentitude of distinct carotenoid oxygenases in plants – *A. thaliana* encodes more than a dozen CCDs and NECDs –, the high degree of conservation of their cyanobacterial orthologs, and their increased expression levels under conditions of elevated ROS (Hihara *et al.*, 2001) clearly indicates an important function of these enzymes, most likely in the turnover of carotenoids. The aim of this work was the study of the carotenoid contents in vivo of three mutant strains lacking putative CCDs under high-light exposure. The absence of a carotenoid phenotype in these strains could have several reasons. For example, the formation of apo-carotenoid species under the tested high-light and carbon-limited conditions could be too low for the detection by the used HPLC system, which did not show traces of carotenoid breakdown products as reported by Ruch *et al.* (2005). Besides, apo-carotenoids could disappear quickly either due to the volatile nature of some of these pigments with chain lengths of 13 or less carbon atoms (Enzell, 1985), or quick downstream processing by (yet unidentified) enzymes, e.g., polyene-specific oxidases and oxygenases. Ke *et al.* (2005) identified a retinoic acid binding cytochrome P450 in *Synechocystis*, which was later characterized as a retinoic

acid hydroxylase by Alder *et al.* (2009). While the designated substrate for this enzyme was all-*trans*-retinoic acid, it also processed apo-carotenals such as retinal (Fig. V-20), although at significantly lower rates.

The functions of cyanobacterial CCDs like the ones studied in this work continue to be a largely unanswered question. Additional steps in the enzymatically controlled breakdown of (apo-) carotenoids remain to be elucidated, and their study will be necessary for the future exploitation of prokaryotic hosts in the production of apo-carotenoid-based vitamin A, aroma compounds and plant hormones.

References

- Alder, A., Bigler P., Werck-Reichhart D., and Al-Babili S. (2009) In vitro characterization of *Synechocystis* CYP120A1 revealed the first nonanimal retinoic acid hydroxylase. *FEBS J* **276**: 5416-5431.
- Bouvier, F., Isner J.C., Dogbo O., and Camara B. (2005) Oxidative tailoring of carotenoids: a prospect towards novel functions in plants. *Trends Plant Sci* **10**: 187-194.
- Burton, G.W., and Ingold K.U. (1984) β -carotene: an unusual type of lipid antioxidant. *Science* **224**: 569-573.
- Carlioz, A., and Touati D. (1986) Isolation of superoxide dismutase mutants in *Escherichia coli*: is superoxide dismutase necessary for aerobic life? *EMBO J* **5**: 623-630.
- Chelikani, P., Fita I., and Loewen P.C. (2004) Diversity of structures and properties among catalases. *Cell Mol Life Sci* **61**: 192-208.
- Enzell, C., (1985) Biodegradation of carotenoids – an important route to aroma compounds. *Pure & Appl Chem* **57**: 693-700.
- Fenton, H.J.H. (1894) Oxidation of tartaric acid in presence of iron. *J Chem Soc Trans* **65**: 899-910.
- Fridovich, I. (1997) Superoxide anion radical (O_2^-), superoxide dismutases, and related matters. *J Biol Chem* **272**: 18515-18517.
- Hihara, Y., Kamei, A., Kanehisa, M., Kaplan, A., and Ikeuchi, M. (2001) DNA microarray analysis of cyanobacterial gene expression during acclimation to high light. *Plant Cell* **13**: 793-806.
- Imlay, J.A. (2003) Pathways of oxidative damage. *Annu Rev Microbiol* **57**: 395-418.

- Jüttner, F., and Höflacher B. (1985) Evidence of β -carotene 7,8(7',8') oxygenase (β -cycocitral, crocetindial generating) in *Microcystis*. *Arch Microbiol* **141**: 337-343.
- Kloer, D.P., Ruch S., Al-Babili S., Beyer P., and Schulz G.E. (2005) The structure of a retinal-forming carotenoid oxygenase. *Science* **308**: 267-269.
- Ke, N., Baudry J., Makris T.M., Schuler M.A., and Schlichting I. (2005) A retinoic acid binding cytochrome P450: CYP120A1 from *Synechocystis* sp. PCC 6803. *Arch Biochem Biophys* **436**: 110-120.
- Latifi, A., Ruiz M., and Zhang C. (2009) Oxidative stress in cyanobacteria. *FEMS Microbiol Rev* **33**: 258-278.
- von Lintig, J., and Vogt K. (2000) Filling the gap in vitamin A research. *J Biol Chem* **275**: 11915-11920.
- Massey, V. (1994). Activation of molecular oxygen by flavins and flavoproteins. *J Biol Chem* **36**: 22459-22462.
- Marasco, E.K., Kimleng, V., and Schmidt-Dannert C. (2006) Identification of carotenoid cleavage dioxygenases from *Nostoc* sp. PCC 7120 with different cleavage activities. *J Biol Chem* **281**: 31583-31593.
- Rodríguez-Bustamante, E., and Sánchez S. (2007) Microbial production of C₁₃-norisoprenoids and other aroma compounds via carotenoid cleavage. *Crit Rev Microbiol* **33**: 211-230.
- Ruch, S., Beyer P., Ernst H., and Al-Babili S. (2005) Retinal biosynthesis in Eubacteria: in vitro characterization of a novel carotenoid oxygenase from *Synechocystis* sp. PCC 6803. *Mol Microbiol* **55**:1015-1024.
- Scherzinger, D., and Al-Babili S. (2008) In vitro characterization of a carotenoid cleavage dioxygenase from *Nostoc* sp. PCC 7120 reveals a novel cleavage pattern, cytosolic localization and induction by high light. *Mol Microbiol* **69**: 231-244
- Schwartz, S.H., Qin X., and Loewen M.C. (2004) The biochemical characterization of two carotenoid cleavage enzymes from *Arabidopsis* indicates that a carotenoid-derived compound inhibits lateral branching. *J Biol Chem* **279**: 46940-46945.
- Spurr, A.R. (1969) A low-viscosity epoxy resin embedding medium for electron microscopy. *J Ultrastruct Res* **26**: 31-43.
- Stratton, S.P., Schaefer W.H., and Liebler D.C. (1993) Isolation and identification of singlet oxygen oxidation products of β -carotene. *Chem Res Toxicol* **6**: 542-547.
- Triantaphylides, C., and Havaux M. (2009) Singlet oxygen in plants: production, detoxification and signaling. *Trends Plant Sci* **14**: 219-228.

Walter, M.H., Floss D.S., and Strack D. (2010) Apocarotenoids: hormones, mycorrhizal metabolites and aroma volatiles. *Planta* **232**: 1-17.